Atmospheric Aerosol Loading, Chemical Composition, and Modelling PM_{10} Concentration in Rustenburg and Klerksdorp Mining Areas of the North-West Province of South Africa

Brighton Kaonga

May 2012

Atmospheric Aerosol Loading, Chemical Composition, and Modelling PM_{10} Concentration in Rustenburg and Klerksdorp Mining Areas of the North-West Province of South Africa

Brighton Kaonga

BSc (University of Zambia, Zambia)
MSc (University of Ghent, Belgium)

A thesis submitted in fulfilment of the requirements for the degree of Doctor of Philosophy in the

Department of Chemistry

Faculty of Agriculture, Science and Technology,

North-West University (Mafikeng Campus)

Supervisor: Prof Eno E. Ebenso

May 2012

Declaration

I, Brighton Kaonga, declare that this thesis entitled 'Atmospheric Aerosol Loading, Chemical Composition and Modelling PM_{10} Concentration in Rustenburg and Klerksdorp Mining Areas of the North-West Province of South Africa' and the work presented in it are my own. I confirm that:

i. This work was done wholly or mainly while as a candidate for a research degree at this North West University (Mafikeng Campus).

ii. Where any part of this thesis has previously been submitted for a degree or any other qualification at this University or any other institution, this has been clearly stated.

iii. Where I have consulted the published works of others, this is always clearly indicated.

iv. Where I have quoted from the work of others, the source is always given. With the exception of such quotations, this thesis is entirely my own work.

v. I have acknowledged all main sources of help.

Signed: 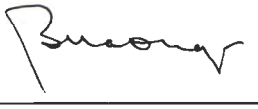

Date: 31-08-2012

Abstract

Atmospheric aerosols emitted from Phokeng, in Rustenburg and Jouberton, in Klerksdorp mining Towns in the North-West Province of South Africa were due to the industrial activities, wind dust, transport and fuel burning. The objective of the study is therefore to collect and analyse atmospheric aerosol data in the mining areas of Rustenburg and Klerksdorp in the North West Province. The Atmospheric aerosols studies were done over a period of 4 years (from January 2008 to June, 2011) for measurement of particulate matter of particle diameter of 10 micrometers (PM_{10}). Data collection was done by retrieval from NASA's MISR system, Cascade Impactor and drawing air through a German Ambient Dust Monitor (which measures in situ concentrations of particulate matter of various sizes). The results obtained were compared to the South African Air Quality Guidelines (2005) and the World Health Organization Air Quality Guidelines (2005). It was observed that the PM_{10} values for 24 hourly periods exceeded the 75 $\mu g/m^3$ maximum permissible limit for the South African Guidelines in a number of instances. According to the World Health Organization Guidelines, since their maximum permissible limits are set for 50 $\mu g/m^3$, it means the study results exceeded these guidelines for more periods compared to the South Africa Air Quality Standards (SAAQS). Chemical composition of the aerosols indicates presence of the following trace elements: Pb, V, Cr, Ni, Hg, Co, Cd, Se, Mn, Ba, and As. Modeling of atmospheric aerosols was undertaken. It was found that there was a good fit between the measured and the modeled values. The research results have pointed towards the possible health risks from the presence of particulate matter in the air. This study therefore offers the first documentation on atmospheric aerosol loading in Rustenburg and Klerksdorp in the Norrth West Province of South Africa.

Acknowledgements

There is ONE without whom I cannot accomplish anything. Yes because of Him, I can accomplish great things. I therefore give thanks and praise, and all the glory to the Almighty God for it is Him who gave me my life accomplishments and He is the reason I was able to embark on this PhD programme....He has enabled me to reach the goal.
May I take this opportunity to acknowledge Dr. Nnenesi Kgabi for accepting me to work with her although circumstances changed.

My utmost gratitude is to Professor Eno E. Ebenso. When I thought I had reached a gigantic barrier on my progress, he reached out his hand and showed me a new path, holding my hand, guiding me, mentoring me through the rest of the challenging study journey. Such men are rare. In my mind, he will permanently be remembered. I thank the North-West University for admitting me to study at the university, for the North-West University postgraduate bursary, and the Emerging Researchers Funds they gave me to help me with the studies.

I acknowledge the CSIR and National Laser Centre of South Africa for providing me with finances, and their facilities at the centre during part of my study there. Professor Sivakumar Venkataraman deserves to be unreservedly acknowledged for through him much progress has been achieved. This work would not be complete without the unmeasured help from Ms Thokozile Ramoroa and the Department of Agriculture, Conservation and Environment. With her I worked and acquired most of my data. I am greatly indebted to her.

I thank Professor Simon Materechera for all the help he rendered to me in shaping my proposal. To Dr. Nandi Mumba for his advice through my data collection, article writing guidance, and thesis writing input, I say thank you. Dr. Mwadham M. Kabanda is highly acknowledged for his part in advising me on the modeling part of this research work. Without him, a significant delay in completing my work could have been unavoidable.
I am also grateful to Mr. Lebogang Motsei for assisting with the operation of the AAS and the ICP-MS.
Who can survive without friends, I ask? Great friends build you up.

My sincere gratitude goes to Dr. JSP Mlatho. He greatly assisted me in both finances and academic work. His friendship is never to be forgotten. Dr. Ashmore Mawire's help in article writing will always be remembered. I remember in the first part of the programme of my study, I was using what I call a museum computer. Dr. Sabata Moloi unselfishly borrowed me his personal laptop for my use for as long as I wanted. To all those (too numerous to mention all) who cared to share a smile with me while so far away from my family, I say thank you....Moses Molefe, Sylvester Thamaga, Abigail Gomolemo, Chester Murulana, my PhD colleague Priya Thomas, and many more.

Dedication

This work is dedicated to each member of my household. Thank you for enduring my absence. Especially the youngest two who though wanted to know me more in their infancy, I was not there for them.

My dear wife, you deserve my deepest thank you for holding the fort day and night while I was away. I love you and God bless you.

List of Publications

1. Brighton Kaonga and Nnenesi A. Kgabi (2010). Investigation into presence of atmospheric particulate matter in Marikana, mining area in Rustenburg Town, South Africa. *Environmental Monitoring and Assessment* 178 (1-4): 213-220.
   DOI: 10.1007/s10661-010-1683-1
   http://www.springerlink.com/content/x483873km1333620/

2. Brighton Kaonga and Eno Ebenso (2011). Book Chapter An Evaluation of Atmospheric Aerosols in Kanana, Klerksdorp Gold Mining Town, in the North-West Province of South Africa. In the book "Air Quality Monitoring, Assessment and Management" edited by Nicolás A. Mazzeo, ISBN 978-953-307-317-0, InTech Publishers, Czechoslovakia, July 7, 2011
   http://www.intechopen.com/articles/show/title/an-evaluation-of-atmospheric-aerosols-in-kanana-klerksdorp-gold-mining-town-in-the-north-west-provin

Table of Contents

List of Figures

List of Tables

List of Symbols

PM	Particulate Matter
PM1	Particulate Matter of diameter 1.0 μm or less
PM2.5	Particulate Matter of diameter 2.5 μm or less
PM10	Particulate Matter of diameter 10 μm or less
μm	Micrometers
nm	Nanometers
Ω	Absorption Coefficient
σ	Attenuation Coefficient
λ	Wavelength
φ	single scatter albedo
τ_e	Optical depth
π	Pi
r	radius of particulate
n	Concentration of aerosols
I_o	Incident light
Q_s	Scattering efficiency
Q_e	Extinction coefficiency
ECM	Extra Cellular Matrix
NO_x	Nitrogen Oxides
SO_2	Sulphur Dioxide
O_2	Oxygen
O_3	Ozone
UV	Ultraviolet
^oC	Degree Celsius
RF	Radiative Forcing
CCN	Cloud Condensation Nuclei
CO_2	Carbon Dioxide
CFC	Chlorofluorocarbons
H_2O	Water

H_2S	Hydrogen Sulphide
H_2	Hydrogen
CO	Carbon Monoxide
HCl	Hydrogen Chloride
HF	Hydrogen Fluoride
He	Helium
Na	Sodium
Mg	Magnesium
Al	Aluminium
Cl	Chlorine
K	Potassium
Ca	Calcium
Sc	Scandium
Ti	Titanium
V	Vanadium
Cr	Chromium
Mn	Manganese
Fe	Iron
Co	Cobalt
Ni	Nickel
Cu	Copper
Zn	Zinc
Ga	Gallium
As	Asernic
Se	Selenium
Br	Bromine
Rb	Rubidium
Sr	Strontium
Mo	Molybdenum
Ag	Silver
Cd	Cadmium

In	Indium
Sn	Tin
Sb	Antimony
I	Iodine
Cs	Cesium
Ba	Barium
La	Lanthanum
Ce	Cerium
Sm	Samarium
Eu	Europium
Lu	Lutetium
Hg	Mercury
W	Tungsten
Au	Gold
Th	Thorium
SOA	Secondary Organic Aerosol
ARM	Atmospheric Radiation Measurement
WHO	World Health Organization
NIOSH	National Institute for Occupational Safety and Health
NAAQS	National Ambient Air Quality Standards
EPA	Environmental Protection Agency
COPD	Chronic Obstructive Pulmonary Disease
PTB	Pulmonary Tuberculosis
PAH	Polycyclic Aromatic Hydrocarbons
L/min	Litres per minute
ICP-MS	Inductive-Coupled Plasma Mass Spectrometer
AAS	Atomic Absorption Spectrometer
AOD	Aerosol Optical Depth
MISR	Multi-angle Imaging SpectroRadiometer
OMSI	Oregon Museum of Science and Industry
NIR	Near Infrared

$\mu g/m^3$	Micrograms per cubic meter
ng/m^3	nanograms per cubic meter
α	Alpha
Ψ	Psi
ρ	Rho
η	Eta
INAA	Instrumental Neutron Activation Analysis
XRF	Photon-induced X-ray Fluorescence
PIXE	Particle-induced X-ray Emission
ICP/AES	Inductively-coupled Plasma with Atomic Emission Spectroscopy
SEM/XRF	Scanning Electron Microscopy with X-ray Fluorescence
EDXRF	Energy Dispersive X-ray Fluorescence
rf	radio frequency
CIE	Commission of Illumination
GDP	Gross Domestic Product
NWU	North West University
m	Metres
l/h	litres per hour
ppb	Parts Per Billion

CHAPTER 1

INTRODUCTION

1.1 Background

Atmospheric aerosols, technically, are considered to be the suspension of fine solid or liquid particles in a gas (Pandis, Wexler and Seinfeld 1995; Hinds, 1999; Seinfeld, 2004; Politis, Pilnis and Lekkas 2008; Ma, Liu and He. 2010). Aerosols are everywhere in the air and are often observable as dust, smoke and haze. This definition of aerosols includes particulates or Particulate Matter (PM), which is defined as tiny subdivisions of solid matter suspended in a gas or liquid. Particles in the air can change their size and composition by condensation of vapour species or evaporation, coagulating with other particles by chemical reaction, or by activation in the presence of water.

Atmospheric aerosols originate from a variety of natural and anthropogenic sources which are geographically localized and experience short lifetimes in the atmosphere. As a result their concentration can vary significantly by location and time. High concentrations can be found near their sources while at remote areas aerosol number drops rapidly. However, even at remote areas atmospheric aerosols can be found in relative abundance during certain events via long range transport processes. Anthropogenically induced aerosol particles, namely sulfate, elemental and organic carbon, nitrate and mineral dust, have been traced at the farmost corners of the globe (Barrie, 1986; Rau and Khalil, 1993).

The production of atmospheric aerosols or atmospheric particulate matter is of great concern. The effects of inhaling particulate matter have been widely studied in humans and animals and these effects include asthma, lung cancer, cardiovascular issues, and premature death (Berglund et al., 1991; Pope and Burnett, 2002; WHO, 2003; Brugge et al., 2007; Ska and Wojtylak, 2010; WHO, 2011). The size of the particle is the main determinant of where in the respiratory tract the particle will come to rest when inhaled. Larger particles are generally filtered in the nose and throat and do not necessarily cause problems, but particulate matter that is smaller than about 10 micrometers (μm), referred to as PM_{10}, can settle in the bronchi and lungs and cause health problems. Seinfeld and Pandis (2006) state that the 10 micrometer (μm) particle size does not represent a strict boundary between respirable and non-respirable particles,

but has been agreed upon for monitoring of airborne particulate matter by most regulatory agencies. Similarly, particles smaller than 2.5 micrometers, $PM_{2.5}$, tend to penetrate the gas-exchange regions of the lung, and very small particles (< 100 nanometers) may pass through the lungs to affect other organs. In particular, a study by Pope and Burnett (2002) indicates that $PM_{2.5}$ leads to high plaque deposits in arteries, causing vascular inflammation and atherosclerosis — a hardening of the arteries that reduces elasticity, which can lead to heart attack and other cardiovascular problems. Aerosols have properties that influence both climate and human health. These are briefly discussed below.

1.2 Properties of Atmospheric Aerosols

As solar irradiance passes through the atmosphere, it interacts with aerosols and experiences a number of effects. Of particular interest is the transformation that light energy undergoes like absorption and scattering. Absorption of light energy is when either atoms or molecules take up this light energy and move from one energy state to a higher energy state. When these aerosols absorb the sun energy, they undergo temperature inversions (at different wavelength from original), leading to earth warming. Scattering is when the incident light rays are diverted or deflected from their original direction to all directions without changing their wavelength (**Figure 1.1 a** and **b**).

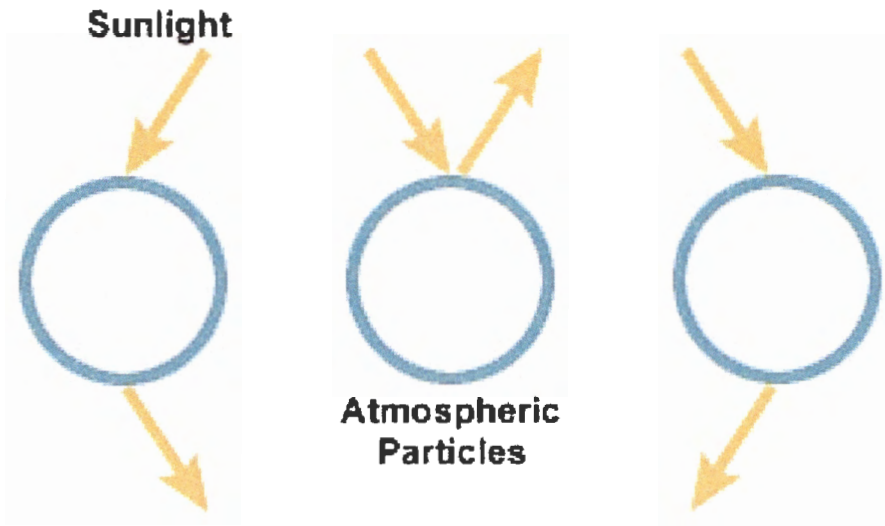

Figure 1.1a: How particles in the air scatter sunlight (source: Reyes, 1997)

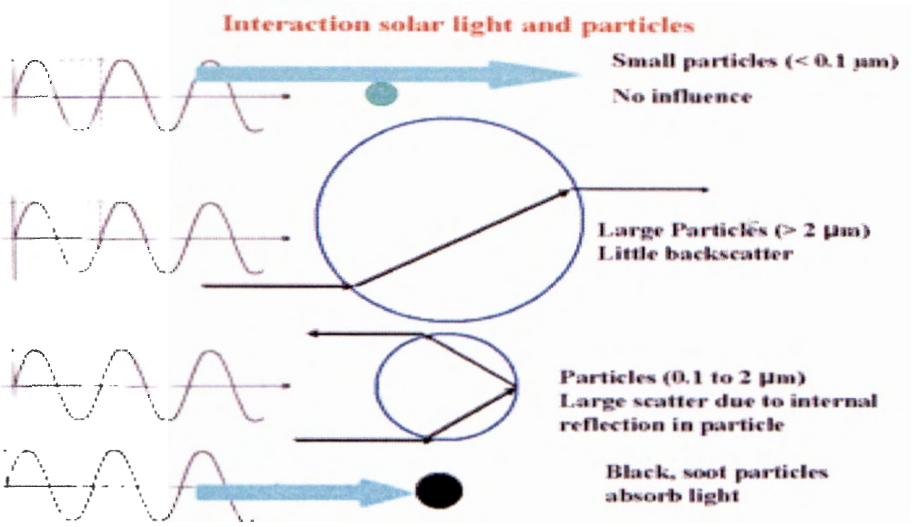

Figure 1.1b: Interaction of solar light and particles (source: Slanina, 2010)

The aerosols simply scatter the original sunlight without undergoing temperature inversions. The amount of scattering is determined by the size of the aerosols. The fraction amount of incident light energy that has passed through aerosols without being absorbed can be determined. If the incident light is denoted by I_o, passing through aerosols for a distance I, then

$$I=Ioe^{-\Omega I} \quad (1)$$

$$dI=-I\Omega dI$$

$$\text{or } dI=\sigma nIdI \quad (2)$$

where Ω and σ stand for absorption and the attenuation coefficient, respectively, and n is the concentration of aerosols. Rayleigh scattering takes place when the diameter of particulates being impinged is very small (<0.1 µm) in comparison to the wavelength (λ) of the incident light energy. This occurs mainly with molecules. Rayleigh scattering or molecular scattering is proportional to λ^{-4} (Şen, 2008; Agranovski, 2010; Sportisse, 2010; Hussein, 2011). If on the other hand, the diameter of particulates being impinged is similar in comparison to the wavelength (λ) of the incident light energy impinging it, the scattering taking place is referred to as Mie scattering. The single scatter albedo, φ, (a measure of the effectiveness of scattering relative to extinction for the light encountering

the atmospheric aerosol particles) is obtained by dividing the scattering coefficient by the extinction coefficient (Bergstrom et al., 2007; Dubovik, 1998; Panchenko et al., 2001)

$$\varphi(r, \lambda) = Q_s(r, \lambda)/Q_e(r, \lambda) \quad (3)$$

Where Q_s is the scattering efficiency; Q_e is the extinction coefficiency.
This helps in the characterisation of atmospheric aerosols. When the single scatter albedo is high, the scattering processes become more important in causing light attenuation. Integration of this extinction coefficient from the Earth's surface to the upper limit of the atmosphere gives the optical depth (OD):

$$\tau_e = \pi r^2 Q_e(r, \lambda) \quad (4)$$

where r is the radius of particulate. Thus the OD characterises the whole attenuation of solar radiation in a vertical atmosphere due the to presence of aerosols.

Light in the blue part of the spectrum is more intensely scattered than in the red part by atmospheric molecules, hence the appearance of a blue sky. On the other hand, sunsets and sunrises appear reddish because the shorter (blue) wavelengths in direct light are removed by scattering through the long path in the atmosphere, leaving the remaining reddish colours of the spectrum seen here in **Figure 1.2**.

Figure 1.2: Los Angeles in the haze at sunset (source: Chin et al., 2009)

Airborne particles undergo various physical and chemical interactions and transformations (atmospheric aging), that is, changes of particle size, structure and composition

(coagulation, restructuring, gas uptake, chemical reaction). Particularly efficient particle aging occurs in clouds, which are formed by condensation of water vapour on pre-existing aerosol particles (cloud condensation and ice nuclei, cloud condensation nucleus and ice nucleus). Most clouds re-evaporate, and modified aerosol particles are again released from the evaporating cloud droplets or ice crystals (cloud processing). If, however, the cloud particles form the precipitation which reaches the Earth's surface, not only the condensation nuclei but also other aerosol particles are scavenged on the way to the surface and removed from the atmosphere. This process, termed "wet deposition", is actually the main sink of atmospheric aerosol particles. Particle deposition without precipitation of hydrometeors (airborne water particles)—that is, "dry deposition" by convective transport, diffusion, and adhesion to the Earth's surface—is less important on a global scale, but is highly relevant with respect to local air quality, health effects (inhalation and deposition in the human respiratory tract), and the soiling of buildings and cultural monuments (Pöschl, 2005). Depending on aerosol properties and meteorological conditions, the characteristic residence times (life-times) of aerosol particles in the atmosphere range from hours to weeks.

Observations have shown that the composition of the atmosphere is changing on a global scale. This is because the atmosphere is the recipient of many of the products of our technological society. Eventually it becomes a 'reaction vessel' in the sense that the chemical fates of aerosols are often intertwined (Seinfeld and Pandis, 2006). Chemical and physical processes take place in the atmosphere and as a result the concentrations and lifetimes of aerosols get affected. The consequence of this is that the original aerosol becomes amplified or dampened. The temperature of the Earth adjusts so that solar energy reaching the Earth is balanced by that leaving the planet (Seinfeld and Pandis, 2006). This global heat engine, in its attempt to equalize temperatures generates climate. Air over the warm oceans absorbs water vapour and then travels to colder regions. The consequence of this is that transportation of aerosols from one place to another is enhanced.

1.3. Atmospheric Aerosols and Air Pollution

As atmospheric aerosols are suspended fine solid or liquid particles in a gas, it follows therefore that their accumulation in the air may lead to air pollution. These particles

include gases, dust, fumes and others. It is now known that particulates in the troposphere (lowest layer of the atmosphere) have residence times of a few days to a week, before they are removed by either settling down or precipitation. Within this period, when they are present in high concentrations, they become a hazard – a health threat.

1.3.1. Human Health

Accumulating evidence suggests that exposure to pollutants and chemicals could elevate the risk of cardiovascular disease; many epidemiological studies report that exposure to fine particles present in ambient air is associated with an increase in cardiovascular mortality - statistically significant relationships between particulate air pollution and ischemic heart disease, arrhythmias, and heart failure have been reported (Bhatnagar, 2006). Air pollution brought about by asbestos particulates is known to affect the lungs and cause asbestosis. Upon inhaling asbestos particles, they cause damage to tissues. The body orders the repair process which involves cell replacement, and tissue replacement. But where these, asbestos particulates cannot be got rid of, this process continues, leading to chronic myofibroblast activation and excessive accumulation of extracellular matrix (ECM) components, which promote the formation of a permanent fibrotic scar (Wynn, 2007) as seen in **Figure 1.3**.

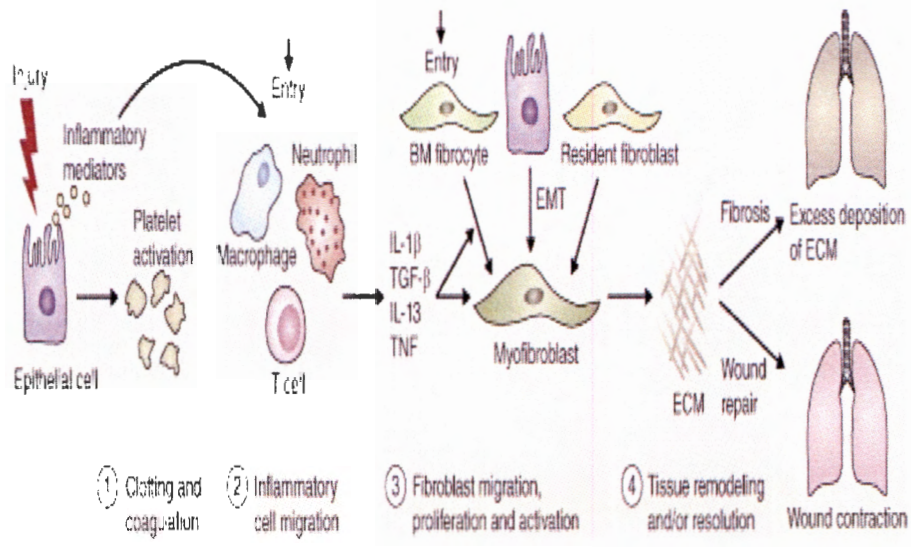

Figure 1.3: Disruptions in normal wound healing contribute to the development of pulmonary fibrosis. (Source: Wynn, 2011).

1.3.2 The Ecosystem

The production and emission of nitrogen oxides (NO_x) and sulphur dioxide (SO_2) causes what is known as "acid rain". This is formed when these gases dissolve in rain water or just get deposited on the earth's surface and eventually become "acid water" on contact with water. Acid rain has negative impact on vegetation, aquatic life as well as on building structures which become corroded. Acid rains have also been known to cause eutrophycation of water systems as a result of the eventual formation of nitrates. This has caused algae blooms in the water systems and depletion of oxygen much needed by aquatic life. A lot of fish and other organisms die for lack of oxygen. Ozone (O_3) on the other hand is a problem to both human health and plants. O_3 naturally occurrs in the stratosphere (upper atmosphere) where it protects life on earth from the sun's ultraviolet (UV) radiation. In the troposphere (lower atmosphere), it is formed by aerosol chemical reactions. This is what is toxic to living things. Aerosols also cause poor visibility. Objects are seen because they reflect sunlight to the observer. But when aerosols are present in the atmosphere, they attenuate the light reflected by the objects hence they appear dim. Smog and fog are all the result of the presence of atmospheric aerosols. Smog causes a smoky dark atmosphere which decreases visibility, and also forms a hazy appearance. It is formed when carbon monoxide, dirt, soot, dust, and ozone that are present as aerosols react with sunlight.

1.3.3 Aerosol Properties and Processes

A very good outline by Ghan and Schwartz (2007) is presented on the aerosol properties and processes. The climate influences of anthropogenic aerosols are very difficult to determine separately from the effects of natural aerosols using observations alone. Hence, these influences are most effectively determined from climate simulations, specifically by simulations with and without anthropogenic aerosols. Increasingly, it has become recognized that aerosols are highly interactive with other components of the climate system, for example, influencing and being influenced by clouds and precipitation. This recognition leads to a requirement for climate that intrinsically incorporates representation of the concentrations and properties of aerosol particles as a function of three-dimensional location and time. Such a representation, in turn, requires an understanding of the governing processes and the dependence of these processes on amounts and properties of particulate matter and gaseous precursors. Direct effects of

aerosols on the energy balance of the Earth depend on the optical properties of the aerosol, specifically the extinction coefficient σ_{ep}, the single scattering albedo ω_0 (a fraction of the extinction coefficient resulting from scattering), and the asymmetry parameter g (the mean of the cosine of the scattering angle). Aerosol indirect effects depend on the number concentration of Cloud condensation nuclei (CCN) as a function of supersaturation s, $N_{CCN}(s)$. These aerosol properties in principle are evaluated as integrals over the properties of the individual particles that comprise the aerosol. The single-particle properties are governed by the particle size and shape, by the properties of the different materials of which the particle is composed, and by the distribution of the materials within the particle. However, because representation of these aerosol properties in such detail is beyond the capability of present climate , as well as those of the foreseeable future, the challenge of climate modelling is to represent this complexity within the constraint of computational resources. This requires compromises and assumptions that accurately account for the most important effects of aerosols within the constraints of practical application.

Aerosol properties that must be accurately represented include mass concentration, particle size and size-dependent composition, optical properties, solubility, and the ability to serve as nuclei of cloud particles. Key processes that must be represented include the emission of primary particles (those emitted directly into the atmosphere), such as mineral dust, sea salt, black carbon, and organic carbon; the emission of aerosol precursor gases, such as Dimethylsulfide (DMS), sulfur dioxide, and volatile organic compounds (VOCs); the oxidation of precursor gases; new particle formation; reversible growth of particles by condensation of nonvolatile and semivolatile gases; coagulation; reversible uptake of water vapor; activation to form cloud droplets; in-cloud scavenging; aqueous-phase reactions in cloud droplets; subgrid vertical transport by clouds; cloud-drop evaporation; dry deposition to the surface; and scavenging by falling hydrometeors. Accurate representation of these processes in climate rests not only on understanding the pertinent processes, but also on developing efficient ways to represent them in large-scale numerical .

1.3.3.1 A Strategy

Because the treatment of aerosol properties and processes in the present Global climate model (GCMs) is highly simplified, opportunities for improving the treatment abound. Four stages in a strategy to represent aerosol processes in climate and examine aerosol influences on climate are summarized in **Table 1.1**. Stage 1 focuses on improving understanding of isolated processes. Stage 2 develops and evaluates modules representing these processes. Stage 3 evaluates the interaction of those modules in integrated aerosol . Once validated, the modules are incorporated within global climate in stage 4 and are again evaluated. At the end of this process the are available to examine the sensitivity of climate to different emissions scenarios.

Table 1.1: Stages of research and model development necessary to examine aerosol influences on climate.

Stage	Activity	Outcome
1	Conduct process research: field and laboratory studies	Improved understanding of processes
2	Develop O-D (modules) representing processes; comparison with process research studies	Modules: model-based representation of understanding
3	Incorporate modules describing aerosol processes in regional to global aerosol ; production runs; assessment of accuracy of aerosol	Evaluated aerosol model incorporating processes
4	Incorporate representation of aerosol processes in climate model; production runs; comparison with observations	Climate relevant runs; assessment of skill of climate model against present and/or prior climate

Field and laboratory studies provide the measurements on which the strategy is founded. These measurements are used to develop and evaluate models of individual processes and properties of aerosols and clouds (necessary for understanding aerosol indirect effects). The resulting suite of process and property are then integrated and evaluated in single-column, cloud-resolving, and regional-scale aerosol . Once validated for a variety of conditions, the aerosol modules are applied to global; here, issues of scale need to be addressed. After a global evaluation of the aerosol properties and processes, the models are coupled to models of the land surface, ocean, and sea ice, and the full climate model is applied to climate change simulations.

Many elements of this strategy have been advocated previously. Penner et al., (1994) and Seinfeld et al., (1996) focused on refining estimates of direct and indirect effects of all important aerosol types, calling for closure studies to evaluate the treatment

of specific aerosol processes and the evaluation of integrated aerosol models using a combination of surface and aircraft observations and satellite remote sensing. The U.S. Department of Energy (DOE 2001) proposed a Tropospheric Aerosol Program that combined laboratory studies, surface and aircraft measurements, and modelling to improve the understanding and representation of aerosol formation, transformation, properties, and removal. Ramanathan et al. (2002) proposed a National Aerosol–Climate Interactions Program that would use new aircraft and satellite measurements to improve estimates of primary emissions, aerosol effects on clouds and precipitation, and direct and indirect effects of aerosols, with an emphasis on black carbon. In the strategic plan for the U.S. Climate Change Science Program, Mahoney et al., (2003) called for expanded laboratory, surface, airborne, and satellite studies to better characterize aerosol properties and processes and to evaluate and improve their representation in integrated aerosol and climate . Diner et al., (2004) and Ackerman et al., (2004) proposed PARAGON, which would integrate data from a variety of aerosol measurement platforms into a global modelling framework.

Elements of this strategy have been supported by several U.S. agencies. NASA has deployed a suite of aerosol remote sensing instruments (SAGE, TOMS, MODIS, MISR, OMI, CALIOP) on multiple satellite platforms (*Aqua, Terra,* CALIPSO), and NOAA has provided aerosol retrievals from its AVHRR satellite instruments. NASA, NOAA, NSF, and DOE have conducted several large-scale field projects, and notable among them are ACE-1, in the vicinity of Tasmania in 1995 (Bates et al., 1998), ACE-2, in the eastern North Atlantic in 1997 (Raes et al., 2000), and ACE-Asia, in eastern Asia and the western North Pacific in 2001 (Huebert et al., 2003); SCAR-B (Kaufman et al., 1998); TARFOX, over the western North Atlantic in 1996 (Russell et al., 1999); INDOEX in 1999 (Ramanathan et al., 2001); TRACE-P in 2001 (Jacob et al., 2003); ICARTT, in northeastern North America and over the North Atlantic in 2004; and the recent MILAGRO project in and downwind of Mexico City, Mexico, in 2006. Projects such as these have provided in situ measurements and remote sensing retrievals to characterize aerosol properties, improve understanding of aerosol processes, and evaluate aerosol process and integrated . Several of these projects have been greatly augmented by international collaboration coordinated through programs such as the WCRP, IGBP, and IGAC. Model

evaluations have been coordinated by the IPCC (Penner et al., 2001, 2002) and the AeroCom project (Kinne et al., 2006).

In parallel with the above work, focusing mainly on climate-related influences of aerosols, much work has focused on the influences of aerosols on air quality. Much work is directly pertinent to the climate influences of aerosols, in the characterization of both aerosol properties and evolution, and more specifically in characterization of aerosol influences on visibility, which is closely related to aerosol direct effects on climate. In the United States much work is supported by the EPA and IMPROVE (Malm et al., 2004). Important contributions from the EPA include laboratory studies of gas-to-particle conversion, the treatment of changes in particle size distribution, estimation of emissions of particulate matter and gaseous precursors, and development of models of transport and transformation of aerosols pertinent to their influence on air quality.

The U.S. Department of Energy (DOE) supports three closely linked research programs that contribute to the improvement of the representation of aerosol properties and processes in GCMs: the ASP, ARM, and CCPP. Each program plays an essential role in the DOE strategy to improve the accuracy and predictive capability of large-scale climate models. ASP and ARM provide field and laboratory measurements that guide the development of models of specific aerosol properties and processes. The ASP has an explicit charge to improve the understanding of chemical, microphysical, optical, and cloud-nucleating properties of aerosol particles and of the processes that control those properties, and to develop numerical models of these processes that are suitable for inclusion in large-scale models. ARM has a broad mission of understanding and quantifying the atmospheric processes and properties that influence radiation, including both direct and indirect aerosol effects, and of developing and evaluating process models. The CCPP supports the application of process models as modules in GCMs so that the influence of anthropogenic aerosol on climate can be quantified in the context of climate change over the industrial period.

1.3.3.2 Generations of Climate

Climate model studies over the past 10 years have shown that aerosol forcing must be represented in climate models in order for these models to accurately represent

temperature change over the industrial period. Early approaches to such representation simply adjusted surface albedo to crudely account for the enhancement of planetary albedo resulting from tropospheric aerosol (Mitchell et al., 1995; Boer et al.,2000; Delworth and Knutson 2000). Subsequently, many models have treated direct effects of aerosol particles using three-dimensional distributions from "offline" simulations with chemical transport models (e.g., Meehl et al., 2003; Delworth et al., 2006; Collins et al., 2006; Meehl et al., 2006). Some GCMs have actively represented certain aerosol components (usually sulfate) and processes (e.g., Stott et al., 2000; Tett et al., 2002; Hansen et al., 2005; Schmidt et al., 2006). It is now recognized that accurate representation of aerosol influences must take into account phenomena such as correlations of aerosol loading with meteorological variables and the influence of aerosol on clouds and precipitation, and hence that aerosol loading and those properties must be represented actively and interactively in climate models. It is this recognition that is driving much of the current effort to actively represent aerosol processes, properties, and effects in climate models.

Much of the practice of climate modelling has become tied to the production schedules for periodic international assessments of the science of climate change by the IPCC. AR4 will be based on simulations completed in 2004 using models that were frozen in 2003. Because these assessments are prepared roughly every 6 years, it may be anticipated that AR5 will be based on climate simulations completed in about 2010 using frozen using about 2009. Likewise, AR6 will be based on frozen roughly in 2015. Each IPCC assessment report is therefore based on a successive generation of climate models, with the timing of the model development and application to some extent being governed by the timing of the assessment process. Although climate modelling predates IPCC assessments by many years, recent generations of climate can be identified by the IPCC report to which they contribute. Thus, it can be said that the fourth generation of climate models contributed to the preparation of AR4.

Inevitably, there is a lag from gaining understanding of processes to representing that understanding in climate models, and this holds true for aerosol processes. Thus, there is a lag from understanding aerosol processes, as represented in zero-dimensional models (box models), to representing this understanding in integrated aerosol models;

and there is a further lag in representing this understanding in GCMs that are used in IPCC assessments, which can be as long as a full IPCC cycle or more. There is a further, similar lag of a full IPCC cycle between the representation of aerosol (or other) processes in GCMs and the use of the results of that generation of models in scenario assessments.

The treatment of aerosols in future generations of climate models will rest on an improved understanding of the processes that control aerosol properties and their evolution as gained in laboratory and field studies carried out in research supported by the DOE ASP and ARM programs, as well as by studies conducted with the support of other U.S. and international agencies. These studies in turn rest on developments in instruments and measurement capabilities to characterize aerosol properties.

Future enhancements will rest also on advances in representing the pertinent aerosol processes in models. Such model development progresses through a hierarchy of approaches. Initially, a subset of aerosol processes is represented in zero dimensions or, for cloud processes, in one (vertical) dimension. These representations are then commonly incorporated into models that are driven by analyzed meteorological data to allow the representation of these processes to be evaluated by comparison with observations at specific locations and times. These process models subsequently become incorporated as modules in integrated aerosol models that are further tested and evaluated. Ultimately these representations become incorporated in climate models. Because climate models must be run for much greater times than is typical for aerosol models, the ability to include aerosol processes will require accurate and efficient representation of aerosol processes and will rest as well on advances in computational hardware and architecture. It is thus clear that representing aerosol influences on climate, at present and for the foreseeable future, will require a suite of approaches.

The incorporation of these approaches in present and future generations of climate models is outlined below, together with examples of research needed to support the development and testing of these new approaches. Aerosol properties that need to be represented in climate models to simulate aerosol influences on climate are presented in **Table 1.2**, together with approaches to model these properties in each model generation. The approaches representing aerosol processes are given in **Table 1.3**.

1.3.3.3 Aerosols in Fourth-Generation Climate Models

The summaries of treatments of aerosol properties and processes in fourth generation climate models presented in **Tables 1.2** and **1.3** are based largely on the three U.S. climate models that participated in AR4: the National Center for Atmospheric Research CCSM3 (Collins et al., 2006; Barth et al., 2000), the Geophysical Fluid Dynamics Laboratory CM2.1 (Delworth et al., 2006; Ginoux et al., 2006; Tie et al., 2005; Horowitz 2006), and the Goddard Institute.

Table 1.2: Treatment of aerosol properties in fourth-, fifth-, and sixth-generation climate .

	Treatment		
Property	Fourth generation	Fifth generation	Sixth generation
Mass concentration and composition	Sulfate interactive (online) with climate model dust, sea salt, hydrophilic and hydrophobic OC and BC prescribed from offline aerosol model simulations	Interactive sulfate, dust, sea salt, hydrophilic and hydrophobic OC, BC, nitrate, ammonia	Interactive sulfate, dust, sea salt, hydrophilic and hydrophobic OC, BC, nitrate, ammonia
Size distribution	Prescribed for each aerosol type except dust; multiple sizes for dust and perhaps sea salt	Variable for each aerosol type (modal)	Variable (sectional, QMOM, or piecewise log-normal)
Mixing state	External	Internal and external mixtures	Internal and external mixtures
Mixing state	Prescribed	Volume average	Volume average treatment of inclusions
Optical properties	Prescribed, for each aerosol type; function of RH	Parameterized in terms of bulk refractive index and wet effective radius	Parameterized in terms of bulk refractive index and wet effective radius
Hygroscopicity	Prescribed	Volume average	Thermodynamic equilibrium
CCN spectrum	Empirical	Köhler theory for external mixtures of internally mixed inorganic and soluble organic salts	Köhler theory for external mixtures of internally mixed inorganic and soluble organic salts plus weakly soluble organics and surfactants

for Space Studies Model-E (Hansen et al., 2005; Schmidt et al., 2006). Although the treatment of aerosols differs somewhat from model to model, for most aerosol properties and processes the differences among models within a given generation of climate models are considerably less than the differences between successive generations.

Most of the important substances that comprise the condensed phase of the aerosol [sulfates, hydrophilic (soluble) and hydrophobic (insoluble) OC, hydrophilic and hydrophobic BC, mineral dust, and sea salt] are treated in fourth-generation climate models. Sulfate chemistry is embedded in the climate models, but concentrations of most other aerosol species are prescribed from offline simulations with global aerosol models.

Table 1.3: Treatment of aerosol processes in fourth-, fifth-, and sixth-generation climate .

	Treatment		
Process	Fourth generation	Fifth generation	Sixth generation
Primary emissions	Prescribed for all species	Sea salt, dust emissions depend on wind speed in host model; also on soil moisture for dust	Sea salt, dust emissions depend on wind speed in host model; also on soil moisture for dust; emission from fires depends on area burned, fuel load, burning efficiency, and emissions factors for each species.
Precursor emissions	Prescribed for all precursor gases	DMS emissions depend on wind speed in host model	DMS emissions depend on wind speed and ocean chemistry in host model
Oxidation of precursors	Reaction of SO_2, DMS with prescribed oxidant concentrations Instantaneous oxidation of VOC with prescribed yield	Reaction of all precursors with oxidants whose concentrations are calculated in the model Multiple hydrocarbon groups Dependence of yield on total organic aerosol	New hydrocarbon treatment
New particle formation	Neglected	Binary homogeneous nucleation	Ternary nucleation ammonia, organics
Condensation of oxidized precursor gases	Instantaneous condensation	Size-dependent mass transfer treatment	Size-dependent mass transfer treatment
Coagulation	Neglected	Brownian coagulation within and between modes	Brownian coagulation within and between modes
Evolution of hygroscopicity of BC, OC and dust ("aging")	Prescribed hydrophobic-tohydrophilic conversion time for BC and OC, neglected for dust	Separate treatment of coagulation and condensation effects for BC and OC, condensation effects for dust	Separate treatment of coagulation, condensation, surface chemistry effects
Water uptake	For external mixtures only; no hysteresis in most models; equilibrium	Internal and external; hysteresis treated	Kinetic effects
Aerosol activation	Prescribed number activated	Maximum supersaturation and number activated parameterized in terms of updraft velocity and external mixtures of internally mixed inorganic and soluble	Kinetic effects; activation to ice crystal

		organic salts.	
Aqueous phase reactions in clouds	Bulk treatment (same for all cloud droplets) pH dependence for prescribed ratio of ammonia/sulfate; poorly constrained cumulus cloud fraction	Bulk treatment (same for all cloud droplets); pH dependence for variable ratio of ammonia/sulfate; physically based stratiform and cumulus cloud fraction	Size-dependent cloud drop composition; reactions in hydrated aerosol
Convective transport and removal	Cumulus parameterization Poorly constrained precipitating area	Cumulus parameterization with physically based precipitating area	Statistics from embedded cloud
In-cloud scavenging	Autoconversion and precipitation rate independent of aerosol Cloud-borne aerosol equals activated aerosol	Autoconversion and precipitation rates depend on aerosol Influence of collision/coalescence on cloud drop number concentration and cloud-borne aerosol; subgrid variability in autoconversion	Statistics from embedded cloud models with microphysics dependent on aerosol scavenging by ice crystals
Subcloud scavenging	Prescribed scavenging efficiency	Size-dependent collection efficiency	Aerosol from evaporated raindrops; precipitation statistics from embedded cloud

Inevitably, this approach for the other species is a compromise, because it does not account for correlations between climatic variables affecting aerosol influences (such as cloudiness) and the concentrations of these species, and further because it does not account for aerosol influences on, for example, the hydrological cycle, which can further influence the concentrations and properties of aerosol particles. The size distribution is prescribed for each aerosol species, so that only the mass concentration of each species is simulated. The aerosol is assumed to be externally mixed, that is, consisting of particles composed wholly of one or another substance, as opposed to individual particles consisting of a mixture of multiple substances. This latter assumption greatly simplifies the representation of aerosol optical properties (absorption coefficient, scattering coefficient, and asymmetry parameter) and their dependence on relative humidity. Optical properties of aerosol particles depend to first order on the refractive index and particle size, and to a lesser extent on particle shape. With the assumption of a prescribed size distribution, and particle shape and composition for each aerosol type, the refractive index and the optical properties and their dependence on relative humidity can be prescribed for each aerosol type; however, this approach cannot account for variability in these properties for a given aerosol type that arises from differences in particle size distribution, particle shape, or

composition. The CCN spectrum NCCN(s), which is the concentration of aerosol particles that can nucleate cloud droplets as a function of supersaturation with respect to water, is either ignored or treated using empirical relationships that are suitable at best only for externally mixed aerosols.

Representation of aerosol processes in fourth generation climate models is highly simplified. Emissions of primary particulate matter and of gaseous precursors of secondary particulate matter are prescribed, rather than treated as being dependent on climate model variables such as wind speed and soil moisture. Concentrations of oxidant species OH, O_3, and H_2O_2, responsible for the conversion of SO_2 and DMS to sulfates, are likewise prescribed, typically at monthly mean values, rather than being generated in the model. In most models VOCs are instantaneously oxidized with a uniform prescribed yield. New particle formation and coagulation are not treated because these processes do not affect aerosol properties when the particle size distribution is prescribed. Condensation of the oxidized precursor gases on particles is assumed to occur instantaneously. If OC and BC are treated as distinct hydrophobic and hydrophilic components, the aging from hydrophobic to hydrophilic is treated using a uniform prescribed conversion time. Aging of dust is neglected. The water content of particles is assumed to be governed by thermodynamic equilibrium with relative humidity, with hysteresis (dependence of the hydration state on the history of its environmental relative humidity) neglected in most models by assuming that particles are always hydrated at humidities above a specified efflorescence point. Aerosol activation is treated by assuming that a prescribed mass fraction of each aerosol type (typically 100% for sulfates, sea salt, and hydrophilic OC and BC, and 0% for dust and hydrophobic OC and BC) forms droplets in clouds, with empirical expressions relating cloud-drop number concentration to mass concentration. A bulk treatment of aqueous-phase chemistry is used, in which oxidation of dissolved SO_2 in cloud droplets is independent of droplet size but depends on droplet pH, with pH diagnosed assuming a prescribed ratio of ammonia to sulfate; cloud properties for chemistry calculations are provided by the host GCM. Vertical transport and removal of aerosol by cumulus clouds is treated using cumulus parameterizations with poorly constrained estimates of precipitation area. In- and below-cloud scavenging are treated using precipitation rates that are not influenced by the aerosol; treatment of cloud scavenging assumes complete of the activated aerosol in clouds.

1.3.3.4 Aerosols in Fifth-Generation Climate Models

Aerosol properties and processes in fifth-generation models will be much more complete than in fourth generation models and is increasingly based on understanding of the pertinent processes. More processes will be represented, and in greater detail. With few exceptions, the advances will build on the current generation of global aerosol models (e.g., Easter et al., 2004; Tie et al., 2005; Koch et al., 2006). Because many aspects of the global aerosol models have already been evaluated in comparisons with observations (Ghan et al., 2001a,b; Easter et al., 2004; Tie et al., 2005; Kinne et al., 2006; Koch et al., 2006; Bates et al., 2006), much of the effort involved in upgrading the aerosol treatment in fifth-generation climate will involve transferring the treatments from the global aerosol models to the global climate models. Within the DOE program this component of the work is carried out largely in the Climate Change Prediction Program. Previous work in the ARM program, which produced treatments of aerosol impacts on clouds (Ghan et al., 1997; Ovtchinnikov and Ghan 2005; Liu et al., 2005) and parameterizations of aerosol radiative properties (Ghan et al., 2001a), will have an impact on the fifth generation models. The ASP provides field measurements and uses them to evaluate specific processes represented in the models.

Aerosol properties for the fifth generation of climate models will have numerous additional degrees of freedom. New species to be included in the models will include nitrate and ammonia/ammonium, and all aerosol species will be simulated online rather than offline, so that concentrations will vary on hourly rather than monthly time scales and will interact with the meteorology that is simulated in the model. The aerosol particle size distribution will be calculated rather than prescribed. Several different methods (modal, quadrature method of moments, and sectional) are available for representing the particle size distribution and composition and their evolution. The simplest modal method (Whitby and McMurry, 1997; Easter et al., 2004; Liu et al., 2005) assumes a lognormal size distribution for each aerosol type and calculates its number and mass concentration from separate conservation equations. The QMOM (McGraw 1997; Wright et al., 2001; Yoon and McGraw 2004a,b) is more general in that it does not assume a lognormal size distribution; aerosol properties and their evolution are calculated from the moments of the particle size distribution by Gaussian quadratures.

The sectional method (Adams and Seinfeld 2002) is most general because the size distribution is explicitly represented, but it requires extensive computational resources in storing, evolving, and transporting large numbers of variables. For this reason the modal method and QMOM are most likely candidates for fifth-generation models. Representation of the aerosol mixing state will accommodate a combination of external and internal mixing so that particles forming by condensation will be capable of being internally mixed with primary particles and/or freshly nucleated particles. Two forms of hydrophobic BC and OC will be treated; one is purely hydrophobic, and the other is internally mixed with sulfates, nitrates, and ammonium. Aging of BC and OC will be expressed in terms of the condensation and coagulation rates, so that fresh BC and OC masses and numbers are transferred to the internally mixed aerosol. Although treating internal mixing can reduce the number of aerosol types, it complicates the representation of optical properties, hygroscopicity, and CCN activity because, as is the case with actual ambient aerosol particles, those properties depend on the now-variable composition. Fifth-generation models will accommodate internal mixing by using mixing rules for refractive index and hygroscopicity pertinent to particle growth with relative humidity and CCN activity. Other mixing rules may be used to represent the optical effects of the inclusion of insoluble material in particles consisting largely of water-soluble material.

Consistent with the online representation of aerosol properties, emissions of DMS, sea salt, and dust will be calculated online using the simulated winds and (for dust) surface moisture and vegetation cover. Likewise, oxidation of aerosol precursor gases will be calculated using oxidant concentrations that are generated online by a gas-phase oxidant chemistry module. VOCs will be separated into multiple classes; the yield of new particulate mass will depend on the total amount of organic aerosol (Chung and Seinfeld 2002; Tie et al., 2005). New particle formation will be introduced as a source of aerosol number, probably using a parameterization of binary nucleation of water and sulfuric acid vapor (Jaecker-Voirol and Mirabel 1989; Harrington and Kreidenweiss 1998; Vehkamäki et al., 2002). Condensation of oxidized precursor gases on existing aerosol particles will be treated using mass transfer theory, so that condensation can be distributed across multiple aerosol types. Coagulation of particles both within each type (which reduces number and increases mean size) and between types will be represented to accurately represent particle number concentration. Dust will age as condensation of sulfuric acid

and secondary organic material onto dust modes changes the bulk hygroscopicity and refractive index of each mode.

Uptake of water by particles will be represented in terms of the bulk hygroscopicity using Köhler theory, with explicit treatment of hysteresis so that dry and hydrated aerosol states are distinguished. Activation of aerosol particles to form cloud droplets will be expressed in terms of updraft velocity and the aerosol particle properties (number, size, and hygroscopicity) for all types (Abdul-Razzak and Ghan 2000; Fountoukis and Nenes 2005), so that aerosol indirect effects and the competition between aerosol types can be treated in a physically based manner. Aqueous chemistry will depend on the pH, calculated from the ratio of sulfate to ammonia, which will be allowed to vary. The cloud fraction will be determined using physically based parameterizations. Convective transport and the removal of aerosol will be improved by using new cumulus parameterizations that diagnose precipitating area and treat cloud microphysics. In-cloud scavenging will be based on the concentrations of the activated particles and will treat the dependence of precipitation development on the number activated. Belowcloud scavenging will use size-dependent collection efficiencies.

In sum, much more detailed representation of aerosol processes and properties is expected in the fifth generation of climate models than in earlier generations. Representation of each of these processes rests on improved understanding of the processes themselves and on improved ability to efficiently and accurately represent this understanding in models, both of which are expected to be greatly advanced by ongoing research.

1.3.3.5 Aerosols in Sixth-Generation Climate

Although it is difficult to anticipate the treatment of aerosol processes in the sixth generation of climate so far out into the future, it is clear that this treatment will rely on advances in understanding provided by programs such as the ASP and ARM. For example, recent work has shown that current understanding of the formation of SOA leads to substantial underestimates in the simulated concentrations of OC (Heald et al., 2005; Volkamer et al., 2006). Laboratory and field experiments will provide the foundation for a new generation of models of SOA formation. The challenge will be to condense that

understanding into process models that are simple enough to be used in global climate simulations, but at the same time provide accurate representation of the process.

It is known from field studies that current models based on binary homogeneous nucleation of sulfuric acid and water yield new particle formation rates that are often far smaller than the measured rate (Weber et al., 1999). In such cases new particle formation rates may be better explained by either ternary homogeneous nucleation of sulfuric acid, ammonia, and water (Napari et al., 2002a,b); of sulfuric acid, organic acid, and water (Jimenez et al., 2003; Zhang et al., 2004); or ion-induced nucleation of sulfuric acid and water (Lee et al., 2003; Lovejoy et al., 2004). Laboratory data for multiple precursor gases can be accurately parameterized by the nucleation theorem (McGraw and Wu 2003; McGraw 2005), but further work is needed to account for the influence of background aerosol on the nucleation rate and subsequent particle growth by condensation and coagulation (McMurry et al., 2005). These parameterizations also need to be evaluated and refined using field measurements and, depending on the outcome, incorporated into the sixth-generation models. It seems clear that treatment of subgrid variability will also be required because the nucleation rate is a highly nonlinear function of the precursor gas concentrations. For these reasons much attention needs to be paid to issues of scale.

Representing aerosol particle size distributions and size-dependent composition is essential. Because explicit representation would seem not to be computationally feasible in climate models, alternative approaches must be investigated. Although representation of the particle size distribution by the modal approach is capable of efficiently representing multiple aerosol types under many conditions (Whitby 1978), the inherent assumption of a lognormal size distribution for each mode can break down. For example, aerosol activation in cloud updrafts typically separates the size distribution into activated particles and particles too small to be activated. The resultant discontinuities in the size distributions of the activated and unactivated particles are not well approximated by lognormal functions (Hoppel et al., 1990, 1994; Zhang et al., 2002). Possible solutions to this problem are provided by the more general and more accurate sectional, QMOM, and piecewise lognormal (von Salzen, 2005) treatments, with differing computational burdens. The ASP and CCPP can contribute to the comparison and testing of these and other potential approaches.

Uptake of water exerts an important and sometimes dominant influence on aerosol particle optical properties. Although the equilibrium Köhler treatment seems appropriate for submicrometer particles, this approach may not work for larger particles, for which the change in particle size may lag changes in relative humidity. Such kinetic effects might be treated by an explicit dynamic form of the Köhler theory. Although this treatment is straightforward for parcel models in which the time dependence of the ambient relative humidity is known, extending it to the Eulerian framework of climate models will require alternate approaches, such as using the turbulence kinetic energy and the vertical gradient of relative humidity.

1.3.4 The Effect of Atmospheric Aerosols on Climate

The emission of atmospheric aerosols into the environment does two things. The first is that aerosols in the atmosphere affect the intensity of sunlight scattered back to space. Scattering of radiation causes a cooling effect (they reflect and scatter solar radiation, slightly reducing the amount that reaches the surface – positive effect), altering the weather and climate. Scattering occurs because the index of refraction of the particles differs from that of the homogeneous medium in which they are imbedded (Houghton, 1985). Although the frequency of the scattered radiation does not change, its phase and polarization may change substantially from those of the incident radiation.

The second is that, aerosols affect the solar irradiance absorbed in the atmosphere that arrives at the earth's surface. Absorption of radiation causes local heating of the earth's atmosphere.

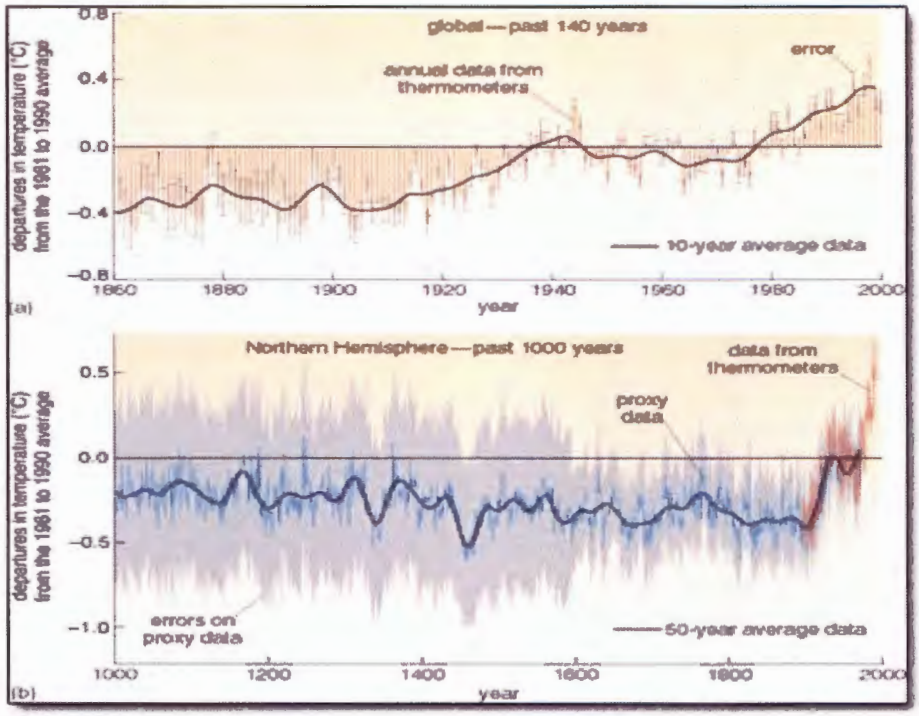

Figure 1.4: Shows deviations in mean surface temperatures from recent average temperatures for two time periods. The first (**Figure 1.4a – upper section**) shows changes in the *global* mean annual surface temperature since 1860. The second (**Figure 1.4b – lower section**) covers the last 1000 years for the Northern Hemisphere (source: OpenLearn, 2012).

As this happens, the stratosphere is locally heated by the absorption of aerosols that can generate winds and temperature inversions.

The effect of sunlight by aerosols is what is called aerosol radiative forcing (RF). Climate change due to atmospheric aerosols is largely dependent on their optical properties. These properties are discussed already in the preceding section. Climate change has an impact on natural phenomena like storms, floods, droughts, melting of ice masses and so on. Human health is affected as well. Many people suffer from heat strokes as a result of heat waves, and some die from extreme cold temperatures. Association between temperature and mortality suggests that climate change as a result of global warming may lead to a reduction in excess winter deaths in the future (Langford and Bentham, 1993). It is established that malaria is distributed during elevated

temperatures whereas viruses like those of flu are transmitted at low temperatures. It means therefore that climate change may influence the distribution of these vector organisms. Agriculture is one other area mostly affected by climate change; some regions have a boost in agricultural production whereas others experience the opposite. This may result in more land being available in some areas, for example, as a result of the melting away of snow, or less land being available as a result of floods. In one scientific study it was estimated that there could be a rise in sea level of about 8cm to as high as 29cm by the year 2070 (Warrick and Oerlemans, 1990). This climate change may be brought about by the fact that atmospheric aerosols absorb and scatter (direct effect) sun energy (solar irradiance). Clouds on the other hand, can also modify sun energy as it passes through towards the earth's surface (indirect effect). Global warming, for instance, is linked to the absorption of sun energy by atmospheric aerosols in the form of black carbon and other greenhouse gases etc. When climate changes, the ecosystem structure is affected and, in turn may also change. Because species respond differently to climatic change, some will increase in abundance while others will decrease (Melillo et al., 1990)

Rain is dependent on clouds. Aerosols influence cloud properties through their role as cloud condensation nuclei (CCN) and or ice nuclei (Chin et al., 2009). Chin and his coworkers stated that increases in aerosol particle concentrations may increase the ambient concentration of CCN and ice nuclei, affecting cloud properties. A CCN increase can lead to more cloud droplets so that, for fixed cloud liquid water content, the cloud droplet size will decrease. This effect leads to brighter clouds (the "cloud albedo effect"). Aerosols can also affect clouds by absorbing solar energy and altering the environment in which the cloud develops, thus changing cloud properties without actually serving as CCN. Such effects can change precipitation patterns as well as cloud extent and optical properties. The presence of sulphur dioxide (SO_2) and nitrogen oxides (NO_x) in the atmosphere causes these substances to react with rain water to produce their acids (acid rain). In turn, these acids affect the ecosystem when they react with carbonate-rich soils and release carbon dioxide (CO_2) into the atmosphere. **Figure 1.5** shows the interactions and effects of aerosols in the atmosphere.

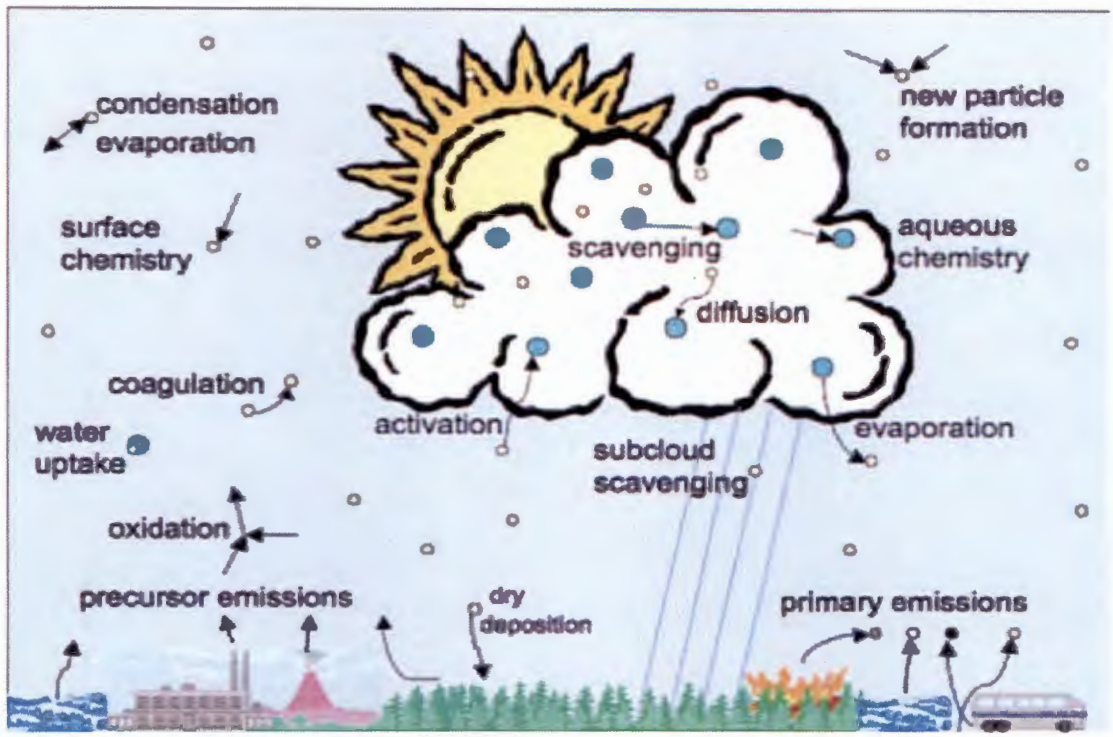

Figure 1.5: Interactions and effects of atmospheric aerosols (source: Ghan & Schwart, 2007).

Summing up the problem statement, a small positive note on aerosols is that cloud formation is dependent upon the presence of small amounts of aerosols such as sea salt and desert dust (Weizmann Institute of Science, 2007). It is proposed that particulates in the atmospheric aerosols offer a platform (seeds) upon which water vapour in the air condenses, thus forming tiny water droplets that rise up as they lose heat. These join together as they collide to form larger water droplets. But when they become too heavy, they fall down as rain. However, particulate matter contributes significantly to the climatic changes. In the topmost sphere of the earth (stratosphere), particulates like chemicals from volcanic eruptions have residence times of over one year. Their accumulation therefore has much impact on climatic changes. Although some passed legislations have been able to cut down on certain particulates like chlorofluorocarbons (CFC's), there still exists those that impact on temperature changes, as well as visibility, rainfall and many other effects.

1.4. PROBLEM STATEMENT

Aerosol production can never be stopped as long as both anthropogenic and natural processes take place. Anthropogenic-generated atmospheric aerosols have

various emission sources. The major emissions come from a variety of industrial processes. Amongst them is mining activities which are of interest in this study. Other anthropogenic emission sources include hospital incinerations, burning of fuels both commercial and domestic, transport, agricultural and others. Emissions from non-anthropogenic sources are quite diverse as well. Some emissions arise as a result of raised dust particles during wind storms, volcanic eruptions, sea sprays and wild fires.

Literature shows that atmospheric aerosols lead to air pollution and thus continues to threaten public health. Despite this, to my knowledge, nothing much has been done with regard to research into atmospheric aerosols in the actively industrial-developing mining areas of Rustenburg and Klerksdorp in the North-West Province of South Africa. This research aims to fill in this gap by collecting and documenting this data so that the short term and long term mitigation steps could be taken by relevant stakeholders.

1.5 OBJECTIVES

The general objective of the study is to collect and analyse atmospheric aerosol data in the mining areas of Rustenburg and Klerksdorp in the North West Province. Mining activities produce toxic metals like mercury (Roulet et al., 1999) and so it is important to establish the contribution of particulate matter in the atmosphere.

The specific objectives of this study are as follows:

a) To determine the concentrations and nature of aerosols in the atmosphere at various meteorological conditions;
b) To determine the optical depth of atmospheric aerosols for analysis of their presence; and
c) To determine trace metals which are present in the aerosols and are hazardous to the respiratory system.

CHAPTER 2

LITERATURE REVIEW

2.1 ATMOSPHERIC AEROSOLS

Atmospheric aerosols are attributed to the causation of various diseases and air quality degradation and yet their production can never be stopped as long as both anthropogenic and natural processes take place. Aerosols have been in existence since volcanic eruptions, forest fires, vegetative emissions, sea sprays, dust storms and since the existence of meteorological conditions namely wind speed and temperature patterns. When a volcano erupts (**Figure 2.1**) due to high temperatures inside the earth, large amounts of gases and dust, as well as moisture, is released into the air. The most abundant gas typically released into the atmosphere from volcanic systems is water vapour (H_2O) followed by carbon dioxde (CO_2) and sulphur dioxide (SO_2); other chemical gases include hydrogen sulphide (H_2S), hydrogen (H_2), carbon monoxide (CO), hydrogen chloride (HCl), hydrogen fluoride (HF), and helium (He) (USGS, 2010).

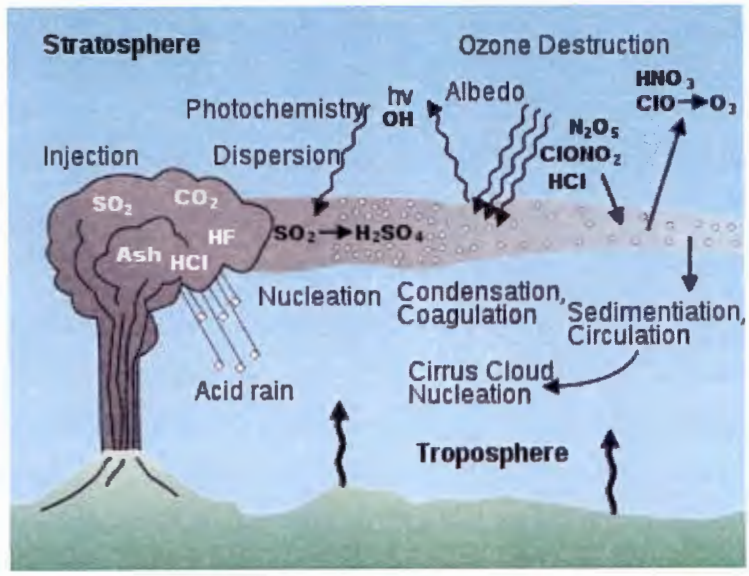

Figure 2.1: Aerosols from a volcanic eruption (source: Turco, 1992)

Volcanoes, sea sprays and wild fires are the natural sources of chemical atmospheric aerosols. Volcanic eruptions can cause great changes to the earth's atmosphere. This is

because they emit huge quantities of volcanic ash into the atmosphere, resulting in poor visibility (**Figures 2.2, 2.3**).

Figure 2.2: Volcanic Ash Emissions Telica, Nicaragua – 2000
(Source: Chemclouds, 2001)

Figure 2.3: Guagua Pichincha, Ecuador – 1999
(Source: Chemclouds, 2001)

Ash from very large eruptions can stay in the atmosphere for months to a few years, and can be transported around the globe (Windows to the Universe, 2011). Although these volcanic eruptions have the bad effect of causing poor air quality (**Figure 2.4**), they do however contribute to the cooling of the atmospheric temperatures.

Figure 2.4: Ashfall Visibility - Mount Spurr, Alaska – 1992
(Source: Chemclouds, 2001)

Wild fires are another source of natural emission of atmospheric aerosols. Smoke from wild fires mainly consists of black carbon known as soot. Smoke can also contain other chemical particulates (from trapped animals and other substances that may be in the area) like nitrogen oxides (NO_x), sulphur dioxide (SO_2). Other substances that could be present are Na, Mg, Al, Cl, K, Ca, Sc, Ti, V, Cr, Mn, Fe, Co, Ni, Cu, Zn, Ga, As, Se, Br, Rb, Sr, Mo, Ag,Cd, In, Sn, Sb, I, Cs, Ba, La, Ce, Sm, Eu, Lu, W, Au, Th (Andreae, Andreae et al., 1998). New knowledge has surfaced that vegetation does emit atmospheric aerosols. These aerosols, secondary organic aerosol (SOA), particles formed from volatile compounds emitted by vegetation, are key players in new particle formation processes. Hence, terrestrial vegetation has an important role as the newly formed particles cool our climate (Virtanen et al., 2010). The new findings will change many features of the understanding of particle behaviour in the atmosphere as the physical state of the particles influences their ability to absorb and release water and other gaseous compounds, as well as their ability to act as cloud or ice nuclei (Virtanen et al., 2010).

Sea sprays generate aerosols as a result of certain physical phenomenon. For example, wind force on the ocean surface is the cause of increasing concentration of airborne salt (Blanchard and Woodcock, 1957; ARM Climate Research Facility, 2011), the breaking of

waves induced by the stress of wind on the sea surface. Thus, primary marine aerosol becomes the principal aerosol component over much of the Earth's surface, providing the dominant aerosol production flux globally by mass and exerting major influences on clouds, radiation and chemistry in the marine environment, and in turn on climate and climate change (ARM Climate Research Facility, 2011).

2. 2 History of the Study of Aerosols

Concerns about the presence of aerosols in the atmosphere began earnestly during the period of the emergence of industry. With the growing knowledge of hospital admissions, and the effects of aerosols on climate, it became evident that there was much need for research into the presence and behaviour of atmospheric aerosols. Health effects of aerosols are evident from the number of research findings as outlined in the sections that follow.

Research into atmospheric aerosols goes way back into the 19th century. About that time, the role of atmospheric trace gases in atmospheric radiative transfer was also recognized – Arhennius, 1896; Rhodhe et al., 1998, as reported by Husar (1999). He further cites the works of Kant (1756), Marcorelle (1784) Verdeil (1783), Hoyer (1819), Schreiber (1844), Benjamin Franklin (1784) and others (Husar, 1999).

Over the past 30 years, major aerosol types have been identified and general ideas about the amount of aerosol to be found in different seasons and locations have been developed but key details about aerosol amounts and properties are needed to calculate even their current effect on surface temperatures, and there are a few observations that reveal the trends in many of these quantities (Kahn et al., 2011). He further reported that the abundance, variations in aerosol size and composition, and the magnitude of aerosol sources and sinks have never been systematically measured on a global basis. In addition, the size of the indirect aerosol effects on climate remains unknown.

In this research, both quantitative and qualitative data will be acquired as well as determining the chemical composition of aerosols in the North-West Province of South Africa.

2.3 Why Study Atmospheric Aerosols?

The much talked about life threatening diseases like cardiovascular diseases, cancers, respiratory diseases, and others; issues surrounding – rising temperatures, flood threats, and other issues certainly are a concern of great magnitude. This, undoubtedly, is a big challenge to the well being of mankind, other living things and the environment at large. This is undoubtedly a major reason to study atmospheric aerosols.

2.3.1 Health Effects Associated with Atmospheric Aerosols

Atmospheric particles with diameters of under 10 μm (PM_{10}) are importantly addressed by Air Quality Standards in several nations. Some epidemiological evidence suggests that mortality in urban areas may be linked to PM_{10} and $PM_{2.5}$ aerosol fractions (Pope et al., 1992; Dockery et al., 1993; Lundgren and Burton, 1995; Schwartz et al., 1996). Generally, the total daily mortality increases by approximately 1% for every 10 μgm^{-3} increase in PM_{10} concentration (Lippmann, 1998). The composition of atmospheric aerosols provides basic data useful in evaluating the optical properties of aerosols (Sloane, 1984; Larson et al., 1988; Pilinis, 1989; Ohta and Okita, 1990; Ohta et al., 1990), which must be known to estimate degradation of visibility, stabilization of the lower atmosphere, and the albedo effect on global climate. Atmospheric aerosols influence the global climate by changing the radiation budget of the earth–atmosphere system by scattering and absorbing solar radiation. This effect of aerosols on climate is called the direct effect or the albedo effect. Coakley et al. (1983) state that the strength of this effect depends on the total amount of aerosols in the atmosphere and their optical properties. The aerosols also affect the climate by changing the cloud albedo by increasing cloud droplets, because water-soluble particles such as sulfate, nitrate or sea salt easily become cloud condensation nuclei. This effect is the indirect effect of aerosols on climate (Nakajima et al., 1991). Atmospheric aerosols must be chemically characterized, and the variation of the major components determined to establish strategies for controlling atmospheric aerosol pollution (Kaneyasu et al., 1995). Airborne particulate matter may have either primary or secondary origins. Primary particles are emitted directly into the atmosphere from sources such as road traffic, coal burning, industry, wind-blown soil and dust, and sea spray. Secondary particles are formed in the atmosphere by the oxidation of sulfur dioxide and nitrogen oxides into sulfate and nitrate particles. Stedman (1997) reported that the contribution of secondary particles to measured PM_{10} is much more

uniform across the country than that of primary particles because the secondary particles are formed relatively slowly in the atmosphere and have a long lifetime therein. Inorganic, water-soluble ions represent a large fraction of the atmospheric particulate mass, the largest contributions to which are made by sulfate, nitrate, ammonium, sodium, chloride, calcium and magnesium (Wall et al., 1988; Harrison and Kitto, 1992).

Increases in respirable particulate matter lead to increased mortality, increased admissions to hospital for respiratory symptoms, increased use of medication by people with asthma, and reduced lung function (World Health Organization, 2000). Main industries and activities around the world in which silica particulate matter exposure has been reported are mining and its related milling operations (National Institute for Occupational Safety and Health, 2002). Research indicates that air pollution in the form of particulate matter (PM), at concentrations currently allowed by national standards (the National Ambient Air Quality Standards, or NAAQS) is linked to thousands of excess deaths and widespread health problems (U.S. Environmental Protection Agency, 2007).

A study on the risk of pulmonary tuberculosis relative to silicosis and exposure to silica dust in South African gold miners was undertaken by Hnizdo and Murray, 1998. The objectives of the study were to investigate, firstly, if silica dust on its own, without the presence of silicosis, was associated with an increased risk of pulmonary tuberculosis (PTB) in workers exposed to silica dust; secondly, whether in the absence of silicosis the excess risk dose was related, and thirdly, what was the predominant chronological sequence between the development of PTB and the development of silicosis after the end of exposure to dust. They took a cohort of 2255 white South African gold miners and followed them up from 1968 to 1971, when they were 45-55 years of age, to 31 December 1995 for the incidence of PTB. They found that exposure to silica dust was a risk factor for the development of PTB in the absence of silicosis (Hnizdo and Murray, 1998).

Another research by Hnizdo, Sluis-Cremer, Baskind, & Murray (1994), aimed at investigating which pathological changes in the lung are associated with impairment of lung function in silica dust exposed workers who were life-long non-smokers. In their method, 242 South African white gold miners who were lifelong non-smokers and who had

a necropsy at death were studied. The pathological features identified at necropsy were the degree and type of emphysema, the presence of airway disease and the degree of silicosis in the lung parenchyma and pleura. These features were related to lung function tests done a few years before death, to the type of impairment (obstructive or restrictive), and to cumulative silica dust exposure. They concluded from their results that the level of exposure to silica dust, to which these miners were exposed, without a confounding effect of tobacco smoking, was not associated with a degree of emphysema that would cause a statistically significant impairment of lung function. Silicosis of the lung parenchyma was associated with the loss of lung function.

A study to determine lung cancer and its relationship to exposure to silica dust, silicosis and uranium production in South African gold miners was conducted by Hnizdo and Murray (1997). They could not reach a definite conclusion in terms of causal association. They however suggested three possibilities. The first possible interpretation was that subjects with high dust exposure who develop silicosis are at increased risk of lung cancer; the second possible interpretation was that high levels of exposure to silica dust on its own is important in the pathogenesis of lung cancer and silicosis is coincidental; and thirdly, high levels of silica dust exposure may be a surrogate for the exposure to radon daughters.

Sluis-Cremer, Walters, and Sichel (1967) did a community-based, cross-sectional study of chronic bronchitis in 827 male residents who were aged >35 and who lived in Carletonville, a South African town with four gold mines. They found that a significant difference existed between the prevalence of chronic bronchitis in dust-exposed smokers and non-dust exposed smokers (51 % and 13 %, respectively).

Pope and Burnett (2002) did a cohort study to evaluate health effects associated with long term exposure to certain fine chemical particulate matter at levels typical in North America. They found a 14 % increase in lung cancer mortality. The first atmospheric species to be identified as being carcinogenic are polycyclic aromatic hydrocarbons (PAH), (Seinfeld and Pandis, 2006).

Ballester (2002), studied the impact of air pollution on mortality in Spain. He found an association between mortality and pollution through particulates among city populations in Spain. Jonathan et al., (2000) assessed the effects of five major outdoor-air pollutants on the daily mortality rates in 20 of the largest cities and metropolitan areas in the United States from 1987 to 1994. The pollutants were particulate matter that is less than 10 µm in aerodynamic diameter (PM_{10}), ozone, carbon monoxide, sulphur dioxide, and nitrogen dioxide. They found consistent evidence that the levels of fine particulate matter in the air are associated with the risk of death from all causes and from cardiovascular and respiratory illnesses.

A group of scientists investigated short-term health effects of particles in eight European cities. In each city, associations between particles with an aerodynamic diameter of less than 10 µm (PM_{10}) and black smoke and daily counts of emergency hospital admissions for asthma (0-14 and 15-64 yr olds), chronic obstructive pulmonary disease (COPD), and all-respiratory disease (65+ yr) controlling for environmental factors and temporal patterns were found (Atkinson et al., 2001). The study confirmed that particle concentrations in European cities are positively associated with increased numbers of admissions for respiratory diseases and that some of the variation in PM_{10} effect estimates between cities can be explained by city characteristics.

U.S. Environmental Protection Agency (2000) writings on toxicity reported that the respiratory tract is the major target organ for chromium (VI) toxicity, for acute (short-term) and chronic (long-term) inhalation exposures. Shortness of breath, coughing and wheezing were reported from a case of acute exposure to chromium (VI), while perforations and ulcerations of the septum, bronchitis, decreased pulmonary function, pneumonia and other respiratory effects have been noted from chronic exposure. Human studies have clearly established that inhaled chromium (VI) is a human carcinogen, resulting in an increased risk of lung cancer. Animal studies have also shown chromium (VI) to cause lung tumours via inhalation exposure. Mercury pollution is a growing concern worldwide (Tesche et al., 2002). All forms of mercury can have some effect on the human nervous system, although the form that is most responsible for human health impacts is methylmercury. Some health effects of particulate matter figures as obtained from the Compensation Commissioner for Occupational Diseases, Johannesburg (Hermanus,

2006), for 2003, indicate that PTB was most prevalent followed by emphysema, silicosis, primary lung cancer asbestosis, mesothelioma, massive fibrosis, coal workers' pneumoconiosis and the lowest prevalent being mixed dust pneumoconiosis.

2.3.2 Deposition of Aerosols in the Respiratory System

A person's ill-health which results from breathing atmospheric aerosols depends mostly on the site of deposition in the respiratory system, and on the aerosol chemical composition. The basic mechanisms of particle deposition in the respiratory system can be determined by dividing the respiratory system into three regions (Hinds, 1999). These regions differ markedly in structure, air flow patterns, function, retention time and sensitivity to the deposited particles. The first region is the Head airways (nose, mouth, pharynx and larynx). The second is the Lung airways or the Tracheobronchial region (trachea up to the terminal bronchioles) and the third is the Pulmonary or Alveolar region, where gas exchange takes place. Inhaled particles are deposited in the various regions of the respiratory system by impaction, interception, diffusion, gravitational settling and electrostatic attraction, or they may be exhaled. The most important of these mechanisms are impaction, settling and diffusion. The extent and location of particle deposition depend on particle size, density and shape; airway geometry, and the individual's breathing pattern. In the head airway region, inhaled air is warmed and humidified while passing in the nasal passage. The large particles are removed by settling and impaction on nasal hairs and at bends in the air flow path. These particles deposited on the ciliated surfaces of the nasal cavity are cleared to the pharynx and swallowed. In the tracheobronchial region, particle sizes of 0.5 – 3 μm get deposited mainly by both impaction and settling. Alveolar deposition is usually expressed as the fraction of the inhaled particles traversing the head airways region that are ultimately deposited in the alveolar region (Hinds, 1999).

According to Hinds (1999), for mouth breathing at an inspiratory flow rate of $1.8m^3$ per hour (30 L/min), approximately 20 % of 5 μm aerodynamic diameter particles and 70 % of 10 μm particles are deposited before the inhaled air reaches the larynx. Under conditions of light exercise and nose breathing, 80 % of inhaled 5 μm particles and 95 % of inhaled 10 μm particles are trapped in the nose. Hinds (1999) went on to state that at an average inspiratory flow rate of $1.2m^3$ per hour (20 L/min) or greater, impaction is the dominant mechanism for the deposition of particles larger than 3 μm in the

tracheobronchial region. For particles 0.5 - 3 µm or flow rates less than 1.2 m^3 per hour (20 L/min), settling is the predominant mechanism of deposition, although overall tracheobronchial deposition for particles in this size range is quite small. Hinds (1999) also reported that, for conditions of light exercise, particles with aerodynamic diameters of 5 - 10 µm that reach the tracheobronchial region are deposited there with approximately 35 % and 90 % efficiency respectively. Significant mixing of inhaled air with the reserve air in the first few sections of the tracheobronchial region due to turbulence in these airways occurs during exercise. This mixing transfers particles from tidal to reserve air facilitating subsequent deposition of submicrometer sized particles in the alveolar region. Ultra fine particles, especially those less than 0.01 µm, have enhanced deposition in the tracheobronchial region due to their rapid Brownian motion.

Salma et al., (2002) carried out an experiment to determine respiratory deposition of elemental mass size distributions in atmospheric aerosols. They collected samples at four different locations in Budapest, Hungary, comprising an urban background site, two downtown sites and a road tunnel. Based on these distributions, deposition fractions for the various elements in the respiratory system were calculated for a healthy Caucasian adult male, female and 5-year-old child under sitting breathing conditions by a stochastic lung deposition model. They found that most of the deposited mass appears eventually in the extrathoracic region of the respiratory system.

In a research to understand the deposition of trace atmospheric aerosols in the respiratory system after inhalation, Johnson (2004) found that ultra fine carbon particles that were radioactively labelled could be detected in the blood within 1 minute, and reach peak concentrations in peripheral blood within 10-20 minutes. Deposition of element-specific particulate matter in the respiratory system of a Caucasian-type healthy adult male and female was computed by a stochastic lung deposition model for different reference levels of physical exertion using mass size distributions in the aerodynamic diameter interval of 0.125–16 µm experimentally determined in urban environments (Salma et al., 2002). The computations presented suggested that the level of physical exertion plays a much greater role in particle deposition than particle size in the diameter range studied. All particle deposition mechanisms considered here are functions of flow rate, thereby affecting the residence time (Brownian motion and gravitational settling) or

the particle velocity (inertial impaction) in human airways. Consequently, computed particle deposition patterns, expressing the fraction of particles deposited during a single breath, depend sensitively on the assumed physical activity. More importantly, however, higher physical exertion also increases the inhaled volume per breath and the number of breaths, thus inhaling many more particles. They further found that the higher deposition at the maximum exertion level is also partly caused by switching from nose-only breathing to mixed nose-and-mouth breathing. Since oral deposition efficiencies are consistently smaller than those for nasal deposition, more particles can reach the bronchial and acinar airways. The slight dependence of particle deposition on gender, as observed in the study, may be caused primarily by differences in related breathing patterns.

Haber, Yitzhak and Tsuda, (2003) carried out a research that hypothesized that the trajectories and deposition of aerosols inside the alveoli differ substantially from those previously predicted. To test this hypothesis, trajectories of fine particles (0.5–2.5 μm in diameter) moving in the foregoing alveolar flow field and simultaneously subjected to the gravity field were simulated. Their results showed that alveolar wall motion is crucial in determining the enhancement of aerosol deposition inside the alveoli. In particular, 0.5 - to 1 μm diameter particles are sensitive to the detailed alveolar flow structure (e.g., recirculating flow), as they undergo gravity-induced convective mixing and deposition. Accordingly, deposition concentrations within each alveolus are non-uniform, with preferentially higher densities near the alveolar entrance ring, consistent with physiological observations. Deposition patterns along the acinar tree were also found to be non-uniform, with higher deposition in the first half of the acinar generations. This they felt was a result of the combined effects of enhanced alveolar deposition in the proximal region of the acinus due to alveoli expansion and contraction and reduction in the number of particles remaining in the gas phase down the acinar tree. They concluded that the cyclically expanding and contracting motion of alveoli plays an important role in determining gravitational deposition in the pulmonary acinus. A research to determine atmospheric particle pollution of PM_{10} and $PM_{2.5}$ was carried out in Nanjing, China. It was found that more than 70 % of total suspended particles were of the size that deposited in the respiratory tract below the trachea, whereas about 22 % mass was of respirable particles that deposited in the alveoli (Wang et al., 2002).

Zemp et al., (1999) investigated the association between long-term exposure to ambient air pollution and respiratory symptoms in a cross-sectional study in random population samples of adults (aged 18 to 60 yr, n = 9,651) at eight study sites in Switzerland. They found that long-term exposure to air pollution of rather low levels is associated with higher prevalences of respiratory symptoms in adults.

U.S. Environmental Protection Agency (EPA) (2007) researchers found that the respiratory dose of particulate matter is similar between young and older adults; they concluded therefore, that dose itself may not be responsible for differences in susceptibility to the health effects of PM by age. Similarly, they found that the overall respiratory dose of particulate matter is comparable between men and women; but, in general, women tended to receive greater doses in their upper airway regions than men, possibly because their airways are somewhat narrower.

The hypothesis that ultra fine PM0.1 (particles with diameters less than 0.1 μm) may be responsible for the association of health effects with ambient PM prompted EPA investigators to evaluate the effect of PM size on deposition efficiency. They found that the ultra fine and coarse PM fractions are deposited in the same areas in a healthy human respiratory tract. While some particles make their way into the deep lung, the majority appear to be removed higher in the respiratory tree. In a study conducted by EPA's research partners, it was found that the total pulmonary deposition of inhaled ultra fine particles was higher than that of fine particles in healthy individuals and was also higher among subjects with asthma and during exercise (U.S. Environmental Protection Agency, 2007).

The study by Johnson (2004) proposed different filtering mechanisms of different particle sizes by the body, as shown in **Table 2.1**.

Table 2.1: Body Filtering Mechanism Vs Particle Size

Particle	Size	Deposition by	Site of Deposition
Large	> PM_{10}	Wall Impact	Conducting airways
Coarse	$PM_{10} - PM_{2.5}$	Wall Impact/Sedimentation	Airways/Bronchioles
Fine	$PM_{2.5} - PM_{0.1}$	Sedimentation	Respiratory Bronchioles
Ultra fine	< $PM_{0.1}$	Diffusion	Alveoli

Peters and Dockery (2001) categorized size particles and deposition in the respiratory system as indicated below:

- >PM_{10} and PM_{10} particles get filtered in nose, larynx and/or bronchial tubes, and removed from the body by cough, sneeze, throat-clearing;
- < PM_{10} and $PM_{2.5}$ sediment out in respiratory bronchioles and get trapped in place; and
- $PM_{0.1}$ either deposits in alveolus due to diffusion, or is breathed back out because it is too small/light weight to deposit in lungs.

2.4 Methods of Analysing Atmospheric Aerosols

The properties of atmospheric aerosols offer many possible ways for their measurement. Some methods make use of optical aerosol properties for measurement, whilst others make use of their mass. Different techniques have been used to identify and characterize aerosols mostly ground-based *in situ* measurements, ground based remote sensing, aircraft *in situ* measurements, and satellite remote sensing (Rios, 2004).

Some methods make use of the absorption properties of atmospheric aerosols for their measurement, specifically carbonaceous particles and mineral dust (Bergstrom, Pilewskie, Russell, Redemann, Bond, Quinn, and Sierau, 2007). The fraction of light absorbed by the deposited aerosol is obtained from a radiative transfer scheme (Petzold and Schonlinner, 2004). Most aerosol measurements, however, provide integrals over time, size, and/or composition. A review of atmospheric aerosol measurements by McMurry (2000), lists a number of techniques to gather information on atmospheric

aerosols. These include; number concentration, CCN concentrations, particle mass concentrations (measurements of particulate mass concentrations are important for regulatory and scientific reasons), epiphaniometer, scattering coefficient, absorption coefficient, aerodynamic particle size, electrical mobility analyzers, diffusion batteries, condensation nuclei counters pulse height analysis and particle density.

Measurements of aerosol chemical composition include laser microprobe mass spectrometry, electron microscopy. Others not included by McMurry (2000), though not exhaustive, include atomic absorption spectrometry and ICP-MS.The present research work used three methods for acquiring atmospheric aerosol data namely: (a) the aerosol optical depth (AOD) measurements, (b) the laser technology measurements, and (c) the particle mass concentration methods for the purpose of comparing outcomes with those of particulate mass concentrations as laid down by regulatory institutions. The AOD measurement is a satellite remote sensing technique that has been developed over the past decades and has enabled the estimate of aerosol radiative forcing on a global scale. The AOD data (vertical integral) were obtained from Multi-angle Imaging SpectroRadiometer (MISR). MISR can retrieve AOD (τ) under cloud free conditions with an accuracy of $\pm 0.05 \pm 0.20\tau$ over land and better than $\pm 0.04 \pm 0.1\tau$ over ocean at mid-visible wavelength; in addition, these and other satellite sensors can qualitatively retrieve particle properties (size, shape and absorption), a major advance over the previous generation of satellite instruments (Remer et al., 2011). The MISR instrument (Maurer, 2001) is an equipment that measures solar radiation bounced off or reflected by, among other things, atmospheric aerosols. MISR is designed to provide data on monthly, seasonal and also long-term trends of atmospheric aerosol concentrations and their types. It also gives information on amount, types, and heights of clouds, as well as distribution of land surface cover, including vegetation canopy structure. As stated by Oregon Museum of Science and Industry (OMSI, 2006), most satellite instruments look only straight down, or toward the edge of the planet. To fully understand Earth's climate, and to determine how it may be changing, there is the need to know the amount of sunlight that is scattered in different directions under natural conditions. MISR is a new type of instrument designed to address this need—it views the Earth with cameras pointed at nine different angles. As the instrument flies overhead, each region of the Earth's surface is successively imaged by all nine cameras in four wavelengths or colors (blue, green, red and near-infrared).

2.4.1 Multiangle Imaging Spectro-Radiometer Operations

The Multiangle Imaging Spectroradiometer (MISR) was launched on board the EOS Terra spacecraft in December, 1999. The orbit is sun-synchronous at a mean height of about 705 km, with an inclination of 98.5°, an equatorial crossing time at about 10:30 am, and an orbit repeat cycle of 16 days. The MISR instrument consists of nine pushbroom (or line imaging) cameras, each of which makes high-resolution images (with approximately 275 m sampling) in four narrow spectral bands located at 443, 555, 670 and 865 nm. These cameras collect data at nine view angles (nadir plus 26.1, 45.6, 60.0, and 70.5° forward and aft of the direction of flight). The time delay between adjacent camera views is 45–60 s with a total acquisition time between the 70.5° aft and 70.5° forward images of about 7 min. In normal operation (called Global Mode) all the data in the red band from all nine cameras and all the data in the blue, green and NIR bands in the nadir camera are saved at the full 275 m sampling. The data of the blue, green and NIR bands of the remaining eight cameras are averaged to 1.1 km. The rest of operational details can be obtained from Diner et al., (1998).

2.4.2 Laser measurements

An important method of studying particulates in the air is the use of ground based laser technology like the Light Detection And Ranging (LIDAR) to measure Aerosol Optical Depth (AOD). The technology makes use of a laser light generated and sent into the atmosphere. The light then interacts with aerosols in the air. These particulates then back scatter some light that is picked up by the LIDAR. Detailed working principles of the LIDAR are presented in a paper written by research scientists at the Council for Scientific and Industrial and Research (Sharma et al., 2009). Laser light (**Figure 2.5**) is generated by a ND:YAG laser and sent into the atmosphere. Back scattered light is received back into the LIDAR. This is translated as voltage by a transient recorder. The transient recorder communicates with a host computer for storage and offline data processing. (Laser light as seen at night in **Figure 2.6**).

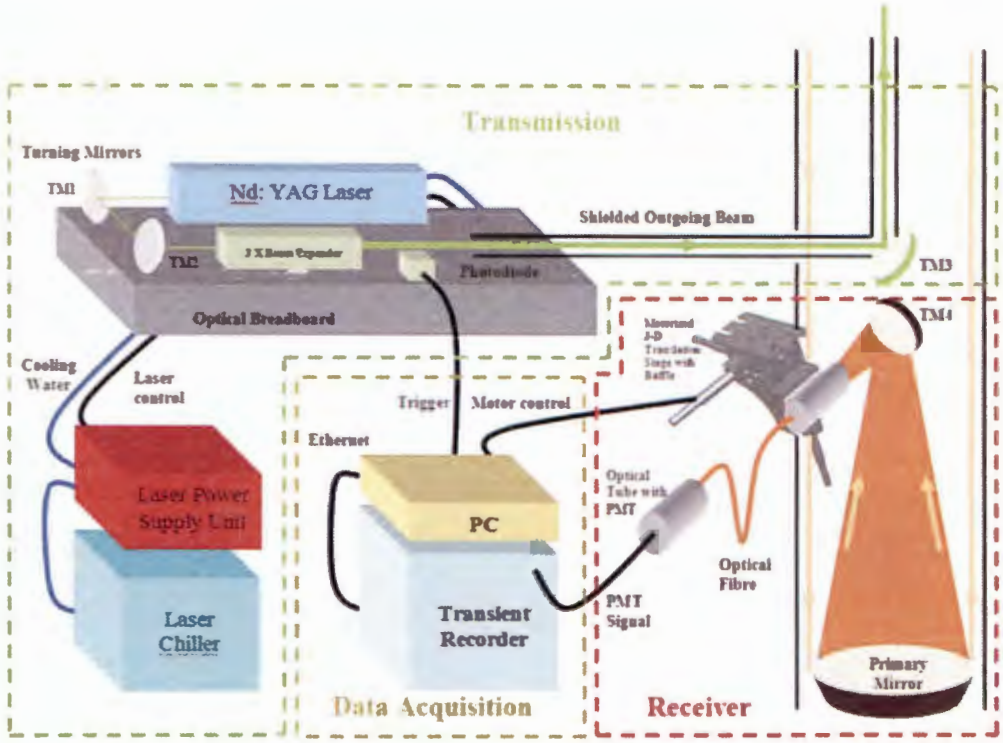

Figure 2.5: Detailed system block diagram showing the transmission, receiver and data acquisition sections of the LIDAR. TM: turning mirror; PMT: photomultiplier tube.
(Source: Sharma et al., 2009)

(a) (b)

Figure 2.6. (**a**) Showing the laser beam exiting the roof of the mobile LIDAR during the first measurements on 23 February 2008. (**b**) Showing the laser beam propagating into the clouds (night).
(Source: Sharmaa Sharma et al., 2009)

In this technique (**Figure 2.7**), particles are measured by the physical principle of orthogonal light scattering. Where particles are illuminated by a laser light in and the scattered signal (**Figure 2.8**) from the particle passing through the laser beam is 180° but collected at approximately 90° by a mirror and transferred to a recipient diode. Each signal of the diode is fed, after a corresponding reinforcement, to a pulse height analyser then classified to size and transmitted in each size channel. These counts are converted each minute to a mass distribution from which the different PM values derive. Results of the measurement are shown on the display in μgm^{-3}.

Figure 2.7: Grimm Laser equipment for taking particulate matter measurements (Source: Grimm # 180 dust monitor manual)

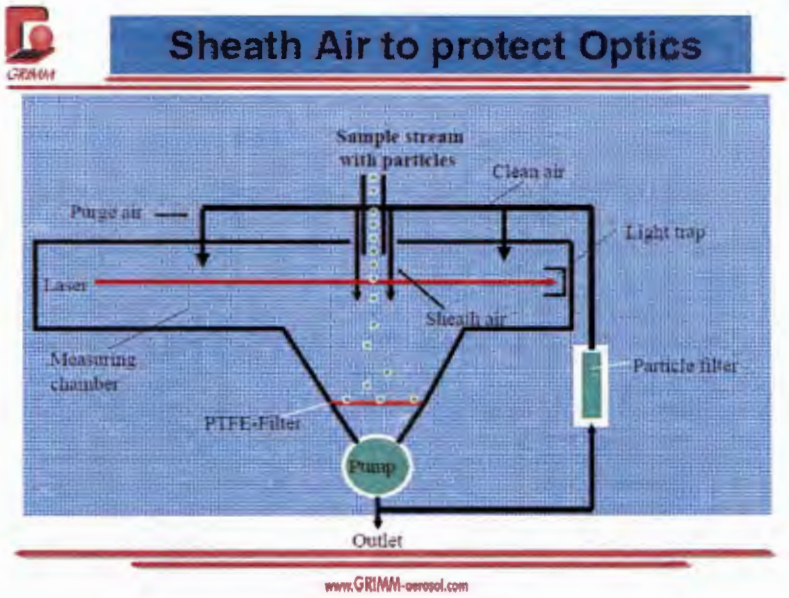

Figure 2.8a: How particles are measured

(Source: Grimm # 180 dust monitor manual)

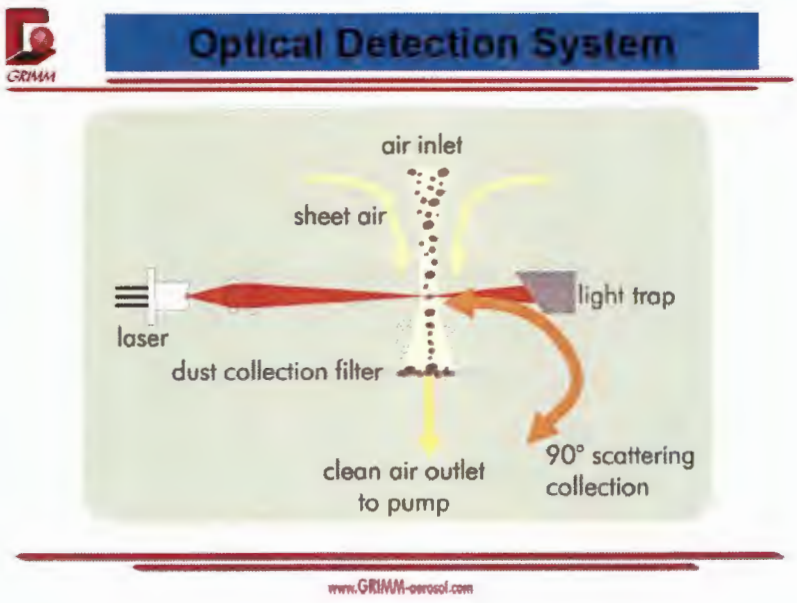

Figure 2.8b: How particles are measured

(Source: Grimm # 180 dust monitor manual)

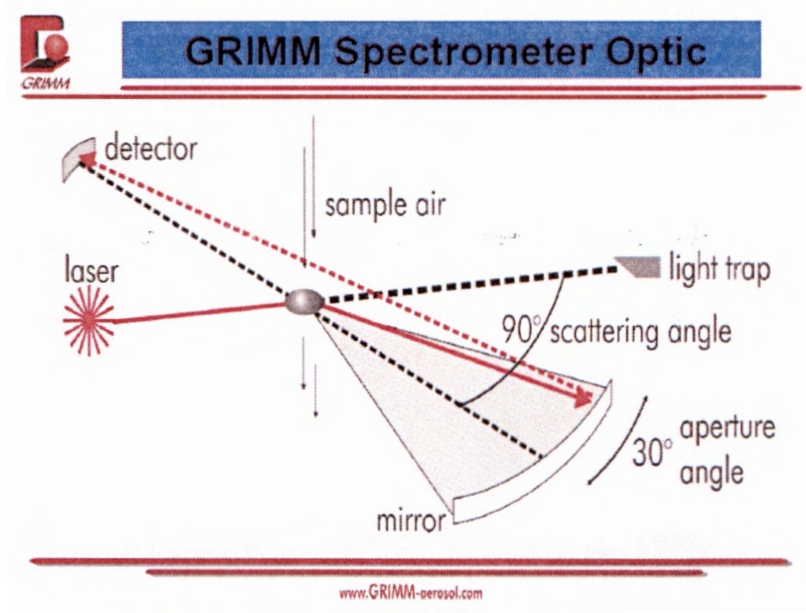

Figure 2.8c: How particles are measured
(Source: Grimm # 180 dust monitor manual)

2.4.3 Impactors

One of the aims of this research was to establish data which regulatory and scientific bodies could use for monitoring ambient air and compare with established Quality Standards. For this purpose, a cascade impactor was chosen. A cascade impactor with different impactor stages was used to collect atmospheric aerosol samples. Cascade impactors are designed to work on the principle of the human respiratory system. In the respiratory system, inhaled particles experience different modes of collection in different respiratory tract sites. Particles greater than PM_{10} get filtered in nose, larynx and/or bronchial tubes, and are removed from the body by cough, sneeze or throat-clearing. The particles smaller than PM_{10} and $PM_{2.5}$ sediment in the respiratory bronchioles trapped. Particles that are smaller than $PM_{0.1}$ get deposited in alveolus due to diffusion and eventually ending in the blood stream.

A cascade impactor collects atmospheric aerosol particle sizes selectively. Aerosol is passed through a nozzle and the output stream directed against a flat plate. The flat

plate, called an impaction plate, deflects the flow to form an abrupt 90° bend in the streamlines. Particles whose inertia exceed a certain value are unable to follow the streamlines and collide (impact) on the flat plate. Smaller particles can follow the streamlines and avoid hitting the impaction plate. They remain airborne and flow out of the impactor. Thus, an impactor separates aerosol particles into two size ranges; particles larger than a certain aerodynamic size are removed from the stream, and those smaller than that size remain airborne and pass through the impactor (Hinds, 1999). There is a cut diameter described as the particle diameter collected with 50 % collection efficiency by the jet stage. The aerodynamic diameter is the diameter of a spherical particle of unit density (i.e. density of 1.00 grams/cubic centimeter) which behaves aerodynamically just the same as the real particle. It has been conventional for many years to use the cascade impactor jet stage cut diameters and aerodynamic diameters with cascade impactor particle size measurements. More recently, the EPA PM_{10} criteria air pollutant for particulate matter less than 10 microns in diameter refers to the aerodynamic cut diameter of 10 microns and $PM_{2.5}$ with the aerodynamic cut diameter of 2.5 microns [EPA proposed Nov. 1996; promulgated July, 1997].

The equation for the cascade impactor jet stage aerodynamic cut diameter da_{50} is given by:

$$da_{50} = \frac{18\mu D_j \Psi_{50}}{CV_j} \qquad (5)$$

Where μ is the gas viscosity, D_j is the diameter of the jet holes in that cascade impactor stage, Ψ_{50} is the inertial impaction parameter at the 50 % particle collection efficiency of that impactor jet stage Ψ_{50} is about 0.145 for cylindrical round jet stages and Ψ_{50} does vary a little with the Reynolds number and other variables), C is the Cunningham slip correction factor for the particle of diameter da_{50}, and V_j is the gas velocity at the inlet (upstream inlet to the jet hole) to the gas jet through the impactor jet stage (Pilat, 1998).

In cascade impactors, downstream filters are added depending on stages required so that all the particles that escape impaction on the plate can be collected. In this way more information can be obtained about particle size distribution. The mass of the particles collected on the impactor plate and of those collected on the filter are determined

by weighing them before and after sampling. The cut-off size is reduced at each stage by decreasing the nozzle size. Reducing D_j increases V_j, and both serve to reduce da_{50} (Equation 5). Since the same volume of gas flows through each stage, only one flow needs to be controlled. Each stage is fitted with a removable impaction plate for gravimetric (or chemical) determination of the collected particles (Hinds, 1999). During sampling, the particles are driven (jetted) toward a collecting surface where they may cling. By changing the velocity (orifice size of the jet), the size of the particles collected is controlled. The size of the jets within each stage is constant, but for each succeeding stage the jets get smaller. Impaction occurs when the particle's inertia overcomes the aerodynamic drag. Otherwise, the particle remains in the air stream and proceeds to the next stage. To keep the cut-point for each stage constant, the impactor must be operated at a constant flow rate. At each stage, the particle impacts on a grease coated filter to reduce bouncing (Rhoades, 2006).

Particle collection is based on Stokes' Law. The stokes number, given in the Stoke's Equation (equation 6), is the parameter that governs collection efficiency defined as the ratio of particle stopping distance at the average nozzle exit velocity to the jet radius or nozzle diameter.

$$\text{Stokes Number} = \frac{4\rho_p C_c d_p{}^2 U}{9n\eta D_N{}^3} \qquad (6)$$

where

ρ_p is particle density, d_p is particle diameter, C_c is 'slip correction' factor, D_N is nozzle diameter, U is air velocity, η is viscosity of air and n is number of nozzles.

The Cascade impactor used for sampling in this study is called a Dekati PM-10 Impactor. It consists of 4 impactor stages connected in series with smaller and smaller cut-point diameters. The first PM_{10} stage removes particles larger than 10 µm off the particle stream. Subsequent $PM_{2.5}$ stage collects particles smaller than 10 µm and larger than 2.5 µm. The third stage collects particles smaller than 2.5 µm and larger than 1.0 µm. The filter stage after the PM_1 stage collects all particles smaller than 1.0 µm. The impactor is designed to work close to atmospheric pressures and between a temperature range of 0

to 80 ^{0}C with three air flow rates of 10, 20 and 30 L/min. Each stage has an impaction plate where the filter is held in place. O-rings hold the collection plates and the jet plate. The collection substrate is held in place by the substrate holder rings onto the plates.

2.5 MEASUREMENT OF CHEMICAL COMPOSITION OF AEROSOLS

2.5.1 Chemical Analysis

Various sensitive instruments used for analysis of contents of suspended atmospheric particles exist: namely Instrumental neutron activation analysis (INAA), photon-induced X-ray fluorescence (XRF), particle-induced X-ray emission (PIXE), atomic absorption spectrophotometry (AAS), inductively-coupled plasma with atomic emission spectroscopy (ICP/AES), inductively-coupled plasma with mass spectroscopy (ICP/MS), and scanning electron microscopy with X-ray fluorescence (SEM/XRF) chemical analytical methods They are all aimed at determining trace elements, which are connected with difficulties relating to small concentration measurements, unknown nature of chemical species as well as the fact that, due to coagulation, condensation and adsorption of gases, each single particle presents complex agglomerate (Tasić, Rajšić, Novaković, and Mijić, 2006).

The primary chemical analysis methods include gravimetric analysis for mass, ion chromatography for anions and cation species, thermal optical transmission for organic carbon, elemental carbon and energy dispersive X-ray fluorescence (EDXRF) for minor and trace elements. Although these are well-established methods, they may not be suitable to all species desired for receptor modelling and understanding atmospheric processes and for obtaining improved relationships between particulate matter and its sources and adverse health effects; and these methods may not be readily available to everyone. For example, detailed organic speciation of the collected aerosol is important for improved receptor modelling, while acidity, soluble transition metals and organic compounds, are potential causal factors associated with adverse health effects.

2.5.1.1 Mass Spectroscopy

As the individual compounds elute from the ICP, they enter the electron ionization (mass spec) detector and are bombarded with a stream of electrons causing them to

break apart into fragments. These fragments can be large or small pieces of the original molecules. The fragments are actually charged ions with a certain mass. The mass of the fragment divided by the charge is called the mass to charge ratio (M/Z). Since most fragments have a charge of +1, the M/Z usually represents the molecular weight of the fragment. A group of 4 electromagnets (called a quadrupole), focuses each of the fragments through a slit and into the detector. The quadrupoles are programmed by the computer to direct only certain M/Z fragments through the slit and the rest bounce away. The computer has the quadrupoles cycle through different M/Z's one at a time until a range of M/Z's are covered. This occurs many times per second. Each cycle of ranges is referred to as a scan. The computer records a graph called the mass spectrum for each scan where the x-axis represents the M/Z ratios and the y-axis represents the signal intensity (abundance) for each of the fragments detected during the scan. The mass spectrum produced by a given chemical compound is essentially the same every time. Therefore, the mass spectrum is essentially a fingerprint for the molecule. This fingerprint can be used to identify the compound (The Shared Research Instrumentation Facility, 1998).

2.5.1.2 Atomic Absorption Spectrometer (AAS)

The inorganic chemical composition and concentrations of the aerosols can be determined by the atomic absorption spectrophotometry (AAS) method. In analytical chemistry, Atomic Absorption Spectroscopy is a technique for determining the concentration of a particular metal element in a sample. Atomic absorption spectroscopy can be used to analyze the concentration of over 62 different metals in a solution (The Shared Research Instrumentation Facility, 1998). The technique makes use of a flame to atomize the sample, but other atomizers such as a graphite furnace are also used. Three steps are involved in turning a liquid sample into an atomic gas: firstly, the liquid solvent is evaporated, and the dry sample remains. Secondly, the solid sample is vaporized to a gas, and thirdly, the compounds making up the sample are broken into free atoms (atomized). The flame is arranged in such away that it is laterally long (usually 10 cm). The height of the flame is controlled by the flow of the fuel mixture. A beam of light passes through this flame at its longest axis (the lateral axis) and hits a detector. The light that is focused into the flame is produced by a hollow cathode lamp. Inside the lamp is a cylindrical metal cathode containing the metal for excitation and an anode. When a high

voltage is applied across the anode and cathode, the metal atoms in the cathode are excited into producing light with a certain emission spectrum. The type of hollow cathode tube depends on the metal being analyzed. For analyzing the concentration of copper in an ore, a copper cathode tube is used, and likewise for any other metal being analyzed. The electrons of the atoms in the flame can be promoted to higher orbitals in an instant by absorbing a set quantity of energy (a quantum). This amount of energy is specific to a particular electron transition in a particular element. As the quantity of energy put into the flame is known, and the quantity remaining at the other side (at the detector) can be measured, it is possible to calculate how many of these transitions took place, and thus get a signal that is proportional to the concentration of the element being measured

2.5.1.3 Inductively Coupled Plasma

Inductively Coupled Plasma (ICP) is an analytical technique used for the detection of trace metals in environmental samples (Bradford and Cook, 1997). The primary goal of ICP is to get elements to emit characteristic wavelength specific light which can then be measured. The technology for the ICP method was first employed in the early 1960's with the intention of improving upon crystal growing techniques. ICP hardware is designed to generate plasma (Bradford and Cook, 1997) which is a gas in which atoms are present in an ionized state as shown in **Figures 2.9, 2.10, 2.11**. The basic set up of an ICP consists of three concentric tubes, most often made of silica. These tubes, termed outer loop, intermediate loop and inner loop, collectively make up the torch of the ICP. The torch is situated within a water-cooled coil of a radio frequency (rf) generator. As flowing gases are introduced into the torch, the rf field is activated and the gas in the coil region is made electrically conductive. This sequence of events forms the plasma.

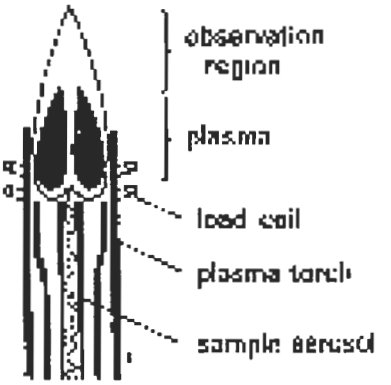

Figure 2.9: Schematic of ICP flame

[Source: Inductively Coupled Plasma (Bradford and Cook, 1997)]

The formation of the plasma is dependent upon an adequate magnetic field strength and the pattern of the gas streams follows a particular rotationally symmetrical pattern. The plasma is maintained by inductive heating of the flowing gases. The induction of a magnetic field generates a high frequency annular electric current within the conductor. The conductor, in turn, is heated as the result of its ohmic resistance.

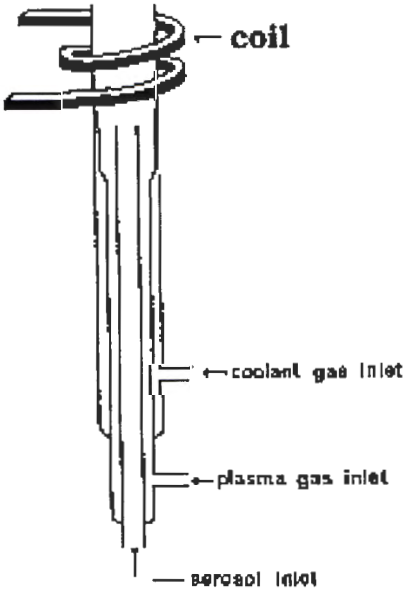

Figure 2.10: A Typical plasma torch.

[Source: Inductively Coupled Plasma (Bradford and Cook, 1997)]

In order to prevent possible short-circuiting as well as meltdown, the plasma is insulated from the rest of the instrument. Insulation is achieved by the concurrent flow of gasses through the system. Three gases flow through the system--the outer gas, intermediate gas and inner or carrier gas. The outer gas is typically Argon or Nitrogen. The outer gas has been demonstrated to serve several purposes including maintaining the plasma, stabilizing the position of the plasma and thermally isolating the plasma from the outer tube. Argon is commonly used for both the intermediate gas and inner or carrier gas. The purpose of the carrier gas is to convey the sample to the plasma.

An ICP typically includes the following components as shown in **Figure 2.11**; sample introduction system (nebulizer); ICP torch; High frequency generator; Transfer optics and spectrometer; Computer interface

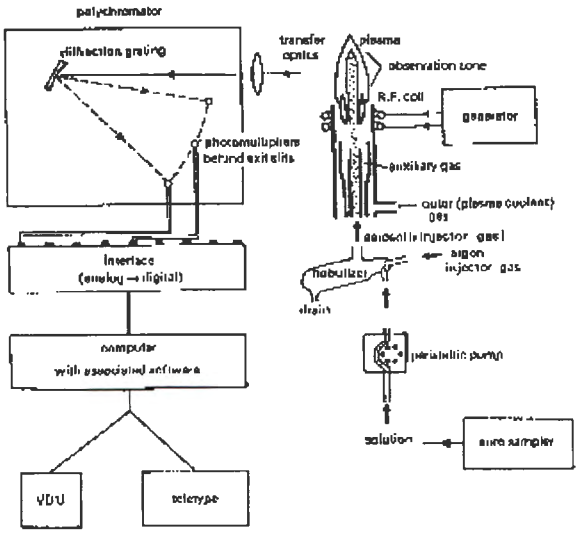

Figure 2.11: Schematic diagram of an ICP system

[Source: Inductively Coupled Plasma (Bradford and Cook, 1997)]

2.6 CLASSIFICATION OF ATMOSPHERIC AEROSOLS

Many definitions of aerosols exist. But, according to the U.S. Climate Change Science Program (CCSP), Atmospheric aerosols are suspensions of solid and/or liquid particles in air. Aerosols are ubiquitous in air and are often observable as dust, smoke, and haze. Both natural and human processes contribute to aerosol concentrations. On a

global basis, aerosol mass derives predominantly from natural sources, mainly sea salt and dust. However, anthropogenic (manmade) aerosols, arising primarily from a variety of combustion sources, can dominate in and downwind of highly populated and industrialized regions, and in areas of intense agricultural burning (CCSP, 2009). Atmospheric aerosols, apart from other substances, can also contain organic carbon compounds such as Organic methyl mercury, and also inorganic chemicals such as lead, cadmium, mercury etc (Pöschl, 2005). Depending on the concentration and nature of particulate matter inhaled through the respiratory system, adverse health effects can result in terms of morbidity and mortality (World Health Organization, 2004).

Atmospheric Aerosols cover a wide range of size. The range is from 1 nm to 100 µm. For better understanding, the aerosols are divided into 2 main classes (Temime, 2012). Class (i) aerosols are defined as *fine*. These have diameter less than 2.5 µm ($PM_{2.5}$). Class (ii) aerosols are defined as *coarse*. These have diameter greater than 2.5 µm. Under class (i) aerosols are the nucleation (or Aitken) mode with diameter less than 0.1 µm, and the accumulation mode with diameter between 0.1 µm to 2.5 µm. These particles originate mainly from the gas phase condensation (example from combustion).
Processes involved in aerosol formation for the nucleation mode can be from:

- Condensation of low-vapour-pressure gaseous species,
- Condensation of a gaseous species on pre-existing particles, or
- Coagulation: the formation of particles through collision and sticking smaller particles together.

Processes involved in aerosol formation for the accumulation mode can be from:

- Coagulation of nucleation mode particles,
- Gas-particle partitioning: condensation of compounds, even at concentration under the saturation concentration,
- Compound either adsorbed on the surface or absorbed in the particle, or
- Partitioning is a function of saturation vapour pressure, particle concentration and temperature.

The class (ii) aerosols (*coarse mode*) originate mostly from sources such as dust, sea spray, and volcanoes.

2.6.1 Chemical Composition of Atmospheric Aerosols

According to Seinfeld and Pandis (2006), atmospheric aerosol particles contain sulphates, nitrates, ammonium, organic material, crustal species, seasalt, metal oxides, hydrogen ions and water. From these species, sulphate, ammonium, organic and elemental carbon, and certain transition metals are found predominantly in the fine particles; and crustal materials, including silicon, calcium, magnesium, aluminium, and iron, and biogenic organic particles (pollen, spores, plant fragments) are usually in the coarse aerosol fraction.

Tasić et al., (2006) describe fine particles as having an aerodynamic diameter less than 2.5μm ($PM_{2.5}$) and that they differ from coarse particles in origin and chemistry. The fine or accumulation mode is ascribed to growth of particles from the gas phase and subsequent agglomeration. Fine particles are categorised as a fraction composed of varying amounts of sulphate, ammonium and nitrate ions, elemental carbon, organic carbon compounds, water, and small amount of soil dust, and trace species (Pb, Cd, V, Ni, Cu, Zn, Mn, Fe etc). This size fraction is generally man-made. Their lifetime is from days to weeks, travelling distance ranges from hundreds to greater than thousands of kilometers and they are associated with decreased visibility (haze) (Pöschl, 2005).

Work on effects of recent human colonization on the presence of mercury in Amazon ecosystems found that gold mining contributed more mercury into the atmosphere than burning activities (Roulet et al., 1999). Large emissions of mercury (Hg) occur in the Amazon Basin as a result of gold mining activities (Artaxo et al., 2000). Palheta and Taylor (1995) carried out an investigation on the dispersion of mercury in environmental and biological samples from a gold mining area in the Amazon region of Brazil. They found that widespread environmental contamination with mercury existed and that further monitoring of environmental, animal and human specimens was necessary.

Schroeder and Munthe (1998), reported on the estimated mercury emission values into the atmosphere (tons per year) for 1990 from the major U.S. anthropogenic source categories as: fossil-fuel combustion (62.1), municipal and medical waste incineration (56.6) manufacturing/smelting (27.7) and other sources (7.7) for a total of 154.1 ton per year.

Organic chemical composition of atmospheric aerosols consists of the carbonaceous fraction which is divided into elemental carbon and a variety of organic carbon (compounds) (Seinfeld and Pandis, 2006). The following organic compounds in the ambient aerosols: n-alkanes, n-alkanoic acids, n-alkanols, aliphatic dicarboxylic acids, diterpenoid acids and retene, aromatic polycarboxylic acids, polycyclic aromatic hydrocarbons, polycyclic aromatic ketones and quinines, steroids, nitrogen containing compounds, regular sterones, pentacyclic triterpanes, and iso- and ante iso- alkanes were identified by Seinfeld and Pandis (2006). Some examples of inorganic chemical components of atmospheric aerosols as identified by Schroeder, Dobson, Kane and Johnson, (1987) are shown in **Table 2.2**.

Table 2.2: Inorganic chemical particulates

Compounds		Elements
NO_3^-	nitrate	Iron (fc)
NH_4^+	ammonium ion	Lead (f)
SO_4^{2-}	sulfate	Zinc (f)
HSO_3^-	bisulfite	Cadmium (f)
SO_3^{2-}	sulfite	Arsenic (f)
Cl^-	chlorides	Vanadium (fc)
metal	oxides	Copper (fc)
NO	nitric oxide	Manganese (fc)
NO_2	nitrogen dioxide	Mercury -
NH_3	ammonia	Nickel (fc)
N_2O_5	dinitrogen pentoxide	Chromium (fc)
HNO_3	nitric acid (vapor)	Antimony (f)
SO_2	sulfur dioxide	Cobalt (fc)
		Selenium (fc)

f => fine particulates; fc => fine particulates + coarse particulates

Torres et al., (1998) write that aerosols affect the radiation budget of the earth-atmosphere system directly by the scattering and absorption of solar and thermal radiation and, as cloud condensation nuclei, they also have an indirect effect by modifying the optical properties and lifetimes of clouds. The net effect on the radiative budget depends upon aerosol composition and physical properties, reflectivity of the underlying surface and altitude of the aerosol layers. Aerosol effects on climate have been the focus of scientific interest for decades. The role of stratospheric aerosol of volcanic origin has

traditionally received most of the attention (e.g., El Chichon and Mt. Pinatubo eruptions), because of the large climate modification potential associated with the long lifetime of injected sulfate aerosols. Tropospheric aerosols, on the other hand, have only intermitently been the subject of research in the context of its potential climatic effects. In the last few years there has been a great deal of interest about the importance of tropospheric aerosols of anthropogenic origin from industrial pollution and biomass burning.

The consequent aerosol effect on climate is usually quantified in terms of radiative forcing, i.e., the net flux change at the top of the atmosphere due solely to the direct aerosol radiative effects. Although there are uncertainties in the estimates of aerosol radiative forcing, it is generally agreed that the averaged global direct effects of anthropogenic sulfate aerosols are not negligible and are probably similar in magnitude but in opposite direction to anthropogenic greenhouse gas forcing (Penner et al., 1992; Charlson et al., 1991). Unlike the greenhouse gases, aerosol physical-chemical properties and abundances exhibit large variability in both time and space that result in large uncertainties on the role of aerosols on climate. Because of this, cooling effects from aerosols do not necessarily result in the cancellation of the greenhouse gases' warming effect.

In addition to the well documented cooling effect of aerosols particles by backscattering of solar radiation, some aerosol types also absorb solar radiation reducing their cooling effect. For instance, absorption by both elemental and organic carbon aerosols from biomass burning and industrial pollution may affect the thermodynamics of the atmosphere by changing its thermal structure and perturbing convection and mixing processes in the planetary boundary layer. Silicaceous aerosols, such as desert dust, absorb solar and infrared radiation so that their direct effect on the climate may be significant. The role of anthropogenic sources of mineral aerosols as a climate forcing factor has been examined (Tegen et al., 1996) and found to be of importance when included in climate change studies . Because of the lack of data on absorbing aerosol physical properties and their spatial and temporal distributions, the heating effects of aerosols particles may not have been adequately included in model calculations. In an effort to improve on the current understanding of the role of aerosols on climate, it has

been suggested (National Research Council, 1993) that a combination of activities including satellite measurements be undertaken.

The effect of aerosols in the ultraviolet radiation field has traditionally been studied in the context of ozone retrieval from space based measurements of backscattered ultraviolet radiation (buv). The wavelength dependance caused by absorbing and non-absorbing aerosols on the buv radiance was first documented by Dave (1978) in his analysis of aerosol related errors in the ozone retrieval from buv measurements. Additional wavelength and angular dependencies have been discussed that arise from the presence of polar stratospheric clouds (Torres et al., 1992) and stratospheric sulfate aerosols (Bhartia et al., 1993, Torres et. al., 1995) on TOMS (Total Ozone Mapping Spectrometer) ozone measurements. Torres and Bhartia (1995) considered the artifacts introduced by stratospheric aerosols on ozone profile retrieval by the SBUV family of instruments. Torres et al., (1995) used the strong angular dependance of the aerosol effect on the TOMS buv measurements to infer optical depth and particle size of the Mt Pinatubo aerosol layer in the tropics. Several works have been recently published on the detectability by the TOMS instrument of tropospheric absorbing particulate matter such as carbonaceous aerosols (Hsu et al., 1996, Herman et al, 1997) and ash aerosols from volcanic eruptions (Seftor et al., 1997; Krotkov et al., 1997). These papers discuss the sources and geographic distribution of absorbing aerosols based on an aerosol index from which optical depth can be derived.

The atmospheric aerosol distribution exhibits large spatial and temporal variability in composition, size and concentration, related to the geographic locations of emission sources, type of emission, diffusive transfer and removal processes (Torres et al., 1998). The fluctuations of meteorological parameters (humidity, temperature, wind speed and direction) have a direct effect on the aerosol vertical and horizontal distributions as well as on the processes of diffusion, sedimentation and coagulation of aerosols. A comprehensive discussion of the variability of aerosols characteristics is presented by d'Almeida et al., (1991). The optical and microphysical properties of the different types of atmospheric aerosols span a wide range of values. A theoretical analysis of all possible aerosol types is very complicated and impractical. Thus, to carry out a sensitivity analysis it is necessary to simplify the problem by selecting a set microphysical representative of

the most commonly observed aerosol types. A brief discussion on the rationale used in the selection of the aerosol is presented next.

2.6.1.1 Non- absorbing aerosols

Two non-absorbing aerosol covering a wide particle size range are used in this study.

(a) A small particle size model, representative of troposheric sulfate aerosols of anthropogenic origin , S1, and a large particle model representative of other nonabsorbing aerosol types such as sea-salt aerosols and stratospheric sulfuric acid aerosols, S2.

(b) Suspended sea-salt particles and sulfate aerosols are the most common type of non-absorbing aerosols. Sea salt aerosols are entirely of natural origin whereas the sources of sulfate aerosol include both natural and anthropogenic mechanisms.

2.6.1.2 Carbonaceous Aerosols

Carbonaceous aerosols generated by biomass combustion consist of a mixture of material with varying radiative properties, both absorbing and nonabsorbing. Among these, the group of volatile organic or inorganic components is relatively non-absorbing. Much of the absorption of carbonaceous particles is due to the fraction of elemental or graphitic carbon (Rosen et al., 1978). Thus, the absorption of smoke aerosol particles depends on the relative amounts of each aerosol constituent. The single microphysical property directly related to the absorptivity of a given material is the imaginary component of its refractive index. The single scattering albedo, a macrophysical measurement of aerosol absorption, is defined as the ratio of the coefficients for scattering and extinction (i.e., the summation of scattering and absorption coefficients). The relation between imaginary refractive index and single scattering albedo is not direct since it also depends on the absorption cross-section of the particles.

Smoke components are produced from four fire stages : pre-ignition, flaming, smoldering and glowing (McMahon, 1983). The relative amount of elemental carbon and consequently the absorption properties of the resulting smoke vary through the combustion process. Analysis of laboratory fires (Patterson and McMahon, 1984) showed significantly larger absorption during flaming combustion than during the smouldering phase of the fire. Radke et al., (1991) measured the single scattering albedo of prescribed

fires as a function of smoke age at altitudes between 2 to 2.5 km in North America in September and October 1987. The observed single scattering albedo rose from an initial value of 0.7 and stabilized at about 0.9 over an hour after the onset of the fire. Westphal and Toon (1991) discussed the dependance of smoke optical properties on the particle size distribution parameters and examined the time dependance of smoke particle size. Their detailed analysis of direct measurements of size distribution and optical depth in several events of aged forest fire smoke indicates that the size of smoke aerosol particles increases systematically with time reaching geometric mean radii between about 0.10 to 0.14 μ in 48 to 90 hours. This range of smoke particle size is consistent with airborne volume density size distributions measurements over Brazilian and African smoke source regions during the TRACE A experiment in September to October 1992 (Anderson et al., 1996). The observed size distributions over both areas show a well defined mode diameter at about 0.25μ characteristic of the accumulation mode aerosols which are a primary combustion product (Radke et al., 1991). As reported by Anderson et al. (1996), the observed aerosol size showed only a slight tendency to increase with smoke age, and no appreciable differences in size distribution were observed between the source areas and the outflow regions. Particle radii derived from sky spectral radiances measured by sun/sky radiometers in Brazil (Holben et al., 1996), also clearly shows the accumulation mode with a well defined maximum volume distribution for radii in the vicinity of 0.1 μ.

It thus appears, that the variability of biomass burning smoke single-scattering albedo over a given area is more likely to be due to the variability of the fraction of elemental carbon in the smoke than to changes in particle size distribution. Based on the documented physical nature of the evolution of biomass burning smoke optical properties, Torres et al., (1998) selected two carbonaceous aerosol (C1 and C2). Both having the same particle size distribution, but differing in the magnitude of the imaginary component of the refractive index. The form of the assumed size distribution being a lognormal function with mode radius 0.12 μ and width 1.5. These parameters were found to adequately represent the nucleation mode of the observed size distribution over Brazilian and African sources as depicted in Figures 4, 8 and 9 of Anderson et al. (1996). Model C1, representative of weakly absorbing smoke aerosols away from the source area, has an imaginary refractive index of 0.02. Model C2, representative of fresh, more absorbing, smoke in the vicinity of the source area has an imaginary refractive index of 0.04. These

are typical values within the range of recommended values based on experimental work (Patterson and McMahon, 1984).

2.6.1.3 Mineral Aerosols

Mineral or dust aerosol is a common type of atmospheric suspended matter characteristic of the earth's arid and semi-arid regions accounting for about one-third of the land-surface area. Because of the high insolation levels and strong convective processes characteristic of arid regions, fine dust particles are easily lifted to high altitudes and horizontally transported by synoptic-scale atmospheric disturbances to areas thousands of kilometers away from their source regions (Carlson and Prospero, 1972). Measurements of desert dust aerosol composition indicate a mixture of different kinds of materials with calcium, silicon (in the form of quartz), and iron (in the form of hematite), identified as the main elemental components (Levin and Lindberg, 1979). Although desert dust from the same source region exhibits relatively uniform physical and chemical properties over large areas, there is considerable variability in aerosol properties associated with the nature of the crustal material from different source regions (Gomes and Gillette, 1993).

The complex refractive index of desert dust is largely determined by the volume fraction of hematite present in the mixture. Empirically-computed aerosol dust refractive index values (Longtin et al., 1988) at 400 nm based on a weighted mixing of measured refractive indices of quartz and hematite vary between 1.56 - 0i (for 0% hematite concentration) and 1.66 - 0.0335i (for 10% hematite concentration). Real refractive index values of about 1.5 are generally used in the visible based on the measurements of Saharan aerosols by Patterson et al., (1977) at 550 and 633 nm. No direct measurements in the near ultraviolet are available. Measured values of the imaginary refractive index at 400 nm at a variety of locations (Deluisi et al., 1976; Levin et al., 1980; Lindberg et al, 1976; Lindberg and Laude, 1974; Patterson et al., 1977; Sokolik et al., 1993) vary from about 0.005 to about 0.02. While part of the observed variability may result from the use of different measuring techniques (Sokolik et al., 1993), these measurements also reflect the differences in composition of desert aerosols from the different regions of the world where the sampling was made.

The size of desert dust aerosol particles shows significant variability over several orders of magnitude, from Aitken nuclei (aerosol radii less than 0.1μ) to ultra-giant particles with radii larger than 30μ. Since the atmospheric aerosol load over deserts is the direct result of the wind's lifting ability, the airborne particle size distribution is closely related to wind speed. Commonly used dust particle size distributions include the three-model representation for background, wind-carried dust and sandstorm conditions developed by d'Almeida (1987), and the wind-speed dependent model of Longtin et al. (1988) . Model representations of long-range transport mineral aerosols have been developed by Schütz (1980) to represent aerosol dust mobilized to maritime environments and by Shaw (1979) and Parungo et al., (1981) for poleward transport.

Carbonaceous aerosols, on the other hand, are generally a mixture of spherical, non-spherical and chain aggregates depending on the type of burning matter, combustion phase and the age of the smoke. Hallett et. al. (1988), used electron microscopy to determine the shape of forest fire smoke aerosols and found the particles to be mostly spherical. The actual shapes and sizes of combustion aerosols were measured by means of scanning electron microscopy (SEM) during the SCAR-B (Smoke, Clouds and Radiation - Brazil) experiment. As reported by Martins et al. (1996), the SEM analysis showed high variability in particle shape during the flaming phase of the fire and nearly spherical particles in the smoldering phase. They also determined the asymmetry of the particles by measuring the percent change in the integrated light scattering as the particles orient themselves along an applied electric field (Weiss et al., 1992). The measured asymmetry factor during SCAR-B was always less than 11% (Martins et. al., 1996). Thus, based on observational evidence, the representation of carbonaceous aerosols as spherical particles seems to be a reasonably good approximation.

For desert dust aerosols, the sphericity assumption is difficult to justify since dry aerosol particles are seldom spheres. Model calculations (Wiscombe and Mugnai, 1988; Koepke and Hess, 1988; Mishchenko et al., 1995) show that the phase function of non-spherical particles significantly deviates from that of spherical aerosols. Modelling results of the effects of non-spherical particles on phase function, single scattering albedo and asymmetry parameter are available in the literature (Mishchenko et al., 1995). The phase function departure from the spherical model is particle size and scattering angle

dependent with the biggest effect at scattering angles between 90° and 140° for particles of effective radii larger than about 0.5μ . The non-sphericity of the particles produces only a small effect in the single scattering albedo and asymmetry parameter. Although the particle shape is important in most of the range of scattering angles relevant to satellite remote sensing, the phase function deviation from sphericity is minimum in the range 150°-160°. Depending on the actual particle shape and viewing geometry, space retrievals of aerosol optical depth at visible wavelengths may be underestimated at backscattering geometries and overestimated at side-scattering angular configurations (Mishchenko et al.,1995).

Because of the large multiple scattering contribution to the total backscattered intensity in the near UV the use of the spherical particle approximation to retrieve optical depth from measurements in the 320-400 nm range may produce smaller errors than a similar estimate in the visible region (Torres et al., 1998). For near UV measurements of absorbing aerosols, the non-spherical particle phase function effect decreases with increasing absorption. Since the desert dust imaginary refractive index in the UV is almost an order of magnitude larger than at 630 nm, the phase function effect and, therefore, the particle shape may also be less important in the UV than in the visible.

2.7 MODELLING OF ATMOSPHERIC AEROSOLS

Air quality has been a cause of concern all over the world with the concentrations of criteria pollutants exceeding the standards at many places, particularly in developing countries. Particulate matter (PM) has been recognized as one of the key pollutants with a negative impact on human health, and a range of regulations have been introduced in order to control PM_{10} levels in urban areas with an increasing focus on $PM_{2.5}$ control. However, in order to design effective programmes and strategies for reduction of PM concentration in the ambient air, it is necessary to have information about the concentrations, sources and their respective contributions.

The term, source apportionment (SA) describes techniques used to quantify the contribution of different sources to atmospheric PM concentrations. There is a wide range of published literature on source apportionment using dispersion and monitoring data (Laupsa et al., 2009; Colvile et al., 2003). Some source apportionment studies have

been conducted using receptor . Receptor form a subset of source apportionment techniques and apportion the pollutant concentrations based on the measured ambient air data and the knowledge about composition of the contributing sources (Henry et al., 1984). The key outputs are the percentage contributions of different sources to pollutant concentration. Such are particularly helpful in cases where complete emissions inventories are not available (Hopke, 1991). Receptor have been used for identification of sources and their respective contributions to airborne particulate matter across the world (Harrison et al., 1997; Kumar et al., 2001; Larsen and Baker, 2003; Begum et al., 2004; Lai et al., 2005; Song et al., 2006; Tsai and Chen, 2006; Chowdhury et al., 2007; Guo et al., 2009; Kong et al., 2010; Stone et al., 2010; Gu et al., 2011).

Receptor can be divided into two broad categories: microscopic and chemical. Microscopic methods, including optical, scanning electron microscope (SEM) and automated SEM analyses are primarily based on the analysis of morphological features of many individual particles in the ambient air (Cooper and Watson, 1980). However, they are not very feasible for large-scale use since they do not produce quantitative results in most cases. Chemical methods, on the other hand, utilize the chemical composition of airborne particles for identification and apportionment of sources of PM in the atmosphere. A number of different methods are included in this category such as enrichment factor analysis, times series analysis, Chemical Mass Balance (CMB) analysis, multivariate factor analysis (including Principal Component Analysis (PCA) and Positive Matrix Factorization (PMF)), UNMIX, species series analysis and Multilinear Engine (ME) analysis (Cooper and Watson, 1980; Henry et al., 1984; Hopke, 1991; Ramadan et al., 2003). Such methods use trace elements, elemental/organic carbon and organic molecular markers for identification of sources and over time have become popular for SA analyses. Since PM is composed of both inorganic (trace metals, cations and anions) and organic species, a range of source markers are used in receptor modelling studies. Traditionally, most studies were carried out using inorganic trace elements like Fe, Zn, Pb, Cr, Al and Ni. However, since many of the trace elements are emitted from a range of sources (e.g., Zn is emitted from tyre wear as well refuse burning), it becomes difficult to apportion the PM to sources with a high degree of confidence. Further, with the removal of elements like Pb and Br from gasoline, there has been a need to develop and use new markers. In the last two decades, research has focused on the identification and

development of organic molecular markers for SA since they can be characteristic of sources, thus reducing the source ambiguity, and creating markers for sources which are difficult to be apportioned solely on the basis of inorganic tracers, e.g., levoglucosan for biomass burning (Harrison et al., 1996, 2003; Schauer et al., 1996; Robinson et al., 2006).

The CMB method requires *a priori* knowledge of the composition of all sources contributing to the airborne pollution, but not their emission rates. The measured air quality is assumed to be a linear sum of the contributions of the known sources, whose contributions are summed over each different sampling period to give the best match to the concentrations of the many chemical species measured in the atmosphere. In more recent studies, organic "molecular markers" which may be only minor constituents of emissions are measured, as these help to discriminate between similar sources (e.g., gasoline and diesel engines).

There is a suite of multivariate statistical methods based upon factor analysis, of which PMF has been developed specifically for the purpose of source apportionment of air quality data, and is the most commonly applied. The method requires no *a priori* knowledge of source composition, but any information on source emissions characteristics is helpful in discriminating between similar sources. The method requires a substantial number (at least 50) of separate air samples and works best with a large dataset in which the number of samples far exceeds the number of analytical variables. A minimum variable to case ratio of 1:3 should be maintained in order to obtain accurate results (Thurston and Spengler, 1985). For a clearer distinction, it is better to have short sampling times so that overlap of multiple point source contributions to a given sample is minimised. The samples are analysed for the chemical constituents, and those constituents from the same source have the same temporal variation, and if unique to that source are perfectly correlated. Typically, however, a given chemical constituent will have multiple sources and there are programs to view correlations in a multidimensional space and can generate chemical profiles of "factors" with a unique temporal profile characteristic of a source. Past knowledge of source chemical profiles is used to assign factors to sources, and typically identification of six or seven different sources is a good outcome. Before PMF became widely adopted, PCA was widely used for the same purpose, but is less refined than PMF (Pallavi et al., 2011). Input data plays an important role in the final results, and care has to

be taken to ensure that this is of good quality and where possible uncertainties can be assigned to individual analytes.

The key differences between CMB and the methods based upon multivariate statistics are summarised in **Table 2.3**. Studies have been conducted to compare results from different (Larsen and Baker, 2003; Ramadan et al., 2003; Shrivastava et al., 2007; Bullock et al., 2008; Lee et al., 2008; Viana et al., 2008b; Yatkin and Bayram, 2008; Callén et al., 2009; Tauler et al., 2009). Multicollinearity can affect the model estimates, particularly in cases where different sources have similar signatures, although multivariate help to reduce that problem substantially (Henry et al., 1984; Thurston and Lioy, 1987). It has been reported that in cases where two different sources have similar signatures, it becomes difficult to distinguish between them and neither CMB nor multivariate can distinguish between sources with similar signatures when additional information (for e.g., meteorology data) is missing (Henry et al., 1984).

Table 2.3 shows comparison between CMB and multivariate (Gordon, 1980; Henry et al., 1984; Thurston and Lioy, 1987; Harrison et al., 1997; Shrivastava et al., 2007; USEPA, 1997; Viana et al., 2008a; Zeng et al., 2010).

Table 2.3: Comparison between CMB and multivariate

CMB model	Multivariate
A key prerequisite is detailed information about the sources/emission inventories	Qualitative information about the potential sources is enough, useful for areas where detailed emission inventories are not available.
Only one sample is required	Require large numbers of samples.
Does not apportion the secondary aerosols	Unable to account for spatial and temporal correlation between emissions (e.g. motor vehicle and road dust) or source identified may contain more than one source.
Cannot take into account the time variation of the pollutant concentration or source emission	Often unable to produce a fine resolution of the sources.
Only non-reactive, stable tracer species can be used	Some of the allow negative contributions to sources which is physically impossible (e.g., PCA).
Near collinearity among source profiles can result in negative source contributions	Information like met data, particle size etc can be incorporated in the analysis.

Hybrid such as target transformation factor analysis (TTFA) and the constrained physical receptor model (COPREM) have been designed to combine the features of CMB and factor analysis with the aim of maximizing the advantages while minimizing the limitations of each model (Wahlin, 2003; Viana et al., 2008). The Multilinear Engine (ME) program also allows the use of source composition data to constrain the model.

Larsen and Baker (2003) compared three different multivariate techniques- UNMIX, PCA/MLR and PMF for SA of ambient polyaromatic hydrocarbons (PAHs) in Baltimore. Although they reported that PCA/MLR is unable to model extreme data effectively, they concluded that the overall source contributions compare well among the various . They also reported that use of different techniques on the same data set could help in identification of missing sources, and increase the robustness of the results. Shrivastava et al. (2007) used PMF and CMB for source apportionment of organic carbon and found good correlation between individual profiles for CMB and factors identified by PMF but with systematic biases that were found to be within an acceptable range (a factor of two). Lee et al. (2008) compared the CMB and the PMF and concluded that although both identify similar sources, they apportion contributions of different sources differently. The authors suggested that a lack of local source profiles, omission of key sources or lack of suitable markers, and the different assumptions regarding aging of the source emissions as the possible causes for the different estimations. Viana et al. (2008b) compared PCA, CMB and PMF for identification of source contributions to PM_{10} in Spain. They reported overall consistency between the different with high correlation in terms of source identification. However, they noted larger differences in terms of the percentage contribution of various sources. They suggested that a combined approach with the use of multivariate techniques for identification and interpretation of emissions sources and use of CMB for source contribution could help in increasing the robustness of the results. Earlier, Thurston and Lioy (1987) had also suggested a similar approach with the consecutive use of multivariate and chemical mass balance to derive better results from receptor modelling studies. Similarly, Shi et al. (2011) tested a combined two-stage PCA/MLR- CMB model and found acceptable results using synthetic datasets with collinearity. They also concluded that maximum uncertainty is generally observed in case of highly collinear sources.

Callén et al. (2009) compared three different multivariate techniques- PCA-ACPS, UNMIX, PMF for source apportionment of PM_{10} and found that the different showed high correlation between modelled and measured concentrations and PCA and PMF were able to identify more sources in comparison with UNMIX with good agreement. Tauler et al. (2009) compared four different multivariate (PCA, PMF, Multivariate Curve Resolution by Alternating Least Squares, (MCR-ALS) and Weighted Alternating Least Squares (MCR-WALS)) and concluded that PMF and MCR-WALS identify sources and apportion the emissions to sources in a similar fashion. The weighted (PMF and MRC-WALS) were found superior in robust and accurate factor identification.

Receptor have been used for regulatory purposes since they were first used in Oregon, USA in the late 1970s (Gordon, 1988). However, there is a caveat regarding the degree of uncertainty associated with the results (Caselli et al., 2006). Other that are used simulate aerosol size distributions. Two such methods commonly used are the modal and the sectional ones (Cousin et al., 2004). (i) In the modal representation, each aerosol subpopulation (mode) is described by an analytical distribution function like lognormal (Binkowski and Shankar, 1995). This approach has the advantage of limiting the number of prognostic variables but forces the distribution function for each mode. In the sectional approach, the size distribution which is approximated by a set of contiguous, non-overlapping discrete size bins appears more suitable for a detailed description of the microphysical processes (Jacobson, 1997; Gong et al., 2003). This allows for flexibility in solving aerosol multicomponent systems involving the processes of coagulation, condensation, absorption and chemical reactions. In the ORISAM module, first developed by Bessagnet and Rosset (2001), there are four bins from 0.03 to 10 µm. These four sectional bins are chosen as follows: bin 1 between 0.03 and 0.156 µm, bin 2 between 0.156 and 0.625 µm, bin 3 between 0.625 and 2.5 µm and bin 4 between 2.5 and 10 µm.

A detailed aerosol speciation that is adopted to represent aerosol composition properly is shown in **Table 2.4** (Cousin et al., 2004). This aerosol module comprised six chemical species: anthropogenic carbon, secondary OC, sulphates, nitrates, ammonium and water. Carbonaceous anthropogenic primary species are partitioned into two primary carbon components, BC and primary organic carbon (OCp). Similarly secondary organic aerosols are partitioned to differenciate between their anthropogenic or biogenic origins.

Nitric acid is produced in the gas phase by NO_x oxidation. Ammonium is considered a primary species converted into the aerosol phase by ammonia neutralization with nitric and sulphuric acids. Secondary Organic Aerosol (SOA) are formed from condensable Volatile Organic Compounds (VOC) using aerosol yields (Moucheron and Milford, 1996) and partition coefficients (Pankow, 1994). Aerosol growth follows condensation/absorption processes on preexisting particles followed with subsequent coagulation. A nucleation process gets added also for sulphates according to Kulmala et al. (1998). A detailed description can be found in Bessagnet et al. (2004).

Table 2.4: List of aerosol species

Model species	Species	Type
BC	Anthropogenic black carbon	Primary
OC	Anthropogenic primary organic carbon	Primary
ASOA	Anthropogenic secondary organic aerosol	Secondary
BSOA	Biogenic secondary organic aerosol	Secondary
H_2SO_4	Equivalent sulphate[a]	Secondary
HNO_3	Equivalent nitrate[a]	Secondary
NH_3	Equivalent ammonium[a]	Primary gas emissions, then secondarily transferred to the aerosol phase
Water	Water	

[a]Ions, molecules, crystals.

(ii) The mesoscale non-hydrostatic chemistry model (Meso-NH-C)

The ORISAM module has been implemented on-line within the mesoscale non-hydrostatic Chemistry model (Meso-NH-C), and a full description of that is given in Cousin et al. (2004). The ORISAM module and the gas-phase chemical module ReLACS (Crassier et al., 2000) derived from RACM (Stockwell et al., 1997) are also coupled on-line with Meso-NH.

Particle dry deposition has also been implemented in Meso-NH-C together with chemistry schemes modified for nitrates following Jacob (2000) so as to account for particle impact on gaseous species.

CHAPTER 3

EXPERIMENTAL PROCEDURES

3.1 DATA ACQUISITION AND TECHNIQUES

This section is divided into three parts. The first part deals with data acquisition using remote techniques. Here, the MISR was used to retrieve data to study the loading of different sizes of atmospheric aerosols in the North-West Province of South Africa. Emphasis was put on collecting data on atmospheric aerosols from two chosen towns, Rustenburg and Klerksdorp, dimmed to be highly loaded. Since this research aimed at acquiring atmospheric aerosols or PM data for comparison with South Africa Ambient Air Quality Standards (SAAAQS), the second part deals with collecting data using a Cascade Impactor. The third part is similar to the second part, the only difference being that an automated equipment was utilised since it proved to be more efficient with regard to data collection.

3.2. Study Sites

Northwest Province lies in the north of South Africa on the Botswana border, fringed by the Kalahari desert in the west, Gauteng Province to the east, and the Free State to the south. It is known as the Platinum Province for the wealth of the metal it has underground (**Figure 3.1**). Rustenburg is South Africa's fastest growing city due to the incredibly lucrative mining industry in the region involving platinum mining (Rustenburg, 2012). Rustenburg and Klerksdorp form the economic heart of North West Province. Klerksdorp is referred to as one of the hubs of South African gold mining industry although it has other minerals like uranium and diamonds being mined. Klerksdorp, together with Rustenburg, is also a major player in agriculture and animal farming. The general qualitative study done by Yigiletu M, Yigiletu V, Botai and Mengistu (2011), on the whole of South Africa indicated that the Upper Part is mostly loaded with atmospheric aerosols of anthropogenic origin. Together with the role Rustenburg and Klerksdorp play in the economy of North West Province, the two towns were chosen as research study areas for both quantitative and chemical composition of atmospheric aerosols in the Province. The North West Province Environment Outlook (2008) lists a number of air pollution sources. These include:

- Industrial and commercial activities

- ❖ Electricity generation (especially from coal burning)
- ❖ Waste treatment and disposal
- ❖ Residential fuel combustion
- ❖ Transport
- ❖ Mining
- ❖ Agriculture.

The province boasts of 94% contribution of South Africa's platinum mining. This activity generates more than half of the North West Province's Gross Domestic Product (GDP) (InfoHub, 2011). For this reason, many other economic activities are formed as linkages in one way or another, to the mining industry. The combined economic activities contribute greatly towards atmospheric aerosol loading in the two towns, and the province as a whole.

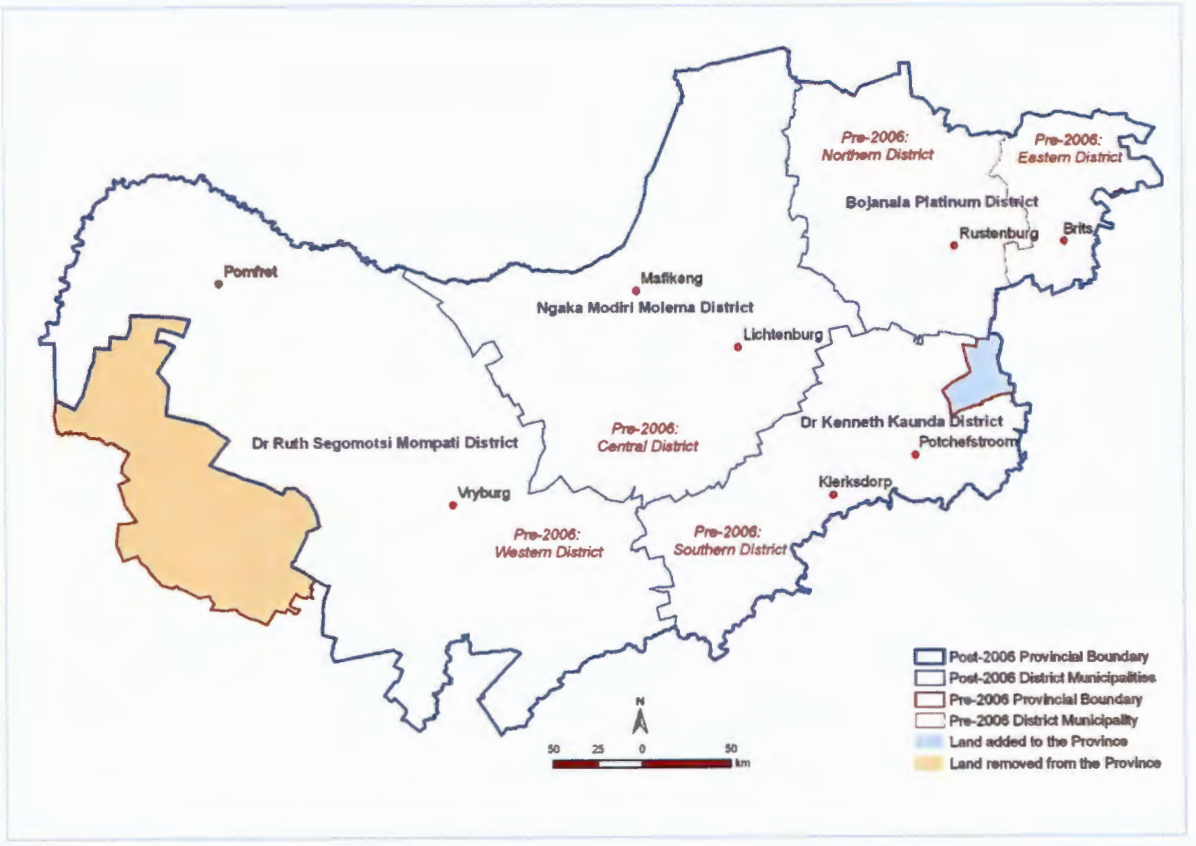

Figure 3.1: Map showing North West Province in South Africa. (Source: MDB, 2008)

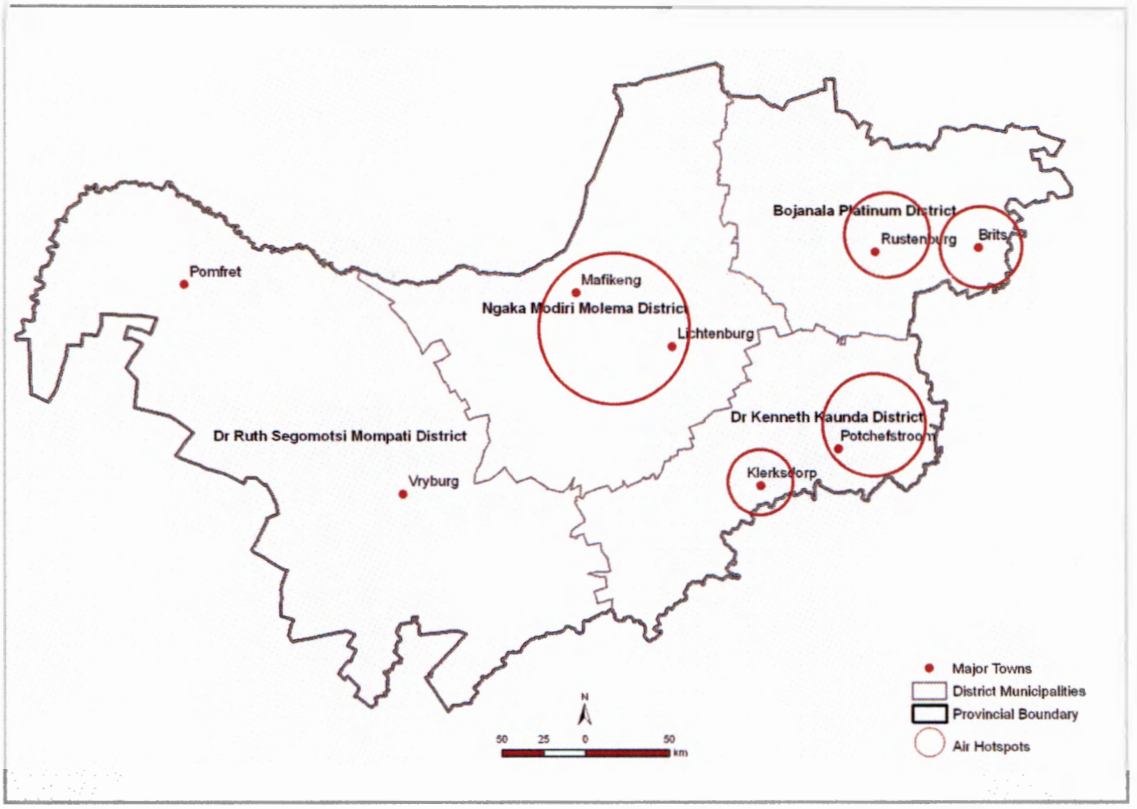

Figure 3.2: Air pollution hotspot areas where ambient monitoring stations needed to be implemented. (Source: MDB, 2008)

Monitoring sites were chosen taking in consideration that many people resided in the area (**Figure 3.3**).

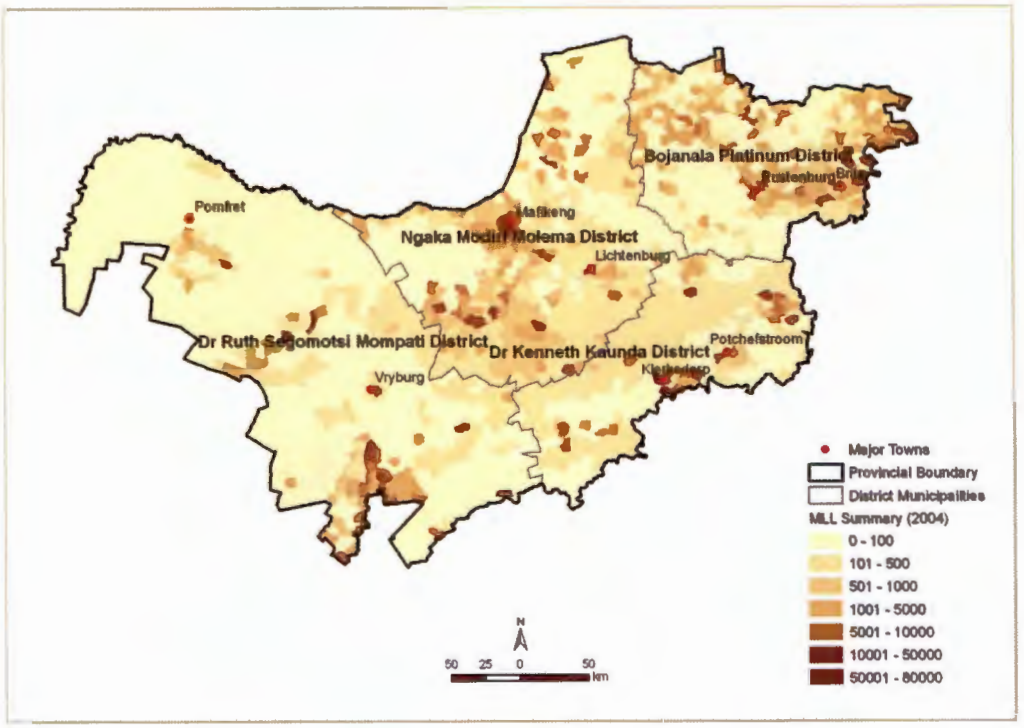

Figure 3.3: Estimated residential population of 2004.

(Source: MDB, 2008)

The chosen study sites are both highly populated (in comparison to surrounding areas), as well as being highly atmospheric aerosol loaded points. **Figure 3.4** shows data collection points in Rustenburg, and **Figure 3.5** shows data collection points in Klerksdorp. Phokeng data collection site can be seen in **Figure 3.4**, with the closest mines in circled in red square. The site is close to the Bafokeng stadium where the world cup was played in 2010. The various other mines are not shown in this map.

Jouberton data collection site can be seen in **Figure 3.5**. The closest mines are to the right after the Klerksdorp industrial, enclosed in red crescent shape. The uranium mines are just before the industrial site.

Figure 3.4: Rustenburg data collection site enclosed in red circle

Figure 3.5: Klerksdorp data collction site enclosed in red circle

3.3 Multiangle Imaging Spectro-Radiometer Data Retrieval

Yigiletu et. al. (2011), showed that the Upper Part of South Africa was dominated by atmospheric aerosols of anthropogenic origin. They reported that the Central Part of South Africa and the Lower Part were not as industrialised as the Upper Part and because of the industrial development in the Upper Part, air quality degradation is mainly attributed to industrial emissions. Classification of South Africa into three broad regions was based on coordinates:

a) Lower part of South Africa (35 1 º S to 31º S; 17.5º E to 30.5º E), includes the Western Cape, Eastern Cape and lower parts of the Northern Cape;

b) Central part of South Africa (31º S to 27º S, 16.5º E to 33º E), includes the middle and upper part of the Northern Cape, Free State and Natal provinces; and

c) Upper part of South Africa (27º S to 22º S, 19.5º E to 32º E), includes North West, Gauteng, Mpumalanga and Limpopo provinces

Yigiletu et al., (2011), did a general study of South African atmospheric aerosol distribution but this work has concentrated on the towns of Rusternburg and Klerksdorp on the basis of their research findings. These two towns are located in the North-West Province of South Africa, in a region described by Yigiletu et al., (2011), as "Upper Part". It is in these two towns that most of the industrial development is concentrated, especially the platinum and gold mining. The technique of data retrieval is described in detail in Yigiletu et al. (2011).

In this study, the Aerosol Optical Depth data on atmospheric aerosols' monthly mean were retrieved from the Multi-angle Imaging and SpectroRadiometer (MISR) for the years January, 2008 to December, 2009. MISR data for January, 2010 to June, 2011, was retrieved to make a comparison with measured PM_{10} behaviour in the same time period. There is a close relationship between atmospheric aerosol sizes and the aerosol absorption exponent (or angstrom extinction/coefficient). Whereas the absorption optical depth (AOD) gives information and describes full aerosol vertical columns, the angstrom extinction differentiates the diameters of the particulates, categorising them into coarse, fine, ultrafine aerosols and so on. The angstrom extinction describes the dependency of the AOD on the wavelenth. This relationship is described by equation (7) below:

$$\frac{\tau_{\lambda 1}}{\tau_{\lambda 2}} = \left(\frac{\lambda 1}{\lambda 2}\right)^{-\alpha} \quad (7)$$

Where $\tau_{\lambda 1}$ is AOD at wavelength λ_1, and $\tau_{\lambda 2}$ is the AOD at another wavelength λ_2. Taking logarithm of the equation gives the angstrom exponent as in equation (8):

$$\alpha = - \frac{log \frac{\tau_{\lambda 1}}{\tau_{\lambda 2}}}{log \frac{\tau_{\lambda 1}}{\tau_{\lambda 2}}} \quad (8)$$

where the angstrom exponent is usually calculated at AOD taken at two different wavelengths. From this calculation of angstrom exponent, the size distribution can be determined. Large values of α means fine particles, mostly from anthropogenic activities, and small values of α means coarse particles mostly of non-anthropogenic sources.

3.4 Sampling of Atmospheric Aerosols – Cascade Impactor

Isopore Teflon membrane filters of 0.4 µm pore size were used to collect particulate matter. Filter preparation was done in the laboratory prior to going out into the field. The filters were first fitted unto impactor plates and then clamped with O rings. Grease (Apiezon M grease) was thinned with analytical toluene and then applied on the filter with a very fine film using a small painting brush. This was done so that loss of particulates because of bouncing off the substrate could be minimised. The filters were then allowed to sit for two minutes to let the toluene to evaporate. The teflon filters were unclamped and weighed with a Shimadzu AY 220 laboratory weigh balance to obtain the weight of the filter alone. The filters were then stored in tubes which were then closed tightly, ready for use in the field. The cascade impactor was assembled and fitted with the pump, in the laboratory, to test their working condition before going to the field. On the selected study site, a firm angle line bar was erected. An arm extension of 0.5m long was made. Filters were fitted onto the impactor plates after which the plates were assembled into two

impactors. The impactors were then clamped to the arm extension. Two plastic pipes from the impactors were connected to two pumps fitted with air flow rate meters and volume measurement meters. The pumps were supplied by 220 volts power. One impactor was set to run for 24 hours. The other impactor was set to run every 3 hours. After the set time runs, the filters were removed and put back into the tubes and stored for further analysis in the laboratory. Fresh filters were then put into the impactor. The filters with PM were measured again in the laboratory. The difference in the initial weight and the new weight gave the weight of collected PM in µg. To calculate the PM concentration, corresponding air volumes for 3 hour measurements and 24 hour measurements were taken respectively. The concentration was calculated by dividing collected mass by the volume and expressed in μgm^{-3}. The filters were retained for element analysis. A total of 72 samples for three hourly measurements, and 9 samples for daily measurements were collected during the period 20 to 22 August, 2008. A total of 72 samples for three hourly measurements, and 9 samples for daily measurements were collected during the period 11 to 13 November, 2008.

3.5 Sampling of Atmospheric Aerosols – Grimm Ambient Dust Monitor

Sampling aerosols using the cascade impactor was discontinued in favour of the Grimm #180 Ambient Dust Monitor mainly for the reason of continuous sampling advantage offered by the automated equipment. The Grimm #180 Ambient Dust Monitor is a stationary monitor installed in a measuring shelter. It measures continuously concentrations of PM_{10}, $PM_{2.5}$, and PM_1. The dust monitor shows the airborne dust particulates in micrograms per cubic meter (μgm^{-3}). The resolution of the mass calculation set by the manufacturer is 0.1 μgm^{-3} with a flow rate of 72 lh^{-1}. The Grimm #180 dust monitor was allowed to take a continuous air sample with a flow controlled pump. In the monitor, the particles are measured by the physical principle of orthogonal light scattering. Particles are illuminated by a laser light and the scattered signal from the particle passing through the laser beam is collected at approximately 90° by a mirror and transferred to a recipient diode. Each signal of the diode is fed, after a corresponding reinforcement, to a pulse height analyzer then classified to size and transmitted in each size channel. These counts are converted each 6 seconds to a mass distribution from which the different PM values are derived. Results of the measurement are shown on the display as mass

distribution in μgm^{-3}: PM_{10}, $PM_{2.5}$, and PM_1. The collected data is stored on an AQWeblogger data logger and retrieved even by remote access.

In this research, it was decided to concentrate on PM_{10} data collection as the South Africa Air Quality Standards (SAAQS) did not give guidelines for $PM_{2.5}$ and PM_1 at the time of this study.

3.6 Meteorological Measurements

3.6.1 For Cascade Impactor Data

Meteorological data was collected at the same time and place as aerosol sampling, by using an onsite weather equipment called RM Young Weather instruments consisting of the following:

- Wind anemometer Model 27005T.
- Relative humidity and temperature sensors Model 41382VC.
- Multi-plate Radiation shield Model 41003.
- Solar Radiation sensor Model 70201.
- Rain gauge and interface.
- Ambient pressure sensor.

3.6.2 For Grimm Equipment Data

Meteorological data for analysis of data from the Grimm equipment was obtained from the South African Weather Services (SAWS). This data was specific to the sites because aerosol sampling points coordinates were provided to SAWS.

3.6.3 Atomic Absorption Spectroscopic Analysis of Atmospheric Aerosols

Elemental standards for chemical analysis were purchased from Merck South Africa suppliers. From these, three different concentrations were made for each element as standards. The sample elements were prepared by carefully transferring the sample filter into a 50 ml round bottomed flask to which 10 ml of concentrated nitric acid was added. This was then refluxed for two hours. After refluxing, the solution was transferred quantitatively to a 100 ml erlenmeyer flask and distilled water was added to bring it to the mark. This solution was analysed using an Aanalyst 200 PerkinElmer AAS instrument made in the US.

3.7 ICP-MS Analysis of Atmospheric Aerosols

A sample which was collected on a teflon filter on 21 August, 2008 was dissolved in a mixture of 6 ml concentrated nitric acid and 2 ml concentrated hydrochloric acid. The sample was taken for 24 hours at Marikana. This was then put into a multiwave microwave 3000 for 40 minutes. The solution was diluted to 100 ml and analysed with an ICP-MS Nexlon 300Q, manufactured in the US.

3.8 Modelling of Parameters

Since there are many data points in the measurements, the polynomial of 9 degree was chosen to be the best fit for the model. All data processing was performed off-line using a commercial software package (MATLAB 6.1, The MathWorks Inc., Natick, MA, 2000). The Polynomial equation utilized was selected from the available polynomial equation in the Matlab programme. The mathematical expression for the forecast obtained has the form:

$$Y = A + B1*X + B2*X^2 + B3*X^3 + B4*X^4 + B5*X^5 + B6*X^6 + B7*X^7 + B8*X^8 + B9*X^9 \quad (16)$$

Where Y is the aerosol concentrations; A is the point of interception of the graph on the Y values; B values represent the slopes of the graph; X represents time in days.

CHAPTER 4

RESULTS AND DISCUSSION

4.1 CASCADE IMPACTOR

Results obtained from sampling in Marikana, Rustenburg show that, particulate matter (PM) values recorded during the measurements ranged from 0 to 135 $\mu g/m^3$.
In the August 2008 measurements, all 3 hourly PM measures were between 06:00 hours to 09:00 hours, and at time period 09:00 hours to 12:00 hours (**Figures 4.1** to **4.3**). It was not possible to set the equipment for the time interval 13.00 hours to evening as there was no access to the site. Daily PM measurements showed recordings of the presence of all the three PM sizes (**Figure 4.4**).

In the November 2008 measurements, 3 hourly PM measures were recorded throughout day time at three hours interval i.e. between 06:00 hours to 09:00 hours, 09:00 hours to 12:00 hours, 12:00 hours to 15:00 hours and 15:00 hours to 18:00 hours (**Figures 4.5** to **4.7**). Daily PM measurements showed recordings of the presence of PM_1, $PM_{2.5}$, and PM_{10} (**Figure 4.8**). The data and the mean were not close to each other as can be seen from the standard deviation error bars (**Figures 4.4** and **4.8**).

4.1.1 Domestic Activities

High values of PM_1, $PM_{2.5}$, and PM_{10} were recorded during the period 06:00 hours to 09:00 hours, 12:00 hours to 15:00 hours and 15:00 hours to 18:00 hours. This could be as the result of domestic activities (**Figures 4.1, 4.2, 4.3, 4.5, 4.6,** and **4.7**). Domestic activities include the burning of fuel for purposes of cooking and the burning of fuel for purposes of keeping warm when surrounding temperatures are low. This activity emits PM into the atmosphere. Cooking times are mostly early in the morning, midday, and evening time. Burning of fuel for purposes of keeping warm could be any time as long as people are at home, but it is mostly in the morning, midday, and evening time. The recorded high PM values during these time periods suggest that this could probably be due to domestic activities. In their study, Cançado and others (2006) showed marked contribution of $PM_{2.5}$ and PM_{10} when they studied emissions from the domestic burning of fuels.

4.1.2 Transport Activities

Transport generates a number of adverse environmental effects from both transport infrastructure and vehicles. But this study is concerned with vehicles. Vehicle exhaust emissions are a major source of air pollution, particularly around busy roads. Pollutants include carbon monoxide (CO), nitrogen dioxide (NO_2), benzene, and particulate matter. Vehicles also emit carbon dioxide (CO_2), which is a greenhouse gas. Particulate matter includes heavy metals and petroleum products. These can contaminate the air, the land and waterbodies since settled PM can be carried far by stormwater. Fine PM has a long atmospheric residence time and may therefore be subject to long-range transport. In addition, a significant contribution to fine PM mass comes from secondary aerosols (inorganics such as ammonium sulfate and ammonium nitrate but also secondary organic aerosols), which are formed in the atmosphere through chemical/physical processes. Although the highest concentrations of particulate matter (PM) are obviously found at close to busy roads, considerable levels can occur even at far areas as a result of being transported over long distances (1000 km or more). This is because fine PM have long residence time in the atmosphere (up to several days).

The recorded PM values in **Figures 4.1** to **4.7** could also be a contribution from transport emissions. There is a busy road about 50 meters from the study site where sampling was done. This road is used by commercial vehicles to transport people from and to Rustenburg for purposes of work in the mines, haulage trucks from the mines and to the mines, as well as private cars. Vehicles emit PM in the atmosphere during the combustion of gasoline. Peak times for vehicle movement are mornings and evenings. This suggests that there is contribution of recorded values of $PM_{2.5}$, and PM_{10} from emissions during 06:00 hours to 09:00 hours, and also 15:00 hours to 18:00 hours as people move to and from work. This is in agreement with the work done by Bogo and others (2003) on atmospheric particulate matter in Buenos Aires City, they reported that vehicle emissions contributed greatly to $PM_{2.5}$ and PM_{10}.

4.1.3 Platinum Mining Activities

Figures 4.1, 4.2, 4.3, 4.5, 4.6, and 4.7, show values of PM recorded during the period 09:00 hours to 12:00 hours. Traffic and domestic activities are markedly reduced at this time. The PM measurements therefore are more likely to have come from mining

activities. The recorded values of PM suggest a contribution from platinum mining during blasting, crushing, processing, handling and also during haulage, but more prominent at these sites. It should be noted that the crushing of the ore is done continuously throughout the day. This activity contributes to recorded PM values at any time of the day.

4.1.4 Wind Direction

Wind direction has a significant effect on measured PM levels and depending on direction from which it is blowing, it could bring in or reduce values of PM recorded. The study site is surrounded by mines and therefore wind blowing from any direction would blow in PM that would contribute to the values measured. For example, south westerly winds during the period 06:00 hrs to 09:00 hrs could have blown in PM from domestic fuel burning and mining, causing high values of 3 hourly $PM_{2.5}$ recorded in **Figures 4.1, 4.2, 4.3,** and **4.6**. A significant amount of PM_1 and SO_2 (**Figure 4.11**) were measured at this time. As there was insignificant traffic (main road is north of study site) from the south western direction. Gas measurements were used to link emissions from the mining activities (SO_2). The PM_1 and SO_2 measured values could have been due to domestic fuel burning and mining activities. Wind direction changed to north westerly direction causing high amounts of 3 hourly measurement of PM_1 at both period of 12:00 hrs to 15:00 hrs and 15:00 hrs to 18:00 hrs (**Figure 4.6**) (~120 and ~90 $\mu g/m^3$ respectively). High 3 hourly values for $PM_{2.5}$ and PM_{10} were measured at these time periods (**Figure 4.6**) (100 and ~60 $\mu g/m^3$ respectively). The PM measured values could have their origin from vehicle emissions (a lot of traffic because of main road), domestic fuel burning and mining activities. Vehicle emissions are supported by the carbon monoxide (CO) and nitrogen oxides (NOx) high values obtained during the period 17:00 hrs to 20:00 hrs (**Figure 4.11**). Gas measurements were used to link vehicle PM contribution as evidenced by CO and NOx.

4.1.5 Wind Speed

Very low south easterly winds (less than 2 m/s) were measured during the period 06:00 hrs to 09:00 hrs (**Figure 4.10**). The highest 3 hourly PM values obtained during this period were for $PM_{2.5}$ and PM_1 (~80 and ~25 $\mu g/m^3$ respectively) (**Figure 4.1**). Since traffic was not much from the south easterly direction (minor traffic on this road, major one is

north of study site), PM sources were most probably from domestic fuel burning and mining activities.

4.1.6 Temperature Effects

Low temperatures cause people to burn more fuel to keep warm especially in Winter. As a result, PM emissions due to domestic fuel burning would be expected to be higher. This was not the case comparing $PM_{2.5}$ (~78 µg/m^3) and PM_1 (~25 µg/m^3) values in **Figure 4.1** to $PM_{2.5}$ (~135 µg/m^3) and PM_1 (~75 µg/m^3) in **Figure 4.6** for instance. This could be due to wind direction. In August, prevailing winds were Southeasteries (**Figure 4.10**) (less populated from that direction). In November, winds blew from Northwest mostly (**Figure 4.12)**. These winds were probably bringing in pollution from that direction. Temperatures are lower in August than in November. The temperature was 16 °C (**Figure 4.10**) on the day of measurement, 20 August 2008, and temperature was 24 °C (**Figure 4.12**) on the day of measurement, 12 November 2008. Measured $PM_{2.5}$ values were higher in November than August by 57 µg/m^3 instead of the other way round. Measured PM_1 values were also higher in November than in August by 50 µg/m^3. The possible explanation is that the south easterly wind on both days was blowing PM from the platinum mining activities as traffic is insignificant from this direction (main road is north of study site). This is supported by the presence of measured high SO_2 values (~350 ppb **Figure 4.9**, and ~400 ppb in **Figure 4.11**). It is important to note that relative humidity, wind speed and wind direction parameters were the same for these particular days.

4.1.7 Relative Humidity Effects

When relative humidity is very high, hygroscopic components in aerosols take up water from the atmosphere so that particles may grow to droplets that are several times their dry weight. And when water vapor molecules interact with aerosol particles, they can be adsorbed onto the surface of the particles or absorbed into the bulk of the particles.
Relative humidity was very high on 20 August, 2008 (**Figure 4.10**), and on 12 November, 2008 (**Figure 4.12**). This is probably the reason PM_{10} is absent at both times (06:00 to 09:00) for these two days (**Figures 4.1** and **4.6**). It is also most probable that ultrafine were growing to give readings of PM_1 and $PM_{2.5}$ (**Figures 4.1** and **4.6**).

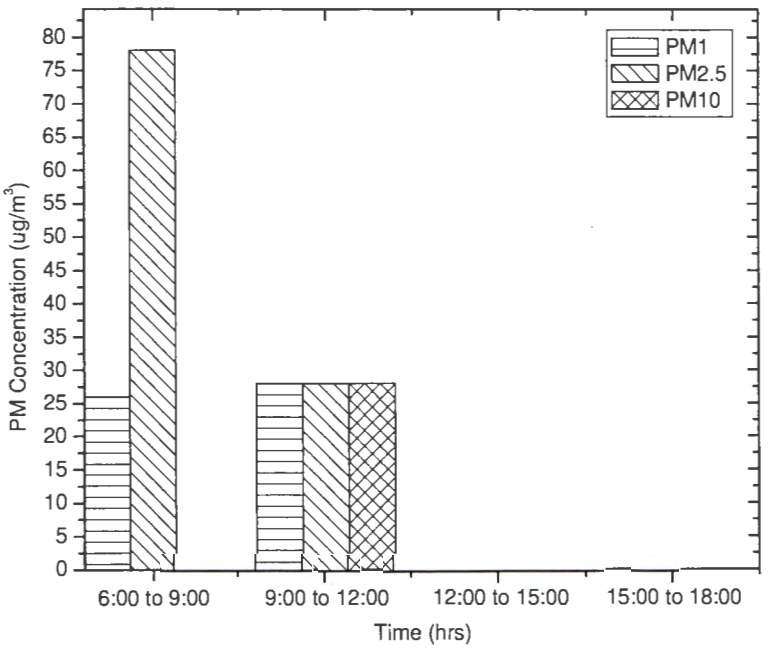

Figure 4.1: Three hourly concentration of PM_{10} for August 20, 2008

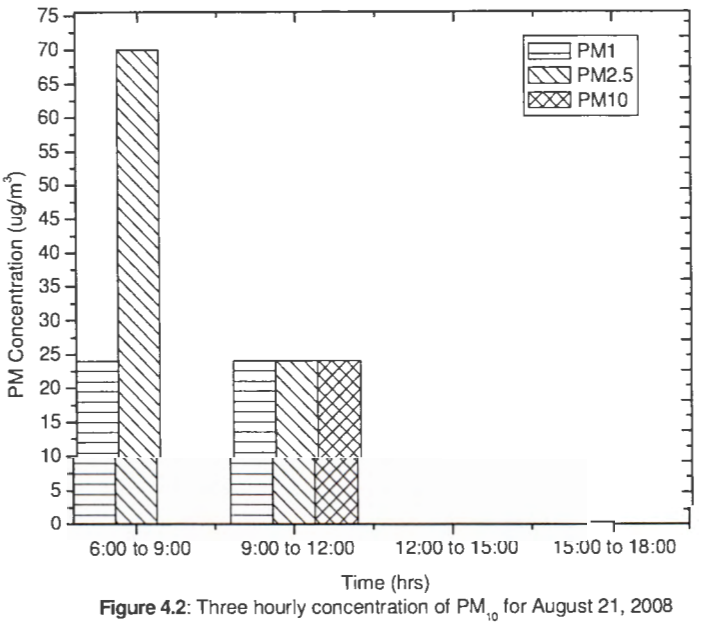

Figure 4.2: Three hourly concentration of PM_{10} for August 21, 2008

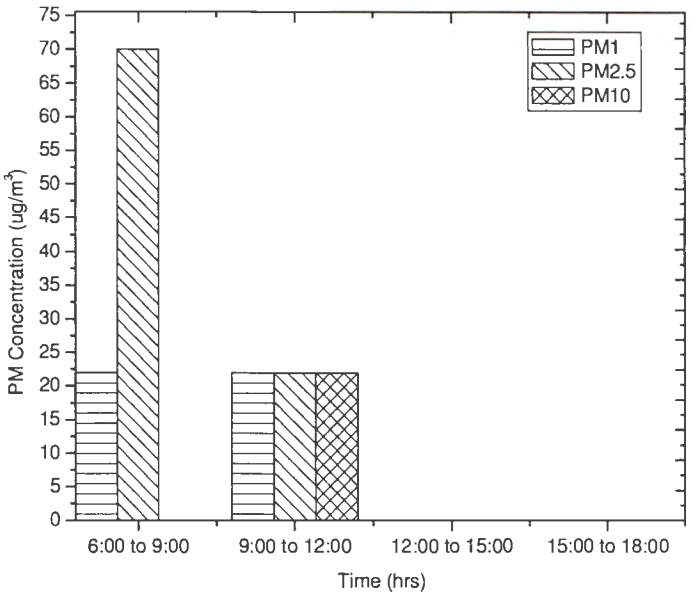

Figure 4.3: Three hourly concentration of PM_{10} for August 22, 2008

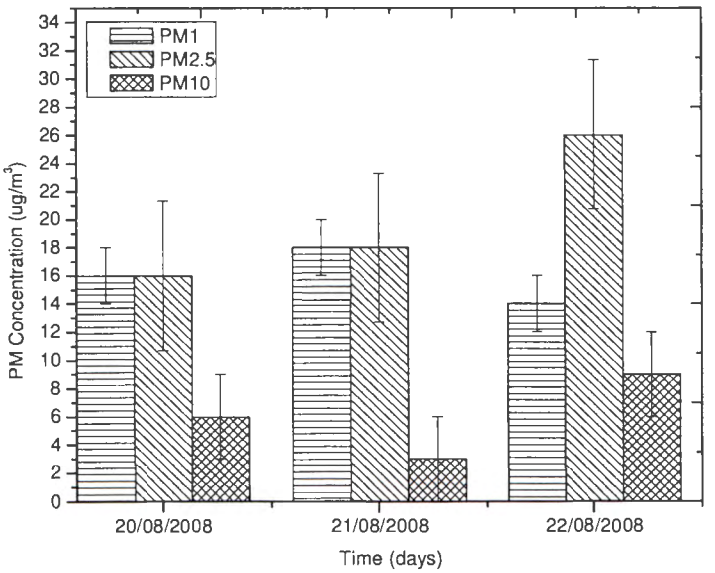

Figure 4.4: Daily concentration of PM_{10} for August 20, 21, 22, 2008

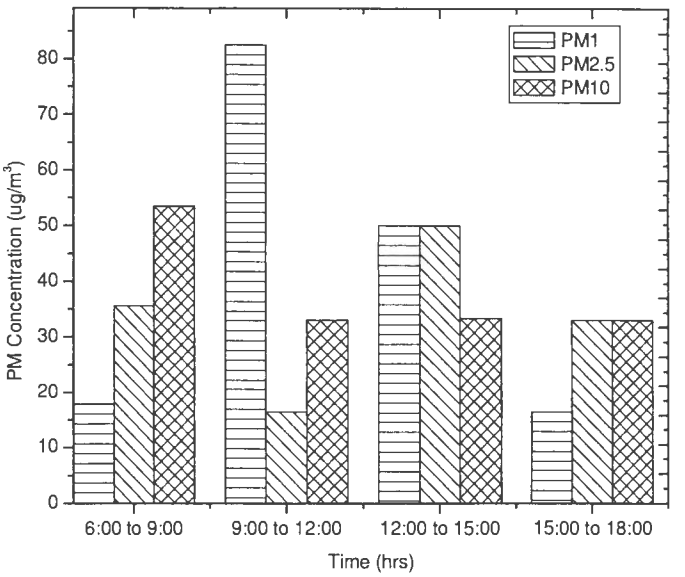

Figure 4.5: Three hourly concentration of PM_{10} for November 11, 2008

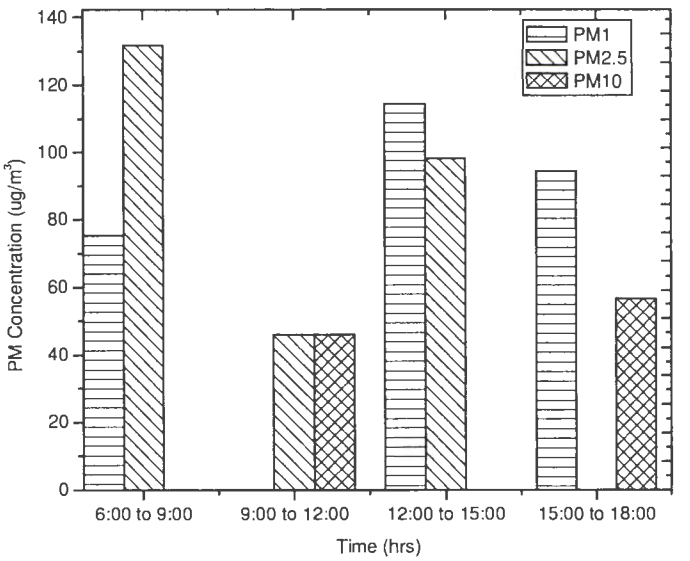

Figure 4.6: Three hourly concentration of PM_{10} for November 12, 2008

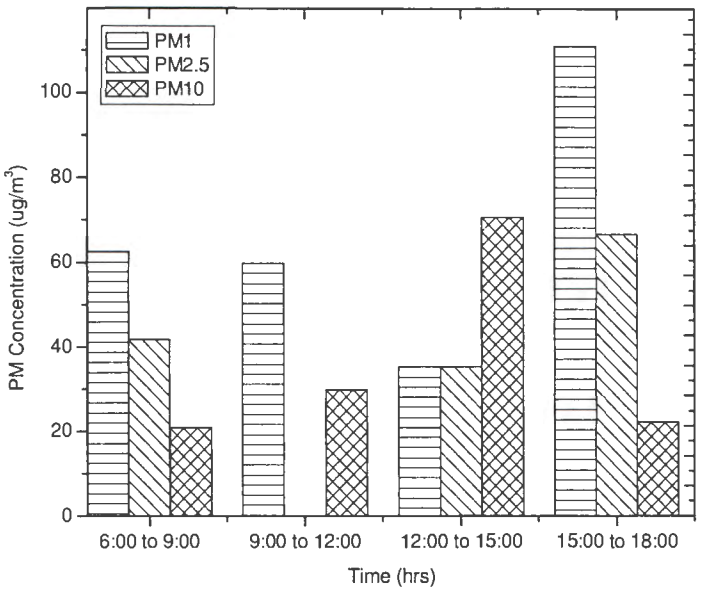

Figure 4.7: Three hourly concentration of PM_{10} for November 13, 2008

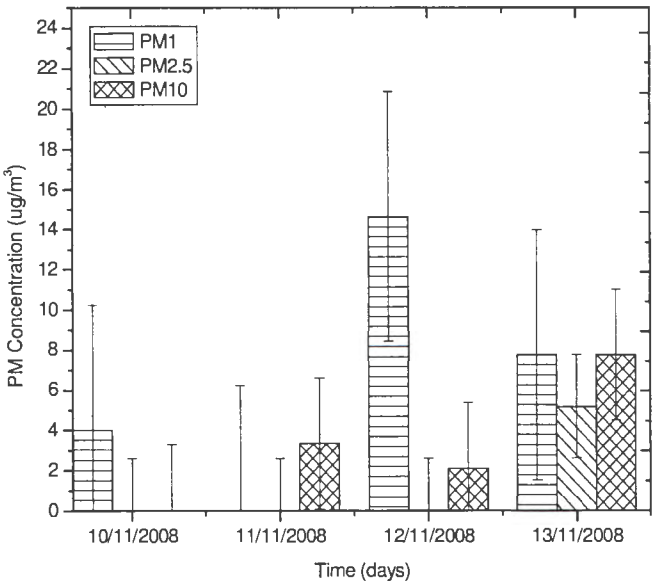

Figure 4.8: Daily concentration of PM_{10} for November 10, 11, 12 & 13, 2008

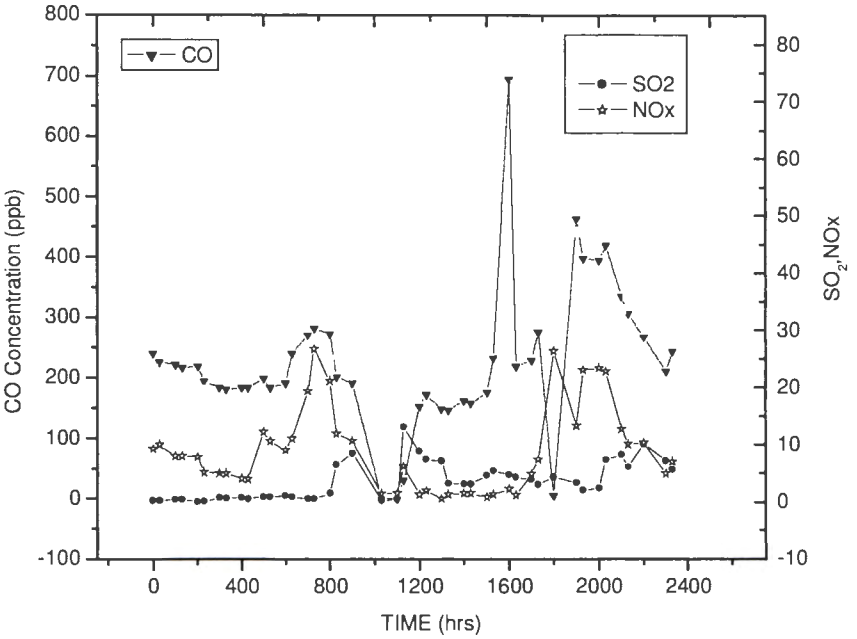

Figure 4.9: Concentration of CO, SO2, NOx versus Time, for August 20, 2008

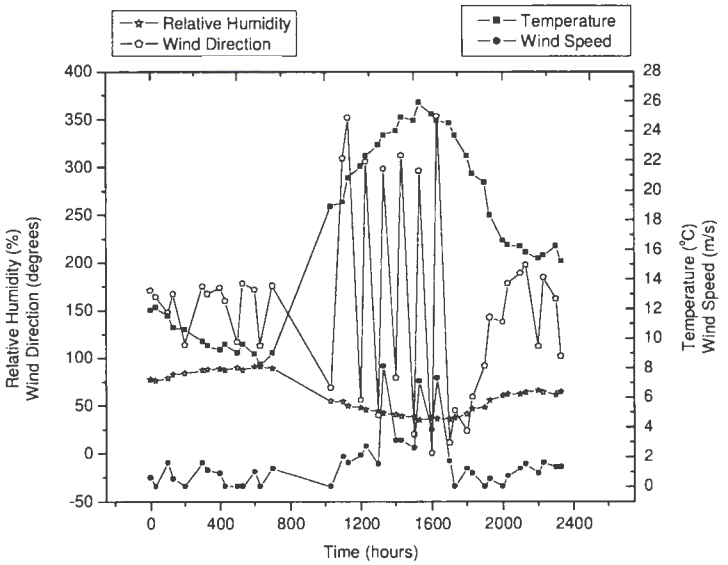

Figure 4.10: Relative humidity, wind speed, wind direction, and temperature versus Time, for August 20, 2008

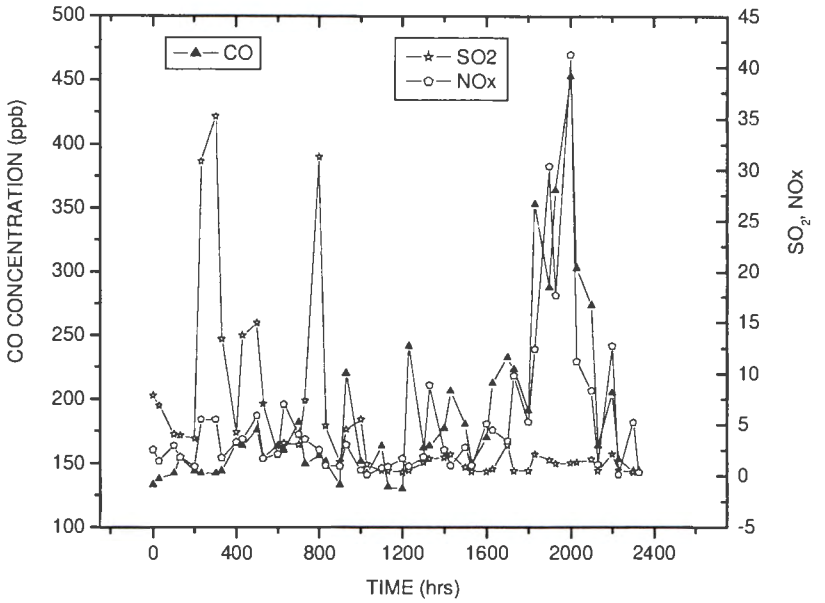

Figure 4.11: Concentration of CO, SO2, NOx versus Time, for November 12, 2008

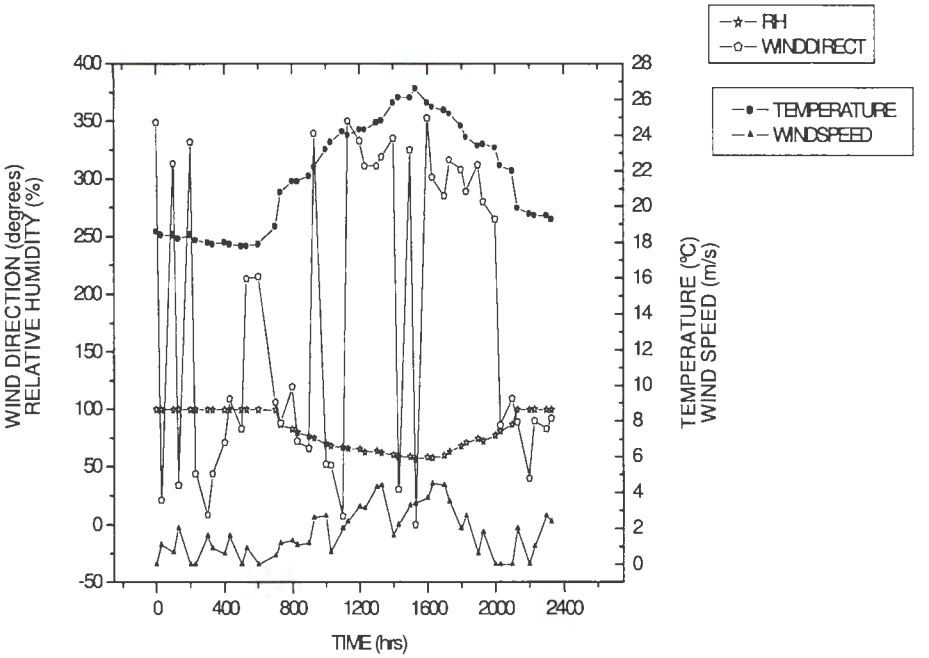

Figure 4.12: Relative humidity, wind speed, wind direction, and temperature versus Time, for November 12, 2008

and then increases again. This behaviour could probably be as a result of precipitation. May is the onset of the Winter season and there is no rainfall during this season. As a result, PM values begin to increase. Since there is no rain from Winter through to Spring, the PM increase trend continues until it reaches maximum values in February.

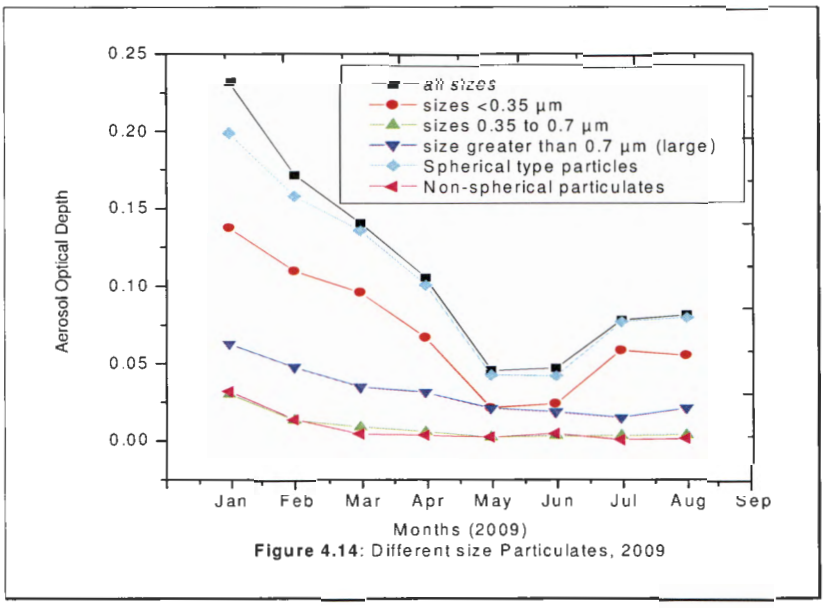

Figure 4.14: Different size Particulates, 2009

Rains begin to fall around November/December. The rain season is at maximum in January/February. This could explain the onset of decreasing values of AOD, as a result of wet deposition of PM. The significance of AOD measurements, apart from giving a qualitative information on the depth of aerosols in the atmosphere, may also help in understanding climatic changes in the environment. The presence of particulates of sizes less than 0.35 µm plays a big role in cloud formation (Eichel et al., 1996). Each aerosol particle attracts ambient moisture and thus behaves as a seed for cloud formation. Smaller PM have longer residence times in the air and however, tend to grow in the presence of ambient moisture, and consequently get deposited on becoming heavy.

4.2 MULTIANGLE IMAGING SPECTRO-RADIOMETER DATA

The **Figure 4.13** displays fractions of different sizes of coarse aerosols PM_{10} and below, for the year 2008 whereas **Figure 4.14** displays fractions of different sizes of coarse aerosols PM_{10} and below, for the year 2009. In both figures, the legend of black graph represents all the sizes combined. The trend of PM behaviour is the same for 2008 and 2009. For example, in both **Figure 4.13** and **Figure 4.14**, it can be seen that of all the combined sizes, the spherical type particles dominate over the non-spherical particles. The particulate sizes less than 0.35 µm contributes, on average 65 % of the total particulate sizes (underlined with a red line in both **Figures 4.13 and 4.14**). This can be so since the ultrafine particulates have longer residence times compared to the larger ones.

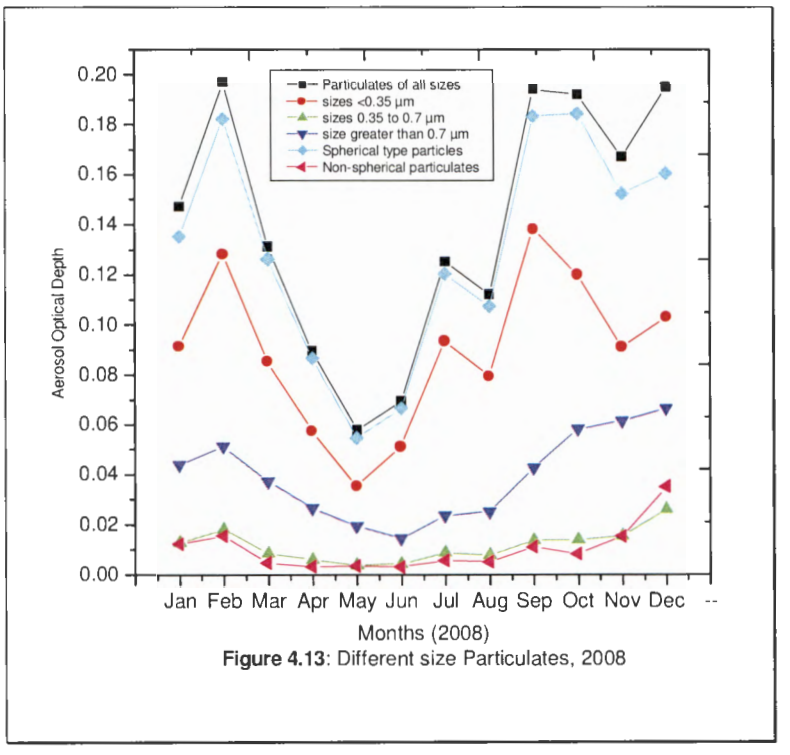

Figure 4.13: Different size Particulates, 2008

Particulate sizes greater than 0.7 µm contribute about 28 % of the total measured aerosols. This fraction includes the 10 µm aerosols. This data gives a qualitative picture of aerosol behaviour in the atmosphere. It does also give a good indication of the vertical presence of PM in the atmosphere. The more the AOD value the more the presence of PM in the atmosphere. From both **Figure 4.13 and Figure 4.14** there is a high load of AOD. This gradually decreases from the months of February to May (minimum values)

4.3 GRIMM EQUIPMENT DATA

4.3.1 Phokeng Study Site

This section covers aerosol measurements done in the town of Rustenburg at Phokeng site. This study site in a major mining area revealed varying aerosol loadings from 0 μgm^{-3} to 200 μgm^{-3} and the aerosols could be linked to both natural emissions as well as anthropogenic origins. The major contributor is human activities as reported in the study conducted by Yigiletu et al. (2011). As can be seen in **Figure 4.15**, in the month of July, measured PM values ranged from 20 μgm^{-3} to 75 μgm^{-3}. This month experienced wind speeds of up to 4 ms^{-1} (**Figure 4.16**), mostly blowing from the northwest (**Figure 4.17**). The temperatures in this month ranged between 0 to 11°C (**Figure 4.18**). Atmospheric moisture content as can be seen in **Figure 4.19**, reached maximum values of about 85%. The month of August was not very different from the previous month in that PM values were within the same range. Minimum values were about 35 μgm^{-3}, and maximum values recorded reached about 80 μgm^{-3} (**Figure 4.15**). Wind speeds in this month were slightly higher, reaching speeds of almost 5 ms^{-1}, blowing mostly from northwest as can be seen in **Figure 4.16.** Temperatures (**Figure 4.18)**, in this month were 2 °C more than the month of July, reaching 14 °C but relative humidity remained the same (**Figure 4.19**). There was a big change in atmospheric aerosol loading in the month of September, with values reaching peaks of almost 200 μgm^{-3}. Lowest recorded values were about 60 μgm^{-3}, (**Figure 4.15)**. This could probably be due to the reduction in atmospheric moisture content (**Figure 4.19**) as winds were still blowing from the northwest (**Figure 4.17**) although blowing at higher speeds, slightly above 6 ms^{-1} (**Figure 4.16**). Temperatures in this month continued to increase, ranging from below 8 °C to 18 °C (**Figure 4.18**). In the month of October, values of PM reduced greatly, from a previous high of 200 μgm^{-3} to a low value of 90 μgm^{-3} (**Figure 4.15**). Wind speeds reduced (**Figure 4.16**) although still flowing from the northwest direction as can be seen in **Figure 4.17.** The only change of interest in meteolorogical conditions was the increase in temperatures, reaching values of 24 °C. Atmospheric aerosol loading for this site continued to record low levels for the rest of the year, 2010. From day 126 to day 172 (November to December, 2010) for 47 days, the Grimm equipment needed servicing from day 288 to day 313 (**Figure 4.15)**. Data during this period was not available due to some minor technical problems which were eventually attended to and the equipment continued to operate

normally. It can be noted that PM levels began to increase gradually in the early 2011 days, reaching levels of 50 μgm^{-3} (**Figures 4.15**). Generally, when wind speeds dropped to less than 2 ms^{-1}, and a corresponding increase in PM can be seen on individual days. Winds (whether from northwesterly or northeasterly), contributed to the increase in concentrations of PM (**Figures 4.15**). Temperature effects on atmospheric aerosol loading cannot be adequately accounted for but their contribution towards a rise in PM cannot be ruled out completely.

Mean monthly PM concentrations and meteorological interactions for Phokeng for the period understudy, (July, 2010 to June, 2011) are summarised in **Figures 4.20, 4.21, and 4.22**.

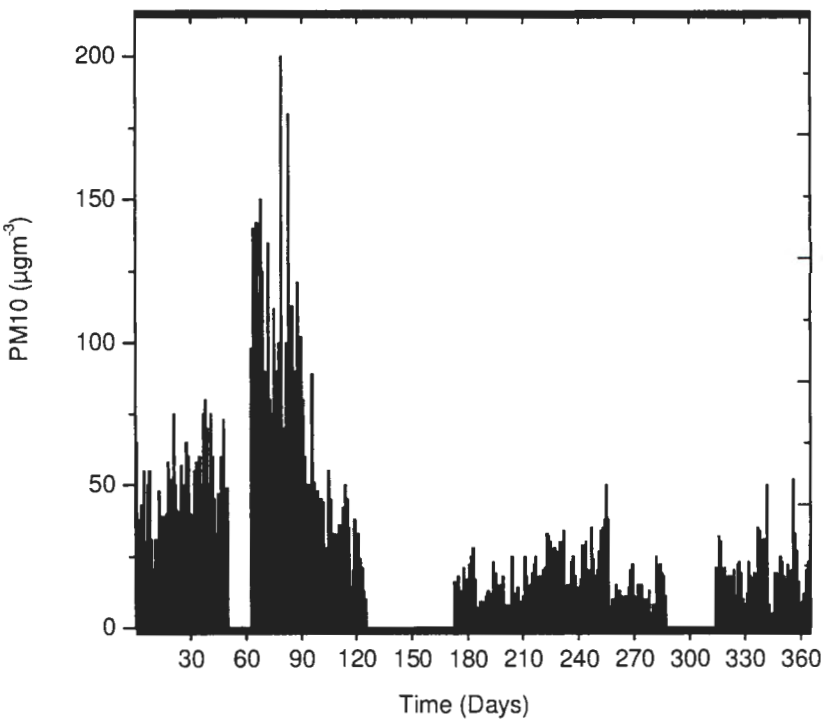

Figure 4.15: Daily mean annual concentration of PM10 for the period of July, 2010 to June, 2011 measured in Phokeng, Rustenburg

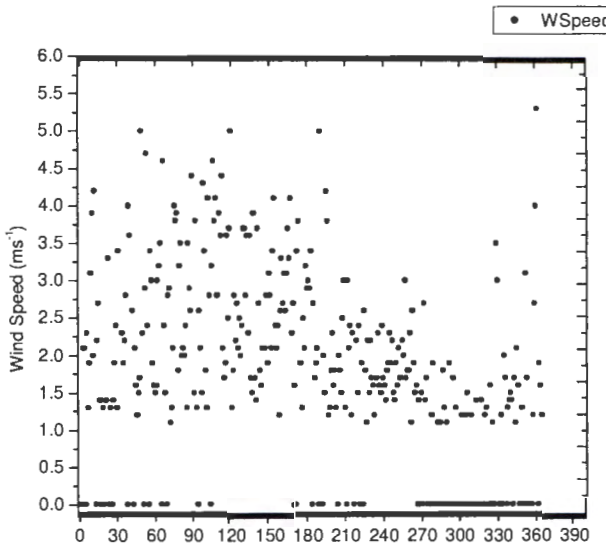

Figure 4.16: Mean annual daily wind speed for the period July, 2010 to June, 2011 in Phokeng, Rustenburg

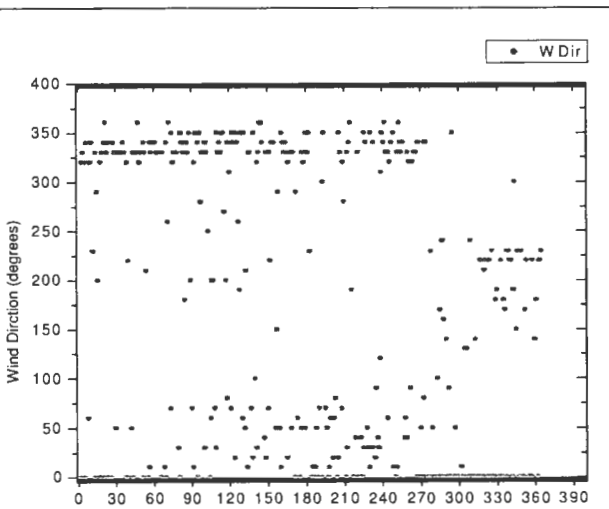

Figure 4.17: Mean Annual daily wind direction for the period July, 2010 to June, 2011 in Phokeng, Rustenburg

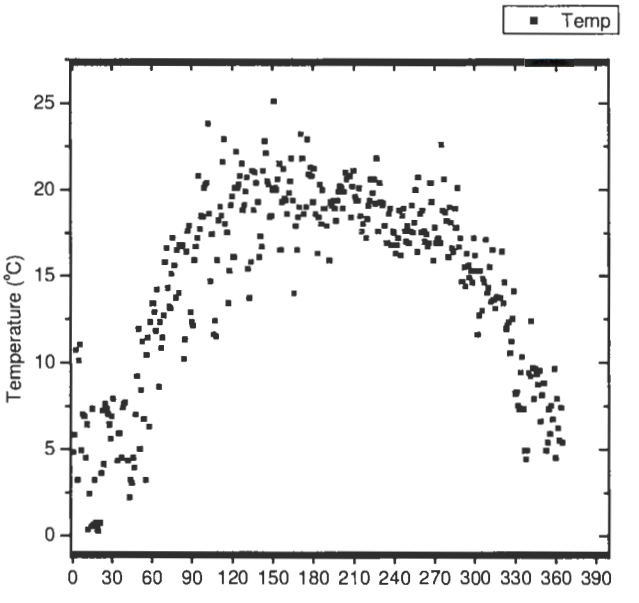

Figure 4.18: Mean daily annual temperature for July, 2010 to June, 2011 in Phokeng, Rustenburg

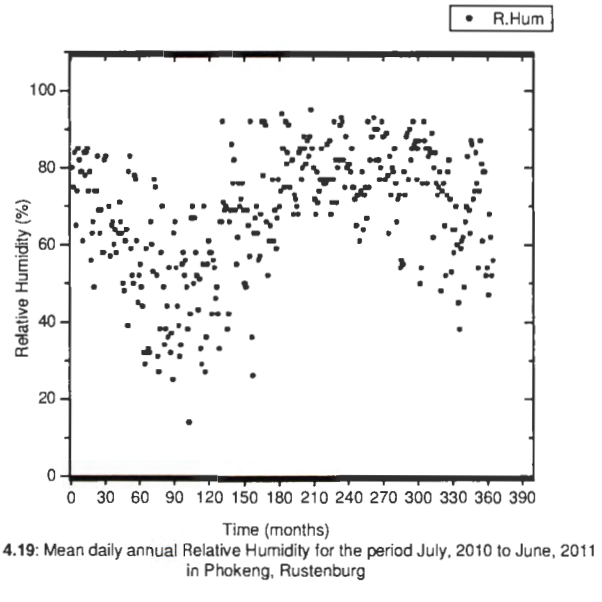

Figure 4.19: Mean daily annual Relative Humidity for the period July, 2010 to June, 2011 in Phokeng, Rustenburg

Mean annual PM_{10} and relative humidity values are presented in **Figure 4.20**. It can clearly be seen that the relative humidity was lowest between the months of July and December. During this period, values of PM_{10} were highest. The high values of the PM_{10} were as a result of the minimal wet deposition as compared to the period between December and June when the relative humidity was high. High values of relative humidity cause the PM_{10} to absorb moisture thereby they become heavier and get deposited easily. Wind speed during the period July to December were low (**Figure 4.21**). This contributed to the values of the relative humidity to remain high resulting in high values of PM_{10}. One other reason is that there was less dilution effects for the PM_{10}. The prevailing winds between the months of July and December were Easterlies (**Figure 4.22**). These could most likely have been one reason of high PM_{10} values. The source of pollution from that direction were contributing to high concentrations of aerosols at this site.

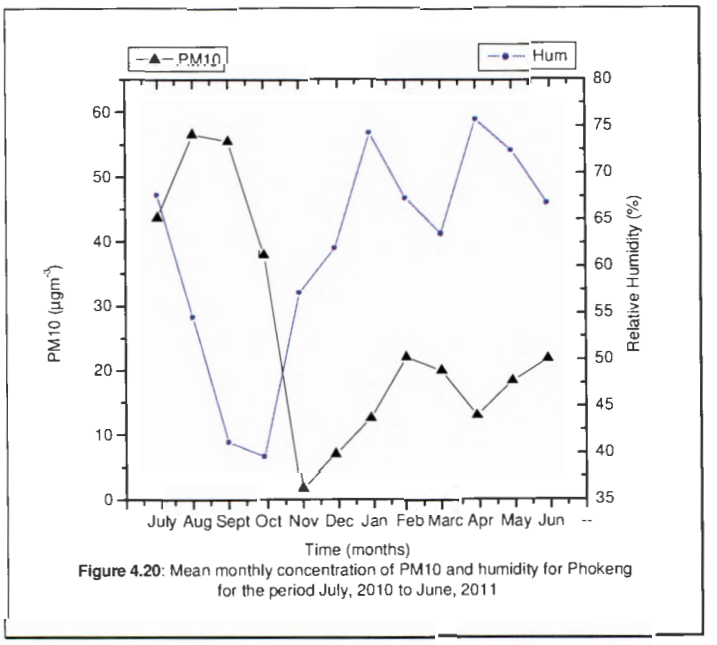

Figure 4.20: Mean monthly concentration of PM10 and humidity for Phokeng for the period July, 2010 to June, 2011

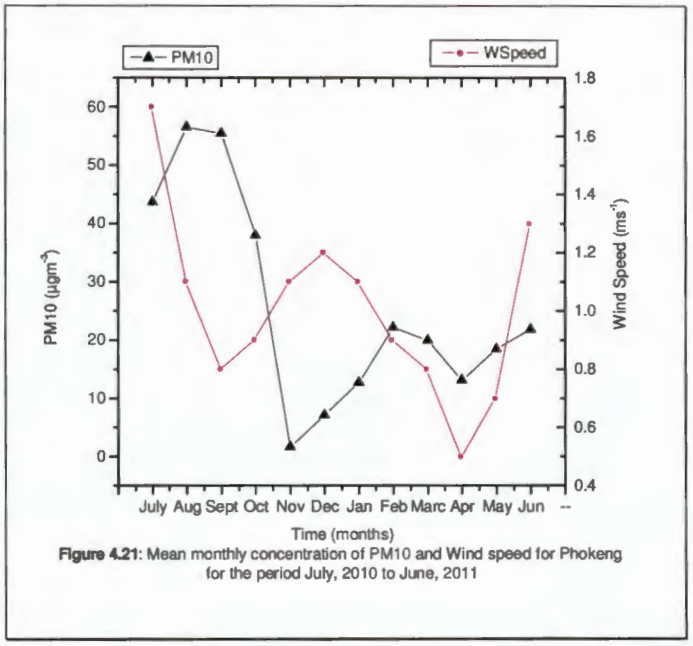

Figure 4.21: Mean monthly concentration of PM10 and Wind speed for Phokeng for the period July, 2010 to June, 2011

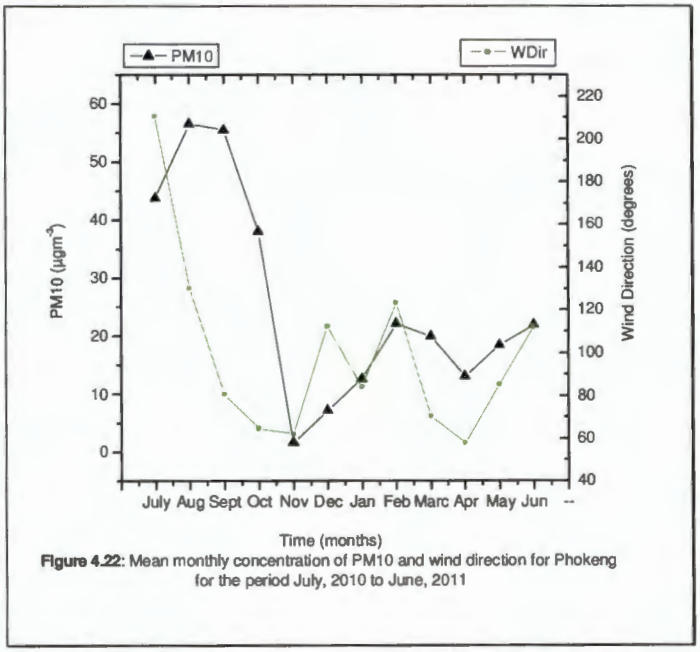

Figure 4.22: Mean monthly concentration of PM10 and wind direction for Phokeng for the period July, 2010 to June, 2011

It is quite evident that there is a higher loading of atmospheric aerosols during winter season than any other season. Winter season begins in June and end in August, but can continue into September. A discussion of the results is presented later in this chapter.

4.3.2 Jouberton Study Site

This study site, located in the town of Klerksdorp mining area, recorded more days of high levels of atmospheric aerosols. The values recorded ranged between 6 μgm^{-3} to 360 μgm^{-3}. The highest aerosol loading in this town happened in the month of August, a winter period (**Figure 4.23**). Almost all the days in this month recorded PM values above 80 μgm^{-3}. Atmospheric aerosol measurements in Klerksdorp were done for 12 months from July 2010 to June 2011, to cover all the seasons.

In the month of July, 2010 (**Figure 4.23**), PM levels were high with all days recording values of over 50 μgm^{-3} with the exception of day 16. Wind speeds ranged from 0 to a high of about 5 ms^{-1} as can be seen in **Figure 4.24**. Wind was blowing from Southeast most of the time - **Figure 4.25**. Temperatures prevailing were below 12 °C in the Winter months (**Figure 4.26**), while atmospheric moisture content ranged from 45 % to 85 % (**Figure 4.27**). This worthy of note is that on the days when the aerosol levels were high, atmospheric moisture content dropped significantly. This implies a marked reduction of wet deposition of aerosols. Another interpretation could be that since wind speeds were also very low, dilution effects were minimal. In the month of August, 2010 (day 60 in **Figure 4.23**), there were no recordings for PM levels below 50 μgm^{-3}. Wind speeds were below 2 ms^{-1} throughout the whole month. The highest aerosol loading was recorded when there was no wind blowing. Since there was no dilution effect of wind movement, accumulation of aerosols in the air prevailed. It is also worthy of note that since there was no wind (calm conditions), the aerosols could be generated from within the locality. Humidity ranged from 20 % to 80 %. Temperatures on the other hand can be seen to have increased, ranging from 7 °C to over 18 °C.

Klerksdorp, like Rustenburg, showed high atmospheric aerosol level recording well into September and beyond. But as pointed out in the case of Phokeng, Rustenburg, although Winter season officially ends in August, it does extend into September. The atmospheric moisture content in September is lower than in either July or August, ranging from below 20 % to slightly above 70 %. Particulate matter concentrations in the air range from 50 μgm^{-3} to 210 μgm^{-3}. Wind speeds were just beginning to rise from zero when the high levels of the aerosols were recorded. The effects of almost zero winds coupled with low levels of humidity allowed for the accumulation of atmospheric aerosols.

Unlike Phokeng, Rustenburg, PM level records still showed above 100 μgm^{-3}. Wind speeds during the days of high PM values were below 2 ms^{-1}, mostly blowing from southeast. Humidity levels for these high PM peak values were on average below 50 %. The contribution of temperatures are not so clear as they averaged highs of above 22 ^{o}C as can be seen from **Figure 4.26**. One possible explanation could be that at high temperatures, irradiance is high. This promotes chemical species to react (endothermic processes) by breaking as well as combining, in the boundary layer, thereby forming molecules that have large diameters. These become heavy and get measured as PM_{10}, on their way to earth surface where they are deposited.

Atmospheric aerosol levels began to show a decrease from the month of November, and this trend continued until December. The month of January, 2011, showed some upward trend of PM values, but declined again slightly. A clear trend of the behaviour of the annual atmospheric aerosol loading in Klerksdorp is shown in **Figure 4.28**. There was more aerosol loading in the Winter than any other season. As in the case of Rustenburg, the days of no wind blowing recorded elevated PM levels. Annual averaged of PM_{10} and relative humidity values are presented in **Figure 4.28**. It can clearly be seen that the relative humidity was lowest between the months of July and December. During this period, values of PM_{10} were highest. The high values of the PM_{10} were as a result of the minimal wet deposition as compared to the period between December and June when the relative humidity was high. High values of relative humidity cause the PM_{10} to absorb more moisture thereby they become heavier and get deposited easily. Wind speed during the period of high PM_{10} values between July October ranged from 1.6 ms^{-1} to 2.7 ms^{-1} (**Figure 4.29**). It would be expected that these speeds could dilute the concentration of the PM_{10}. However, this is not the case. A possible explanation is that since these winds were blowing mostly from the Westery direction (**Figure 4.30**), more aerosols were being transported from that direction to the study site. As observed in the Phokeng site, the PM_{10} values were significantly more during the period July to September. This is a Winter period. The high PM_{10} values in this site are also recorded in Wirter season.

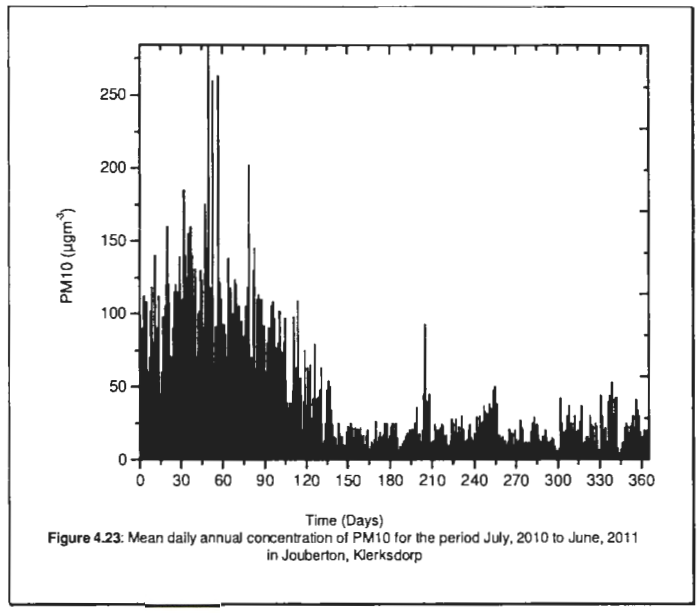

Figure 4.23: Mean daily annual concentration of PM10 for the period July, 2010 to June, 2011 in Jouberton, Klerksdorp

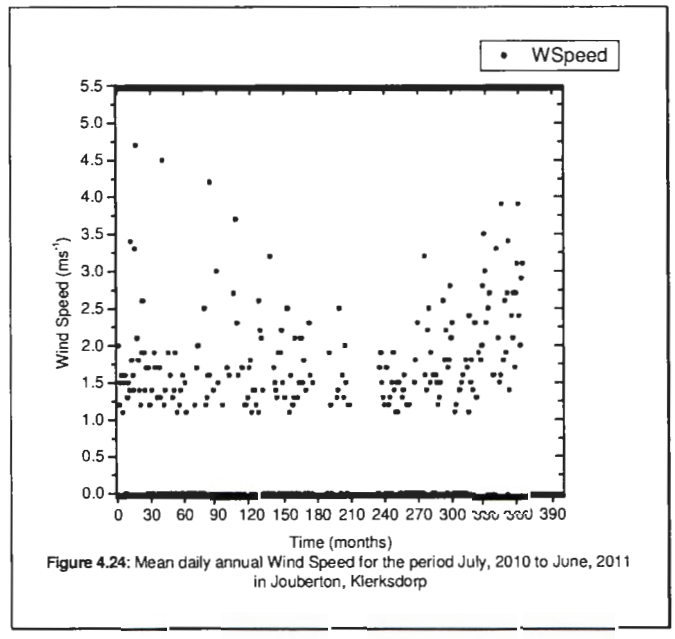

Figure 4.24: Mean daily annual Wind Speed for the period July, 2010 to June, 2011 in Jouberton, Klerksdorp

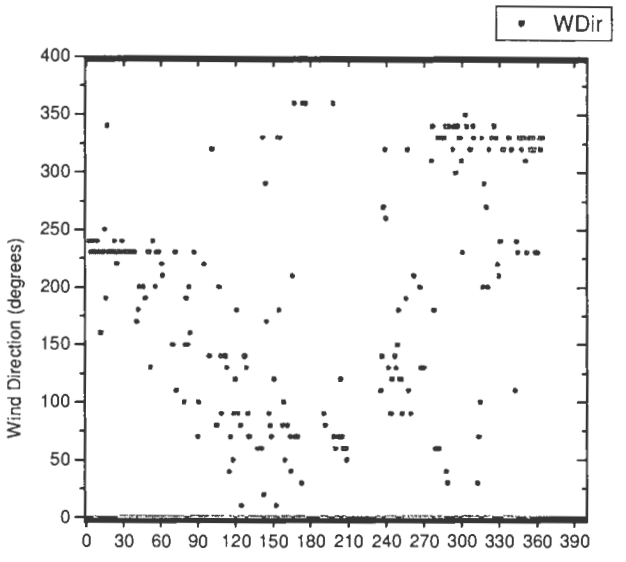

Figure 4.25: Mean daily annual Wind Direction for the period July, 2010 to June, 2011 in Jouberton, Klerksdorp

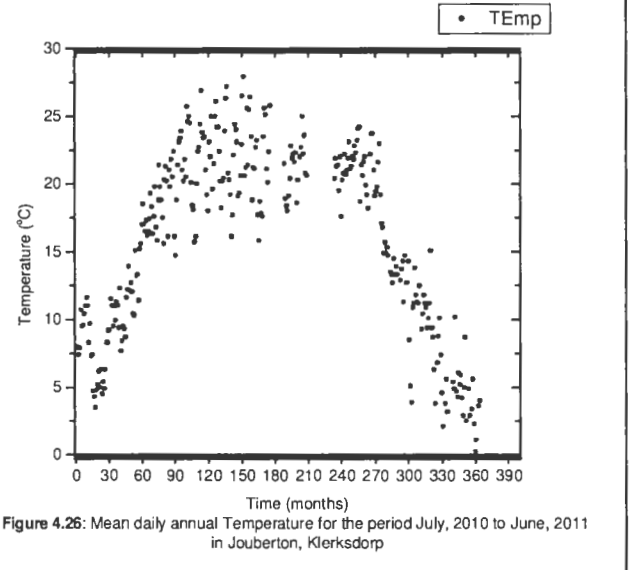

Figure 4.26: Mean daily annual Temperature for the period July, 2010 to June, 2011 in Jouberton, Klerksdorp

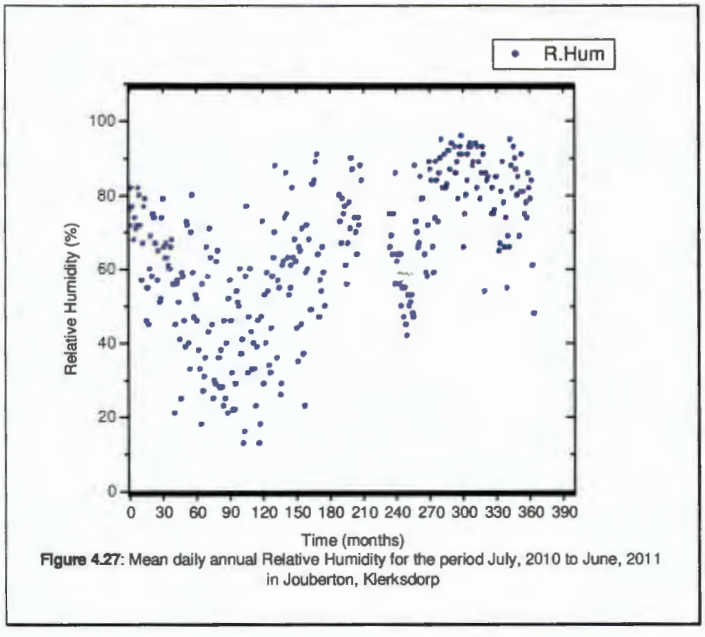

Figure 4.27: Mean daily annual Relative Humidity for the period July, 2010 to June, 2011 in Jouberton, Klerksdorp

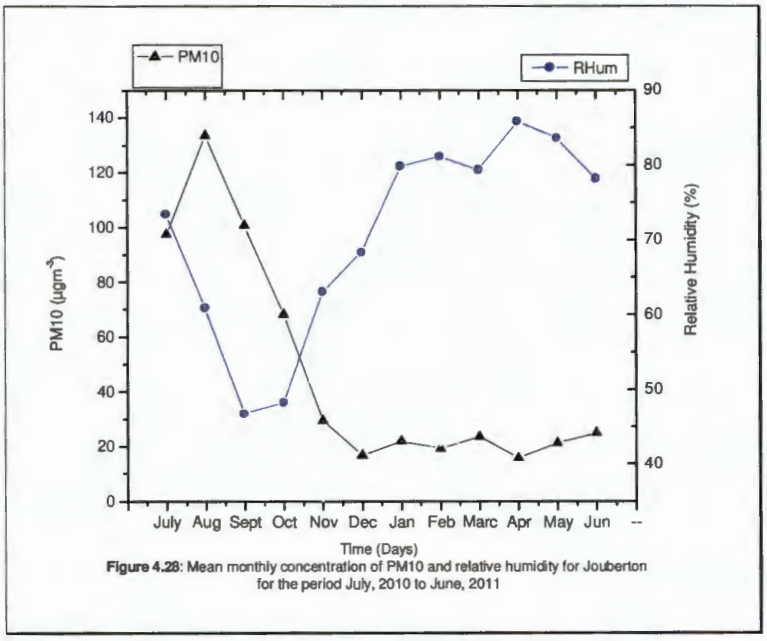

Figure 4.28: Mean monthly concentration of PM10 and relative humidity for Jouberton for the period July, 2010 to June, 2011

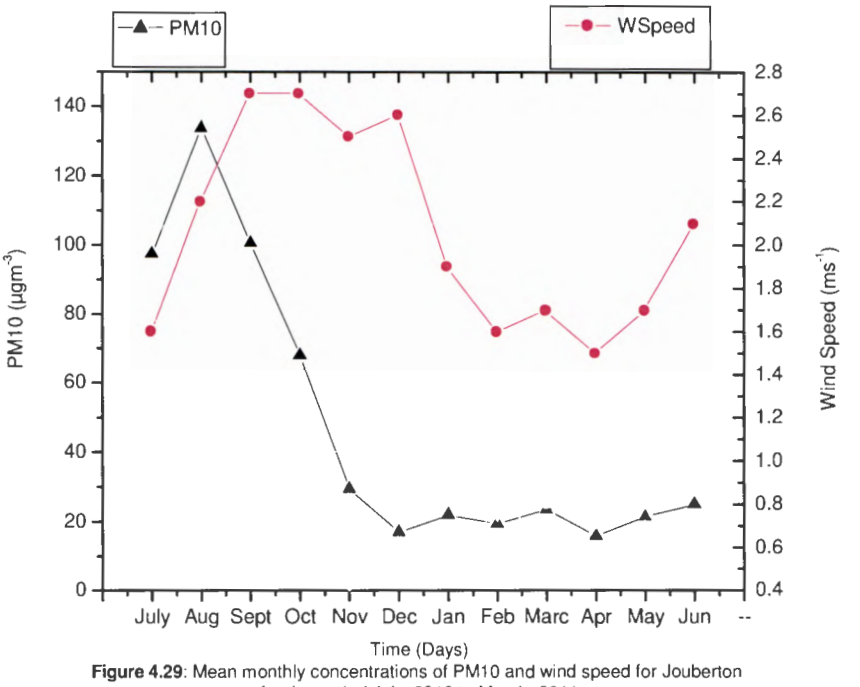

Figure 4.29: Mean monthly concentrations of PM10 and wind speed for Jouberton for the period July, 2010 to March, 2011

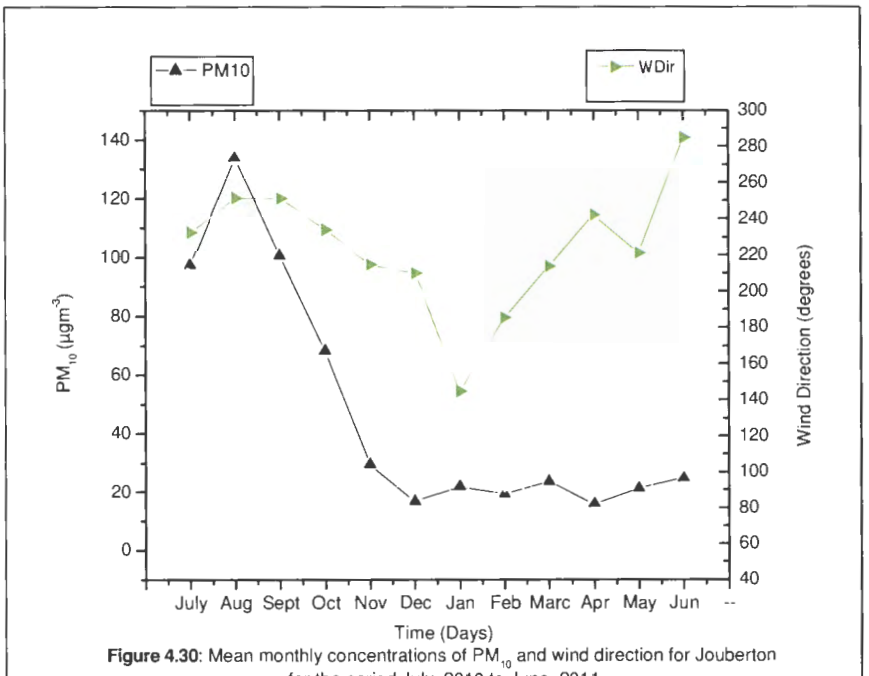

Figure 4.30: Mean monthly concentrations of PM_{10} and wind direction for Jouberton for the period July, 2010 to June, 2011

4.3.3 Mafikeng Comparison

Mafikeng town is the capital city of the Northwest Province and is relatively undeveloped town in terms of industrial activities in comparison to Klerksdorp and Rustenburg. The main commercial activities found in this town are tourism related. Ground-based atmospheric aerosol measurements were done in April to June 2009, using the Grimm equipment and in 2011 using LIDAR. The objective of this study was also to make a comparison between the industrialized zones (Klerksdorp and Rustenburg) and the non industrialized zone (Mafikeng). Representative plots show the PM_{10} values obtained are presented in **Figures 4.31, 4.32, and 4.33**. From the results presented in the three Figures, it can be seen that all the PM_{10} values lie below the South African Air Quality Guidelines for the 24 hour average of 75 μgm^{-3}. This is very far below those of Rustenburg and Klerksdorp.

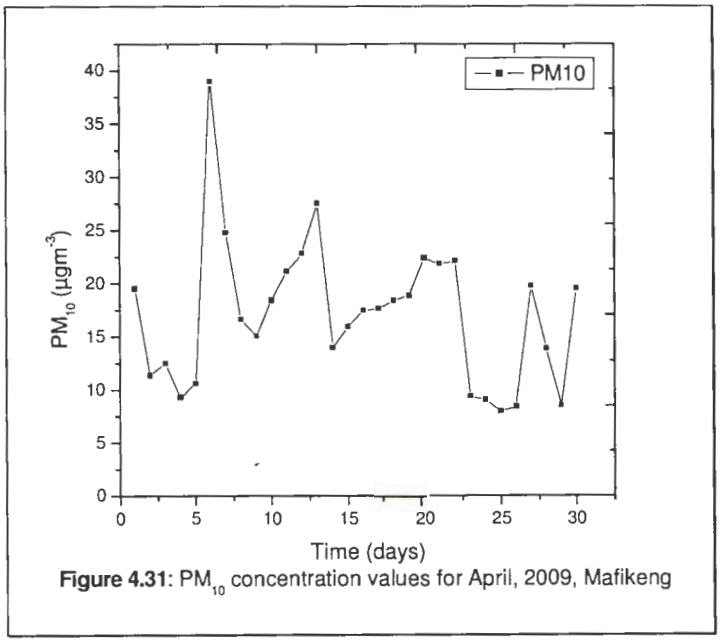

Figure 4.31: PM_{10} concentration values for April, 2009, Mafikeng

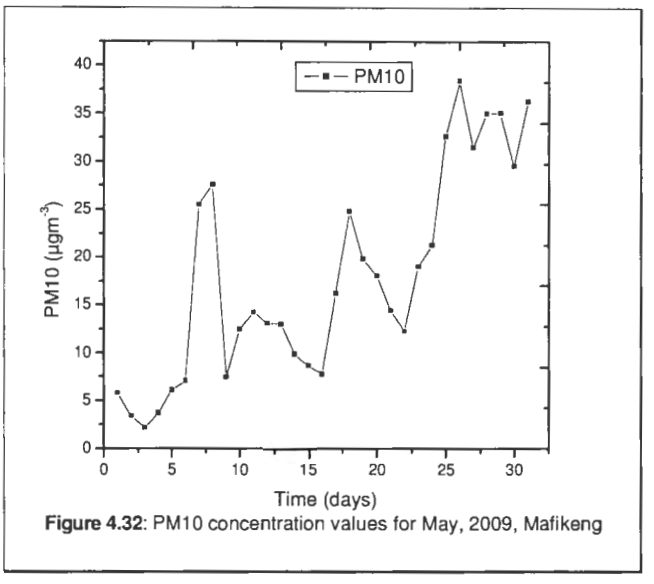

Figure 4.32: PM10 concentration values for May, 2009, Mafikeng

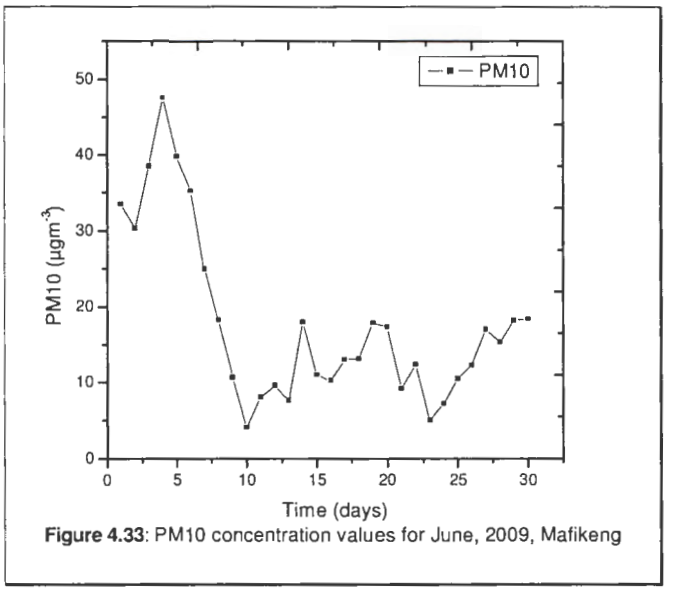

Figure 4.33: PM10 concentration values for June, 2009, Mafikeng

AOD values were obtained over three days, 6 to 8 September, 2011. Angstrom coefficient was also calculated to determine the sources of particulates in Mafikeng. The data is presented **Figures 4.34 and 4.35**.

The boundary layer in **Figure 4.34** shows increase of aerosols in the atmosphere from 16:00 and got to the peak at 18:00. The same behaviour is observed in **Figure 4.35**. The scale next to the figure explains the meaning of different colours. The deep red

signifies the presence of aerosols. Skull (1988), describes the atmospheric boundary layer as the part of the troposphere that is directly influenced by the presence of the earths surface, and responds to surface forcings with a time scale of about an hour or less. The solar heating causes thermal plumes to rise, transporting moisture, heat and aerosols. Since there are almost no aerosol generating industries in Mafikeng, the peak in the boundary layer can only be attributed to traffic. **Figure 4.34** is showing the red band of length 0.5 km at 11:00 hours. This red band increases towards 1 km as time approaches 12:00, drops a little and increases again between 13:00 hours and 14:00 hours. The increase in the height of the band is as a result of traffic increase towards lunch hour. It lowers slightly as people settle for their lunch, but increases again as they go back to their work places. As the temperature rises in the day, it promotes chemical reactions of atmospheric aerosols in the atmosphere thereby keeping the boundary layer in the high levels. Afternoon traffic increase contributes to high PM concentrations. This is observed in the continuous high level of the red band, indicating contribution of PM from traffic **Figure 4.35**. Red band height begins to lower as traffic reduces after 20:00 hours. A further contribution towards the lowing of the red band is the drop in temperatures after 18:00 hours.

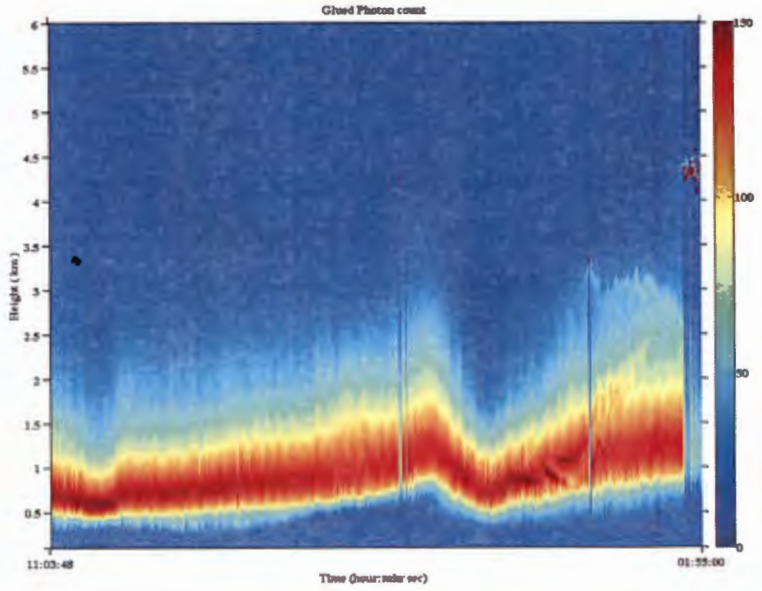

Figure 4.34: Atmospheric Aerosol Measurement by LIDAR on 27 September, 2011, Showing Boundary Layer

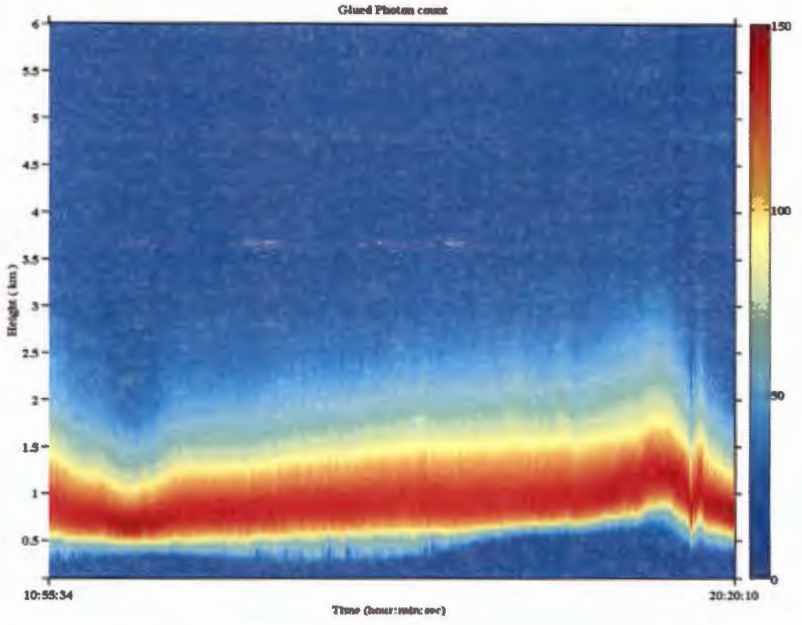

Figure 4.35: Atmospheric Aerosol Measurement by LIDAR on 28 September, 2011, Showing Boundary Layer

4.3.4 Kanana Site, Klerksdorp

Measurements of PM_{10} were done in 2009 in Kanana, another area in Klerksdorp but logistical problems necessitated the relocation to Jouberton. The results are presented below. The results obtained from air samples in the months of April, May and June, 2009, for Kanana, a Klerksdorp Gold Mining Town, are as presented **Figures 4.36 – 4.44**. April and May are autumn months in South Africa. June is one of the months of winter season. In the month of April, high values (above 70 μgm^{-3}) of particulate matter appear 18 times as can be seen from **Figure 4.36**. The highest value of particulate matter recorded was about 130 μgm^{-3} on 20 April, 2009. On the days 18 – 20 April, winds blowing were mostly South easterlies as can be seen in **Figure 4.37**. The probability that these winds are responsible for the high particulate matter values are high. Low wind speeds were recorded during these three days – **Figure 4.38**. Low wind speeds favour high particulate matter values. In the month of May, high values (above 70 μgm^{-3}) of particulate matter appear 11 times as can be seen from **Figure 4.39**. The highest value of particulate matter recorded was about 200 μgm^{-3} on 29 May, 2009. Northwest winds prevailed during the time of high recorded values of particulate matter (**Figure 4.40**). Wind speed for this

period was below 2ms^{-1}, favouring high particulate matter values (**Figure 4.41**). Wind direction appears not to be the conclusive contributor of high recorded values of particulate matter as can be seen in **Figure 4.36, 4.39** and **4.42**. The winter month of June shows the highest value of particulate matter recorded as about 206 µgm^{-3} on the 4th day of the month. However, high values (above 70 µgm^{-3}) of particulate matter appear 9 times as can be seen from **Figure 4.42**. In April, on the average, winds were mostly southeast for most of the month. These winds appear to have caused the high values of the particulate matter recorded. From **Figure 4.38**, it can be noted that these winds were mostly having speeds of about 2 ms^{-1}. The month of May experienced winds blowing from Southeast as well. In this month the high values for the particulate matter appear to be blown in from all directions. Wind speeds for these high values were relatively low, less than 2 ms^{-1} (**Figure 4.41**). In the month of June (just like April and May), on average winds, were mostly Southeast (**Figure 4.43**). These winds again appear to have caused the high values of the particulate matter recorded. From **Figure 4.44**, these winds were mostly having speeds of less than 2 ms^{-1} as in May. It can be observed from the PM_{10} graphs and wind speed graphs that wind speeds above 2 ms^{-1} had a scouring effect, that is, they tended to lower the values of the particulate matter recorded in all the three months.

Aerosol behaviour in Kanana is similar to that of Jouberton, both areas are in Klerksdorp. This implies that Klerksdorp receives high atmospheric aerosol loading, especially in the winter season. The range of PM concemtrations found in Kanana (200 µgm^{-3} to 300 µgm^{-3}) are similar to those Harrison et al, (1997) found in Birmingham, U.K.

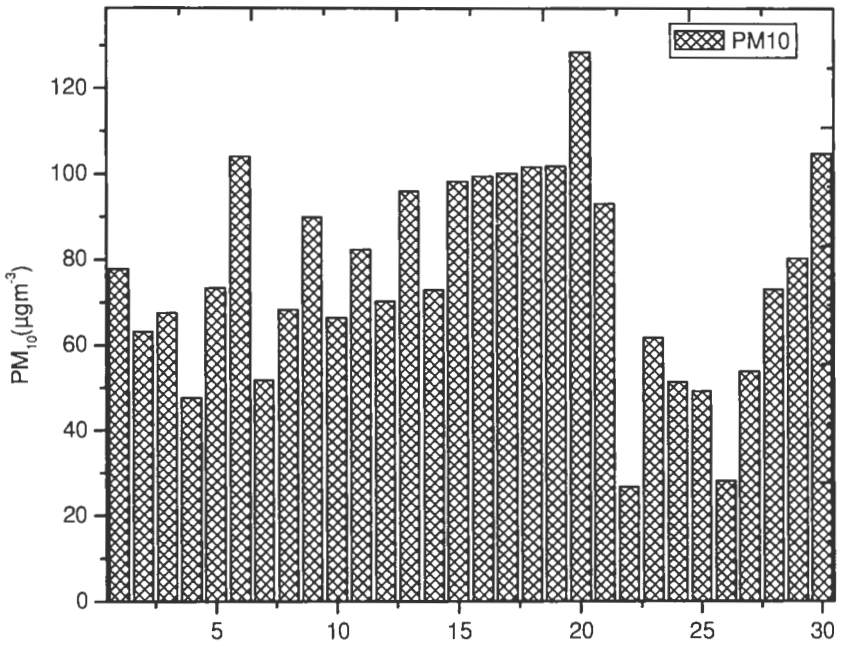

Figure 4.36: Mean daily concentrations of PM10 for the period of April, 2009, in Kanana

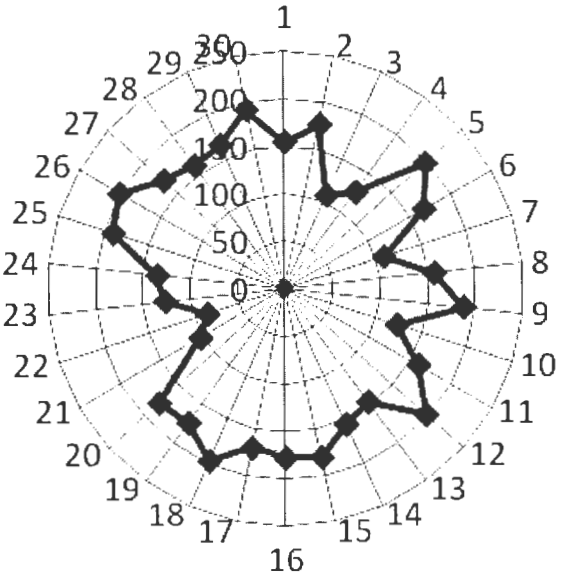

Figure 4.37: Wind direction conditions for each day in the month of April, 2009, in Kanana

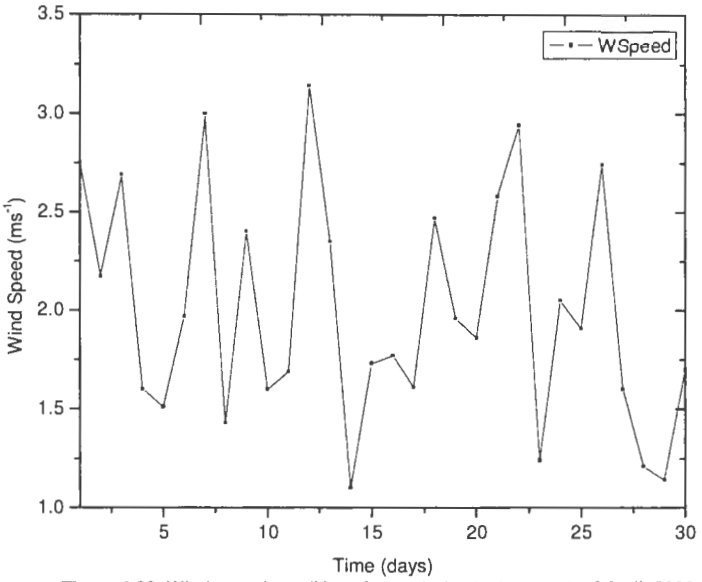

Figure 4.38: Wind speed conditions for each day in the month of April, 2009, in Kanana

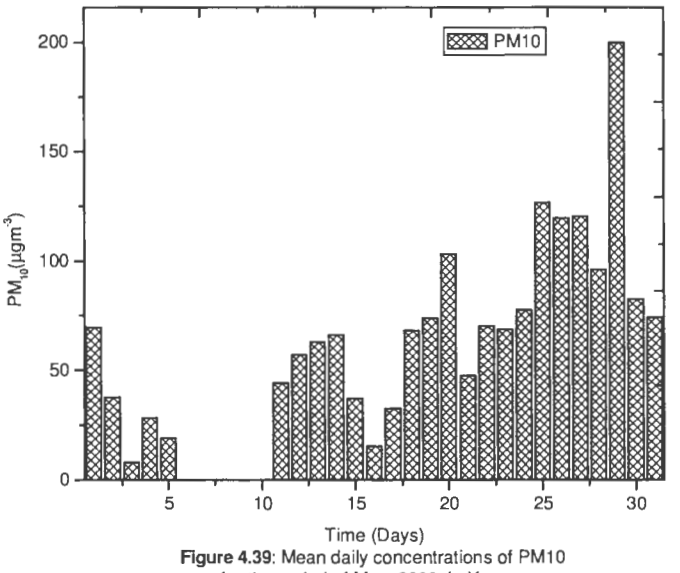

Figure 4.39: Mean daily concentrations of PM10 for the period of May, 2009, in Kanana

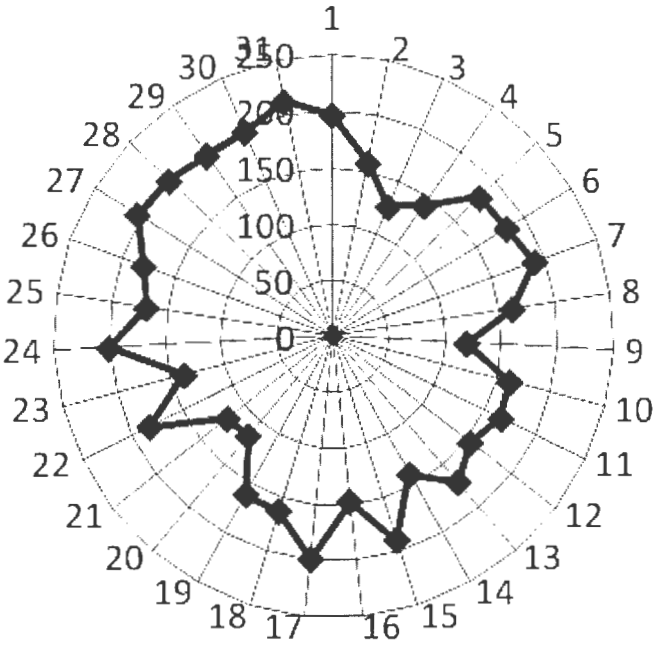

Figure 4.40: Wind direction conditions for each day in the month of May, 2009 in Kanana

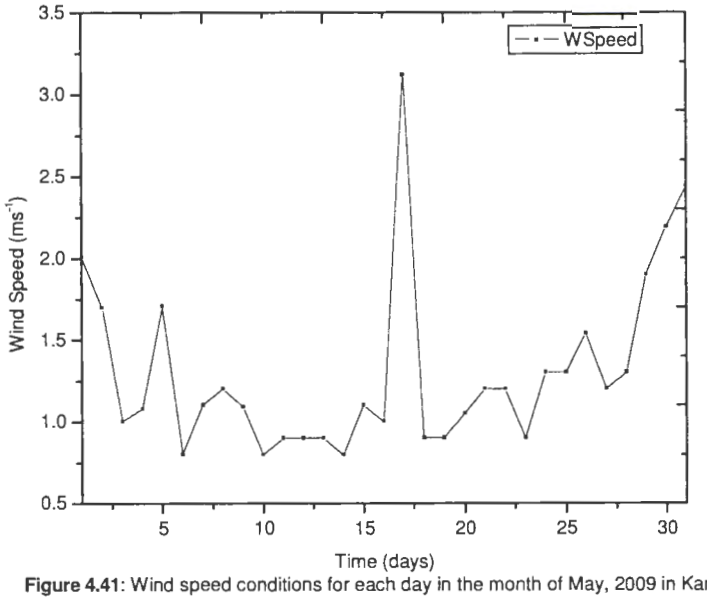

Figure 4.41: Wind speed conditions for each day in the month of May, 2009 in Kanana

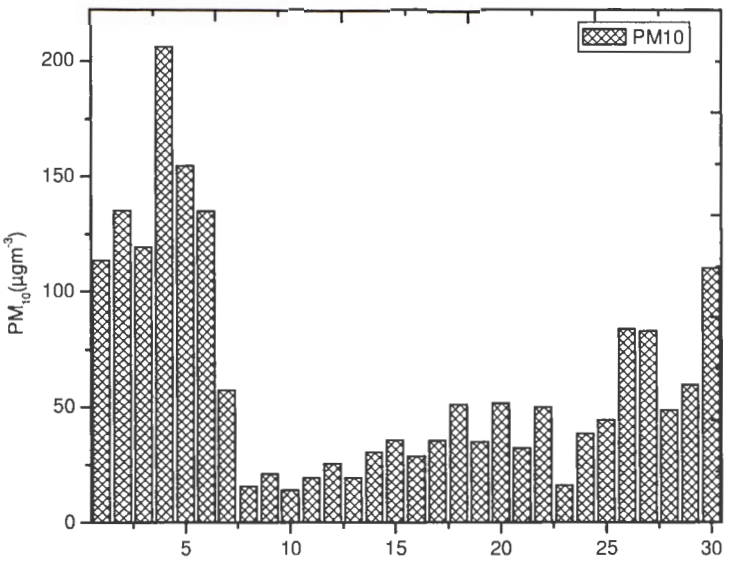

Figure 4.42: Mean daily concentrations of PM10 for the period of June, 2009, in Kanana

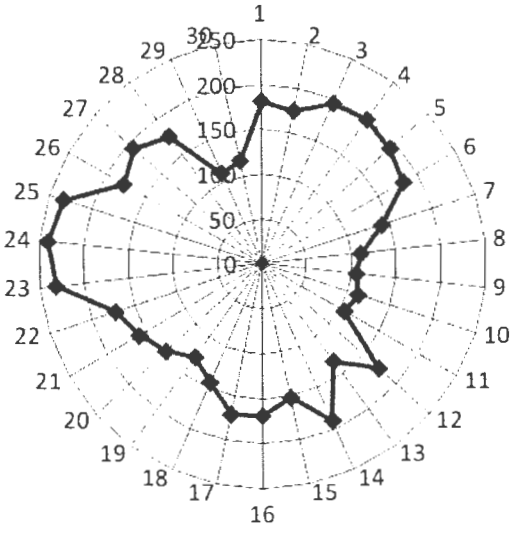

Figure 4.43: Wind direction conditions for each day in the month of June, 2009 in Kanana

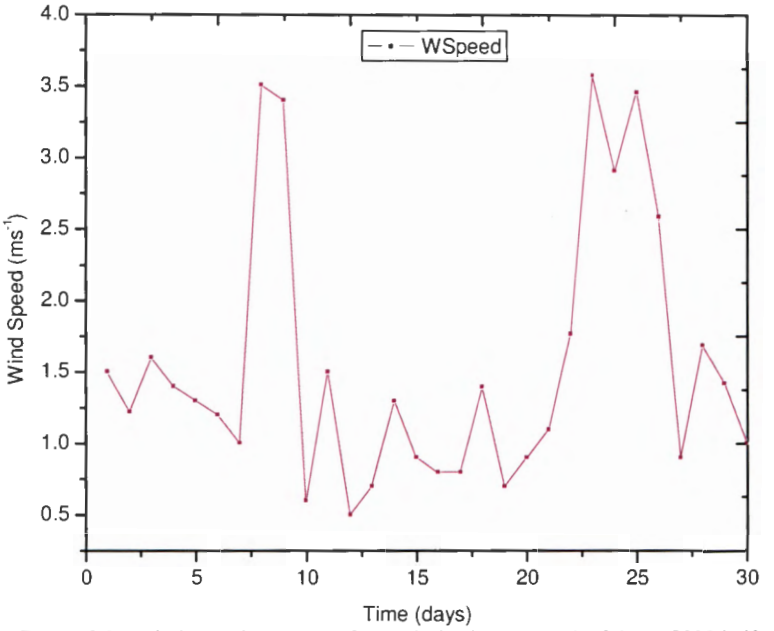

Figure 4.44: Wind speed conditions for each day in the month of June, 2009 in Kanana

4.3.5 Comparison of Concentration of PM_{10} for Phokeng, Rustenburg and Jouberton, Klerksdorp Sites

A comparison of the two study sites (Rustenburg and Klerksdorp) shows that there is a higher atmospheric aerosol loading in Klerksdorp than in Rustenburg (**Figure 4.45**).

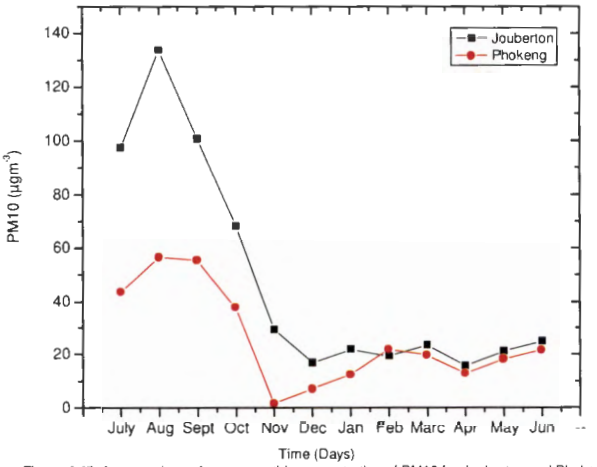

Figure 4.45: A comparison of mean monthly concentration of PM10 for Jouberton and Phokeng for the period of July, 2010 to June, 2011

Although **Figure 4.46** shows that the mean monthly humidity was higher throughout the year in Jouberton than in Phokeng, Jouberton shows higher PM values than Phokeng. There should have been more aerosol wet deposition in Jouberton than in Phokeng. This, however, was not the case. A logical explanation could be that although there is more wet deposition in Jouberton (Klerksdorp), the town generates more atmospheric aerosols compared to Phokeng (Rustenburg).

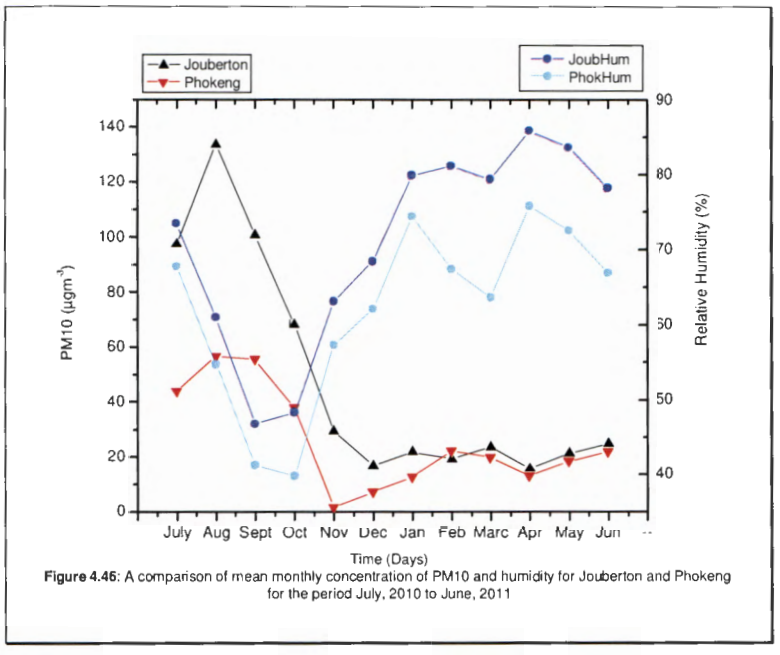

Figure 4.46: A comparison of mean monthly concentration of PM10 and humidity for Jouberton and Phokeng for the period July, 2010 to June, 2011

Klerksdorp is a gold mining area whereas Rustenburg is a platinum mining area. It is difficult however to conclude that gold mining activities generate more aerosol loading than platinum mining activities. A consideration must be taken into account the development in other sectors like industry, transport network, or let alone agriculture, in these towns. On analysing prevailing wind speeds (**Figure 4.47**), again Jouberton recorded higher wind speed values than Phokeng. An effect of more atmospheric aerosol dilution is expected in Jouberton than in Phokeng; but this is not the case.

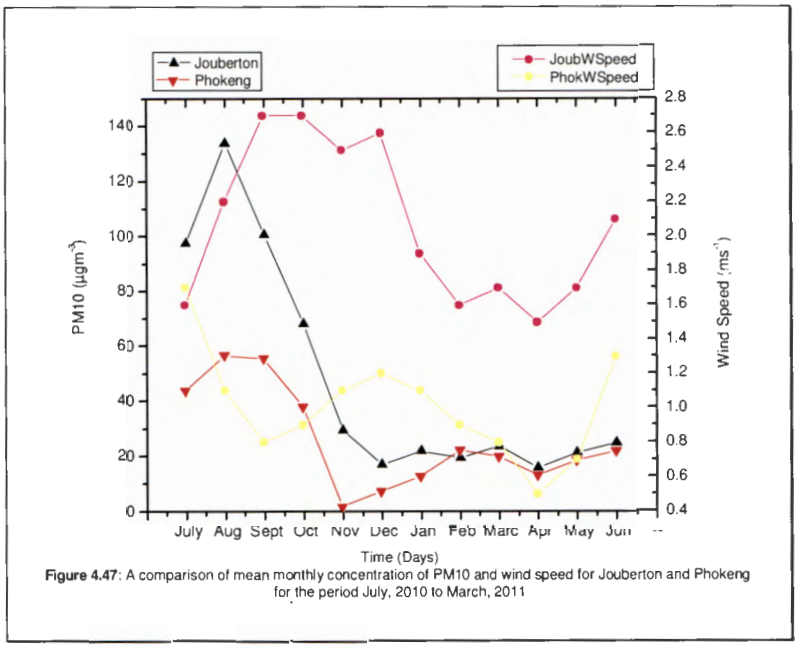

Figure 4.47: A comparison of mean monthly concentration of PM10 and wind speed for Jouberton and Phokeng for the period July, 2010 to March, 2011

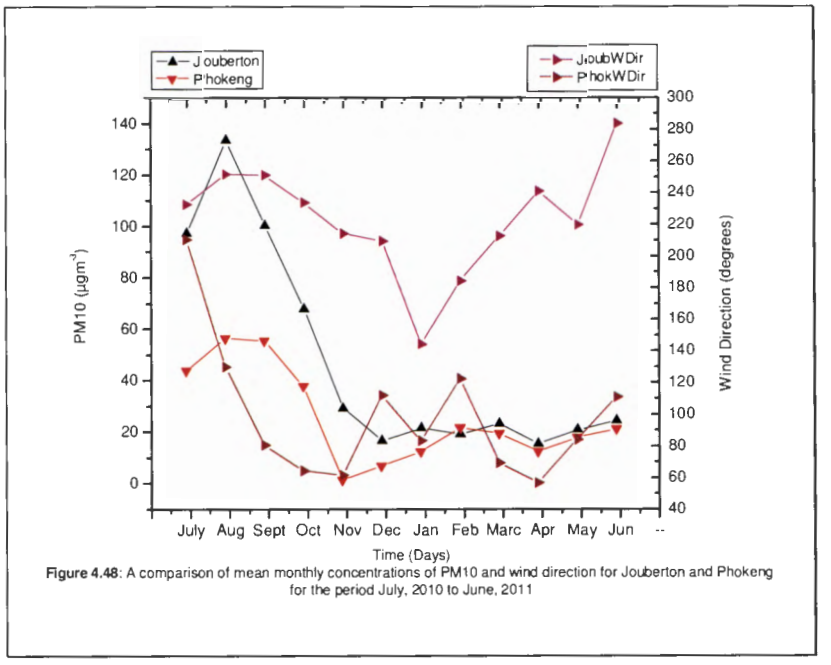

Figure 4.48: A comparison of mean monthly concentrations of PM10 and wind direction for Jouberton and Phokeng for the period July, 2010 to June, 2011

The winds in Jouberton were mostly southwesterlies from July, 2010, through to May, 2011, whereas Phokeng received mostly north-northeasterly winds throughout the 12 months study period (**Figure 4.48**). A probable explanation could be that Jouberton was receiving aerosol loadings from some industries lying from its Southwest direction, and

perhaps from the neighbouring towns. Phokeng receives winds from its Northeast direction, a region of minimal industrial development.

Figure 4.49: Positions of Rustenburg and Klerksdorp
Source: http://www.maplandia.com/south-africa/2012

As can be seen in **Figure 4.49**, North and Northeast of Rustenburg is covered mostly by game parks. There are almost no industrial activities to generate PM of anthropogenic origin. Most of the PM recorded are generated locally, within Rustenburg. During high PM levels, winds blew from the Southeast where towns like Pretoria and Johannesburg regions have industries like power generating and coal mines. These could have contributed to the levels of atmospheric aerosols in Rustenburg. Klerksdorp is flanked by towns that have mines and industries. The main point sources of pollutants in the Highveld are coal-fired power stations, petrochemical industry, as well as mining and metallurgical industries. The major pollutants released by these industries include SO_2, NOx and particulates, whilst the petrochemical industry additionally emits VOCs, H_2S and NH_3 (Cardoso et al., 1997). During winter a significant contribution of pollutants originates from domestic burning in informal settlements for cooking and space heating (June–August) and wild and managed fires (June–September). These emissions contain NOx, CO, VOCs

and particulate matter (PM), with the largest contribution from black carbon. In addition, windblown dust from soil and the mining industry contribute to high PM concentrations (Laakso et al., 2010). A possibility of measured PM_{10} in the environment of both Rustenburg and Klerksdorp is that of particulate growth. Data retrieved from MISR measurements indicated the presence of ultrafine particulates (**Figures 4.13** and **4.14**). This PM size type in the atmosphere tends to grow on interaction with the moisture, especially if there are chlorides, sulphates, and nitrates of sodium (Na) (Hu et. al., 2010). These inorganic salt aerosols are hygroscopic in nature, thus their size, phase and subsequently the optical properties are strongly influenced by the ambient relative humidity (RH) (Hu et. al., 2010). Results in both towns clearly indicates that particulate concentrations are mostly influenced by meteorological conditions (wind speed, wind direction and relative humidity).

4.3.6 Effect of Season Variation on PM_{10} Concentrations

Rustenburg and Klerksdorp both experience the climate of the North-West Province which is characterised by well-defined seasons (summer, winter, autumn and spring) with hot summers and cool sunny winters. The climate and rainfall varies from the more mountainous and wetter eastern region to the drier, semi-desert plains of the Kalahari in the west. Summer is the wet season with rains usually occurring from October to March. Temperatures range between 22°C and 34°C. Winter on the other hand, brings with it dry, sunny days and chilly nights. The average winter temperature is 15.5°C but can range from an average of 2°C to 20°C in a single day.

Results obtained from measurement of PM concentrations indicate higher PM values in winter as compared to summer (**Figure 4.45**). The major reason for this is that winters are mostly dry. The emitted PM remain in the atmosphere for longer periods. The fine aerosols especially (diameter <2.5 µm) tend to have longer residence times. There is no rain to wash them down (wet deposition). At the same time, the relative humidity is low (**Figure 4.**46) to promote particle growth which will eventually lead to larger PM diameters. Larger diameters cause aerosols to become heavier thus causing them to get deposited to the ground. Summers are usually wet because of the onset of rains. The rain tend to washdown the PM. This leads to low atmospheric PM concentrations. The higher relative humidity (**Figure 4.46**) promotes growth of atmospheric aerosols. The aerosols then

acquire larger diameters. The larger diameters cause the atmospheric aerosols to become heavier. As a result, the weight promotes wet deposition of the PM. High relative humidity thus contributes to low atmospheric aerosol concentrations.

4.3.7 Comparison of PM_{10} and Aerosol Optical Depth

AOD retrieved from MISR data for the period of January, 2010 to June, 2011 for Rustenburg and Klerksdorp is presented in **Figure 4.50**. It is clear that there is more particulate matter in the atmosphere in the month of September. Lower AOD values (near zero) imply minimal aerosol loading; there is very little backscattered light, meaning there is little or no particles in the atmosphere to scatter light. High AOD values mean high aerosol loading in the atmosphere; meaning more particulate matter present in the atmosphere blocking light and scattering it.

Comparing PM_{10} Grimm equipment measurements and AOD MISR measurements, both show high peak levels during the Winter season (**Figure 4.51**). Both measurements show a decline in levels as winter comes to an end. The MISR measurements and the laser technology (Grimm) measurements are therefore in agreement within reasonable limits. The results obtained from the MISR data is in agreement with the work of Laakso et al., (2010). They found that the aerosol optical properties obtained from measurements have a clear seasonal cycle, and that it applied to both the extensive properties scattering coefficient and absorption coefficient, as well as the intensive properties Angstrom exponent of scattering and single-scattering albedo (Laakso et al., 2010). The largest scattering and absorption coefficients were observed in the winter and spring months (June–October) and the lowest in summer and autumn (December–March) (**Figure 4.50**). The seasonality of both the emissions and the meteorological conditions are likely the cause. In winter the industrial activities (e.g. higher electricity consumption) and domestic space heating are at their most active state. There are also large emissions due to wildfires in these months. Additionally in winter the mixing height of the boundary layer is lower and the atmospheric residence times due to atmospheric re-circulation and limited wet deposition are longer, leading to an accumulation of the aerosol particles. In summer, mixing height is higher, which leads to lower pollutant concentrations due to more dilution. Other reasons for lower concentrations are frequent below- and in-cloud scavenging, and

less persistent weather types leading to advection of pollutants out of the Highveld area (Laakso et al., 2010).

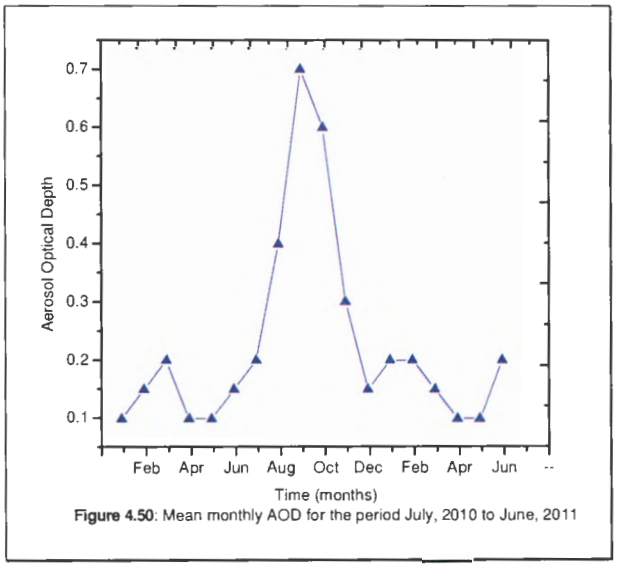

Figure 4.50: Mean monthly AOD for the period July, 2010 to June, 2011

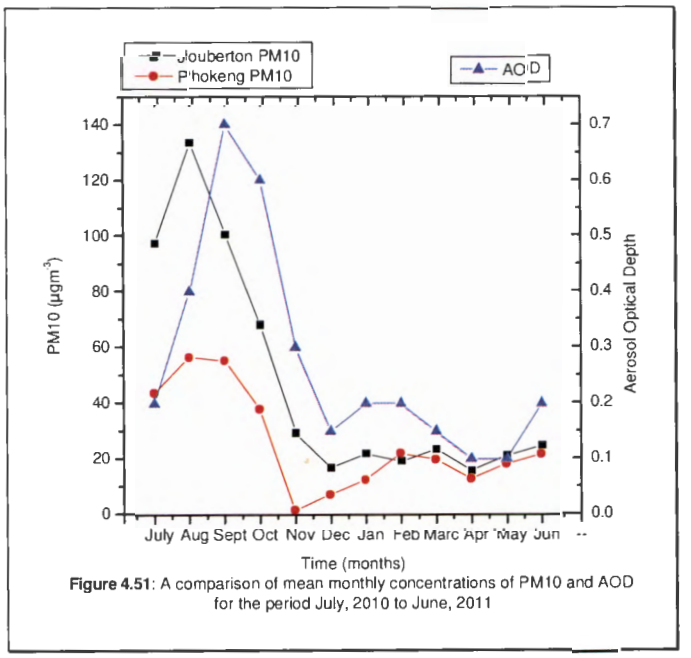

Figure 4.51: A comparison of mean monthly concentrations of PM10 and AOD for the period July, 2010 to June, 2011

4.3.8 Measured PM_{10} Values Versus Standards

24 hourly averages:

SAAQG permitted 24 hourly values: 75 μgm^{-3}

WHO permitted 24 hourly values: 50 μgm^{-3} per day

24 hourly measured values in numbers in red font in **Table 4.1** are times measured PM_{10} values which have exceeded the allowable 24 hourly values of SAAQG for each month in each town.

Table 4.1: 24 hourly Measured PM_{10} Values Versus Standards

Month	Jul	Aug.	Sept	Oct	Nov	Dec	Jan	Feb	Mar	Apr	May	Jun
JBTN[a]	23/31	29/31	25/30	9/31	0/31	0/31	1/31	0/28	0/31	0/30	0/31	0/30
PKNG[b]	0/31	1/30	3/31	26/30	0/31	0/31	0/31	0/28	0/31	0/30	0/31	0/30

[a]Jouberton, [b]Phokeng

Average annual measured values in:

Jouberton – 47.76 μgm^{-3}

Phokeng – 25.9 μgm^{-3}

SAAQG permitted annual values 40 μgm^{-3}

WHO permitted annual values 20 μgm^{-3}

Here, only Jouberton has exceeded the SAAQG permissible 40 μgm^{-3} level. Both towns have however exceeded the WHO permissible 20 μgm^{-3} level.

4.4 CHEMICAL ANALYSIS

4.4.1 AAS Analysis

Sample was analysed for two trace metals (As and Cr). The results indicated that they were present in the atmospheric aerosols.

Mean concentration for As found was: 0.031 μgm^{-3}

Mean concentration for Cr found was: 0.0014 μgm^{-3}

4.4.2 ICP-MS Analysis

The ICP-MS analysis carried out was a semi quantitave one aimed at determining what chemical elements were present. The only standards prepared were for metals of interest (Pb, V, Cr, Ni, Hg, Co, Cd, Se, Mn, Ba, and As). Results revealed that the atmospheric aerosols contained the following elements: Li, Be, Na, Mg, Al, Si, Sc, Ti, Pb, V, Cr, Ni, Hg, Co, Fe, Mg, Si, Ca, Al, Cu, Cd, Se, Mn, Ba, Zn, Ga, Ge, As, Se, Rb, Sr, Y, Zr, Nb, Nb, Mo, Ru, Cs, Rh, Pd, Ag, Cd, Sn, Sb, Te, Ba, La, Ce, Pr, Nd, Sm, Eu, Gd, Dy, Ho, Er, Tm, Yb, Lu, Hf, Ta, W, Pt, Au, Hg,Ti, Pb, Bi, Th, U. Almost all elements were in trace quantities except for Na – (0.71 μgm^{-3}), Mg – (0.38 μgm^{-3}), Al – (0.1 μgm^{-3}), Si – (0.42 μgm^{-3}), K – (0.4 μgm^{-3}), Ca – (1.18 μgm^{-3}).

In this study, the elements of concern, however, are Pb, V, Cr, Ni, Hg, Co, Cd, Se, Mn, Ba, and As because they are of health hazard. Heavy metals or metal elements with the density of greater than 4-5 μgm^{-3} (Moon and Chae, 2007). Some of these heavy metals, such as copper, nickel, chromium and iron, for example, are essential in very low concentrations for the survival of all forms of life (CAOBISCO, 1996). Only when they are present in high concentrations do they become toxic. Metals like lead, cadmium and mercury are toxic at very low concentrations and can cause metabolic anomalies (CAOBISCO,1996). Increasing industrialisation has been accompanied throughout the world by the extraction and distribution of mineral substances from their natural deposits. Following concentration, many of these have undergone chemical changes through technical processes and finally pass, finely dispersed and in solutions, by way of effluent, sewage, dumps and dust, into the water, the earth and the air. Lead has been mined since ancient times and has been processed in many ways. The main sources of lead pollution in the environment are: Industrial production processes and their emissions, road traffic with leaded petrol, the smoke and dust emissions of coal and gas-fired power stations, the laying of lead sheets by roofers as well as the use of paints and anti-rust agents (CAOBISCO,1996). WHO guideline for lead in water is 0.050 μgm^{-3}. Cadmium exists in low concentrations in all soils (CAOBISCO,1996). It is actively extracted from its ores for commercial purposes and is also emitted in industrial processes such as metal melting and refining, coal and oilfired power stations, electroplating plants, etc. Cadmium is concentrated particularly in the kidneys, the liver, the bloodforming organs and the lungs. It most frequently results in kidney damage (necrotic protein precipitation) and metabolic

anomalies caused by enzyme inhibitions. It is now known that the Itai-itai sickness in Japan (with bone damage) is a result of the regular consumption of highly contaminated rice. Mercury or "quicksilver" was already being extracted in ancient times. In 1965, the consumption of fish from regions of the sea contaminated by effluent led to the appearance of the so-called Minamata sickness in Japan and, in 1972, bread cereals contaminated with fungicides containing mercury led to epidemic poisoning in Iraq (CAOBISCO,1996). Mercury in the form of its methyl compounds is specifically the most toxic of the heavy metals. When consumed orally, it first passes into the liver, the kidneys and the brain. Accumulation only takes place temporarily. A large part is excreted with the faeces. The salts of bivalent mercury, in the case of chronic consumption, first cause tiredness, loss of appetite and weight loss. Eventually, the kidneys fail. Muscular weakness and paralysis are typical (CAOBISCO,1996). Arsenic is the most common cause of acute heavy metal poisoning in adults and is number 1 on the The Agency for Toxic Substances and Disease Registry's (ATSDR) "Top 20 List" (LifeExtension, 2012). Arsenic is released into the environment by the smelting (Washington Department of Health, 2003) process of copper, zinc, and lead, as well as by the manufacturing of chemicals and glasses. Arsine gas is a common byproduct produced by the manufacturing of pesticides that contain arsenic. Arsenic may be also be found in water supplies worldwide, leading to exposure of shellfish, cod, and haddock. Other sources are paints, rat poisoning, fungicides, and wood preservatives. Target organs are the blood, kidneys, and central nervous, digestive, and skin systems (Roberts 1999; ATSDR, 2007).

Results for 21 August, 2008 and 10 November, 2008 samples for chemical analysis of the heavy metals and their concentrations are given in **Tables 4.2, 4.3** and **4.4**.

Table 4.2: Elements analysed and their composition (21 August, 2008)

Element	Pb	V	Cr	Ni	Hg	Co	Cd	Se	Mn	Ba	As
Conc. ($x\ 10^{-3}\ \mu gm^{-3}$)	1	59	19	11	0.04	0.3	0.003	0.1	3.4	1	12

This data was for atmospheric aerosols recorded as 18 μgm^{-3} on 21 August 2008, in Marikana. The following are percentage contribution of each element:

Table 4.3: Percent composition contribution of each element analysed (21 august, 2008)

Element	Pb	V	Cr	Ni	Hg	Co	Cd	Se	Mn	Ba	As
Percentage (x 10^{-4} %)	66	3278	1056	611	2	17	0. 2	6.6	189	66	667

Table 4.4: Elements analysed and their composition (10 November, 2008)

Element	Pb	V	Cr	Ni	Hg	Co	Cd	Se	Mn	Ba	As
Conc. (x 10^{-3} μgm^{-3})	0	0	0	0	0	0	0	0	0	0	0

With these findings, it can be stated that the atmospheric aerosols, apart from high levels established especially during the Winter season, have a chemical composition of mentioned trace metals of concern. Samples taken on 10 November, 2008 showed no presence of PM_{10} (**Figure 4.8**). The zero values indicate that the elements were absent in the samples. This could be as a result of rain washdown. This is the reason for absence of heavy metals (**Table 4.4**) in the chemical analysis.

4.5 Modelling of PM_{10} Concentrations

Atmospheric formation and removal of PM are governed by a number of complex dynamic processes, including nucleation, condensation, coagulation, chemical transformation in the gas, and in the aqueous (cloud and fog) phases, interphase exchange and equilibria, and wet/dry deposition (Meng et. al., 1998). The longer the residence time of these PM, the higher their concentration. The impacts of PM have inspired the need to develop models that could be utilized to predict their atmospheric concentrations. Such a prediction mechanism would help in the study of the concentration of PM for cases in which the PM cannot be measured. It may also be utilized to develop efficient and economic monitoring systems. The modelling of the PM concentrations, NOx and O_3, and the chemical components of the atmospheric aerosols is currently under intensive research and improvement by different research groups (Pey et al., 2010). The large number of variables influencing the air pollutant concentrations and its variability in the atmosphere make the development of a predictive model for PM a complex issue (Pey et al., 2010). Because of these limiting effects, it is often necessary to consider the effects

of some of the variables as constant and then study the influence of selected variables. Several models have been developed to predict PM atmospheric concentrations, PM deposition, or even PM distribution, some of which include the mathematical model for dry deposition (Bessagnet et al., 2004).:

$$V_d = \frac{1}{r_a + r_b + r_a r_b V_s} + V_s \qquad (9)$$

Where r_a, r_b, respectively, are the aerodynamic and quasilaminar resistances for particles and V_s the sedimentation velocity (Bessagnet et al., 2004).

Wet deposition assumes a different mathematical expression (Bessagnet et al., 2004):

$$\left[\frac{dQ_i^k}{dt}\right]_{incl} = -\frac{\varepsilon_i p_r}{w_i h} Q_i^k \qquad (10)$$

Other rely on thermodynamic equilibrium principles to forecast PM states. This line of thought is based on the idea that phase state of PM mixture (especially electrolytes) in the atmosphere at a given temperature and relative humidity will tend to thermodynamic equilibrium with the gas phase (Amundson et al., 2005).

The work of Amundson et al., (2005), highlighted two general features:

a) The method of computing activity coefficients of the aerosol-phase species, and
b) The numerical technique that is used to determine the equilibrium state.

Nonlinear algebraic equations derived from mass balances and chemical equilibrium or performing a direct minimization of the Gibbs free energy may be utilized to estimate the composition of atmospheric aerosols. Mathematical expressions utilized in thermodynamic equilibrium include (Amundson et al., 2005):

$$G(n_i, n_g, n_s) = n_g^T \mu_g + n_i^T \mu_i + n_s^T \mu_s \qquad (11)$$

Subject to $n_g>0$, $n_i>0$, $n_s\geq 0$, and

$A_g n_g + A_i n_i + A_s n_s = b$

Where n_g, n_i, n_s are the concentration vectors in gas, liquid, and solid phases, respectively; μ_g, μ_i, μ_s are the corresponding chemical potential vectors; A_g, A_i, A_s, are the component-based formula matrices, and b is the component-based feed vector.

The chemical potential vectors being:

$$\mu_g = \mu_g^0 + RTlna_g \quad (12)$$

$$\mu_i = \mu_i^0 + RTlna_i \quad (13)$$

$$\mu_s = \mu_s^0 \quad (14)$$

Where R is the universal gas constant, T is the system temperature, μ_g^0 and μ_i^0 are the standard chemical potentials of gas and liquid species, respectively, and a_g and a_i are the activity vectors of the gas and liquid species. This is discussed in detail in the article by Amundson et al., (2005).

Seinfeld and Pandis (2006) proposed the Eulerian Box Model to predict concentrations of atmospheric aerosols. Their model uses the following mathematical expression shown below:

$$\frac{d}{dt}(c_i \Delta x \Delta y H) = Q_i + R_i \Delta x \Delta y H - S_i + uH\Delta y(c_i^0 - c_i) \quad (15)$$

Where HΔxΔy is the volume of the Eulerian Box (a region of atmosphere where air mass is mixing), c_i is the air mass concentration, i, is the species in the air mass, Q_i is the mass emission rate of i (kgh^{-1}); S_i is the removal rate of i (kgh^{-1}); R_i is the chemical production rate ($kgm^{-3}h^{-1}$); c_i^0 the background concentration, and u is the wind speed.

In this study, a nonlinear multiple regression quadratic equation was utilized to correlate the time (days) with the measured concentration of the PM_{10}. Polynomial fit for forecasting has been used in various scientific disciplines including biological data (Motulsky and Christopoulos, 2012). In order to do this, the PM_{10} data from the measured values using the Grimm equipment was employed. One year data-sets for both Rustenburg (Phokeng) and Klerksdorp (Jouberton) were taken from **Figures 4.14 and 4.23**, respectively as a representation. A mathematical model of polynomial fit was employed. Since there are many data points in the measurements, the polynomial of 9 degree was chosen to be the best fit for the model. All data processing was performed off-line using a commercial software package (MATLAB 6.1, The MathWorks Inc., Natick, MA, 2000). The Polynomial equation utilized was selected from the available polynomial equation in the Matlab programme. The mathematical expression for the forecast obtained has the form:

$$Y = A + B1*X + B2*X^2 + B3*X^3 + B4*X^4 + B5*X^5 + B6*X^6 + B7*X^7 + B8*X^8 + B9*X^9 \quad (16)$$

In this expression, Y represents the concentration of the PM_{10}, and X represent the time in days. A is the intercept and B are coefficients (slopes). Values for the determined polynomial equation are reported in **Table 4.5** and **Table 4.6**), including error values.

Results are presented in **Figures 4.52** and **4.53**.

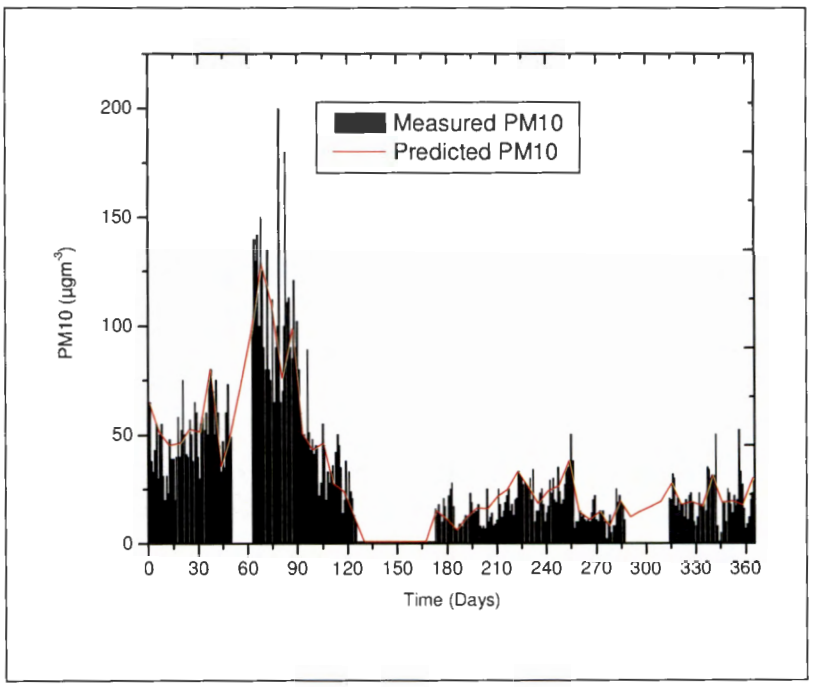

Figure 4.52: Modelling of annual mean daily concentrations of PM_{10} for the period July, 2010 to June, 2011 in Phokeng, Rustenburg

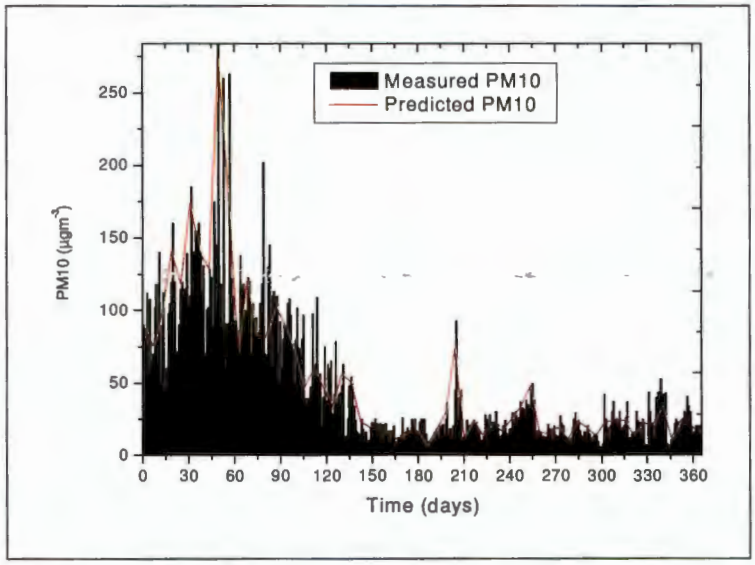

Figure 4.53: Modelling of annual mean daily concentrations of PM_{10} for the period July, 2010 to June, 2011 in Jouberton, Klerksdorp

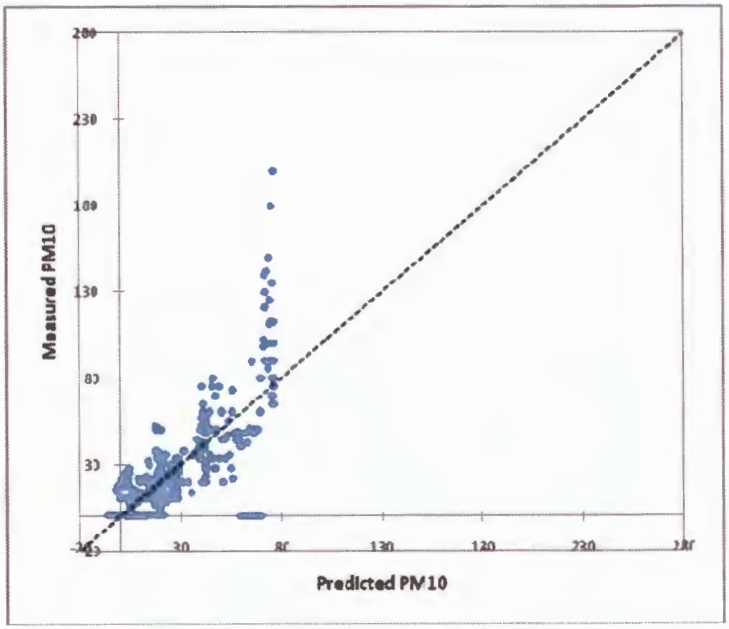

Figure 4.54: Correlation between Measured PM_{10} and Predicted PM_{10} for Phokeng, Rustenburg

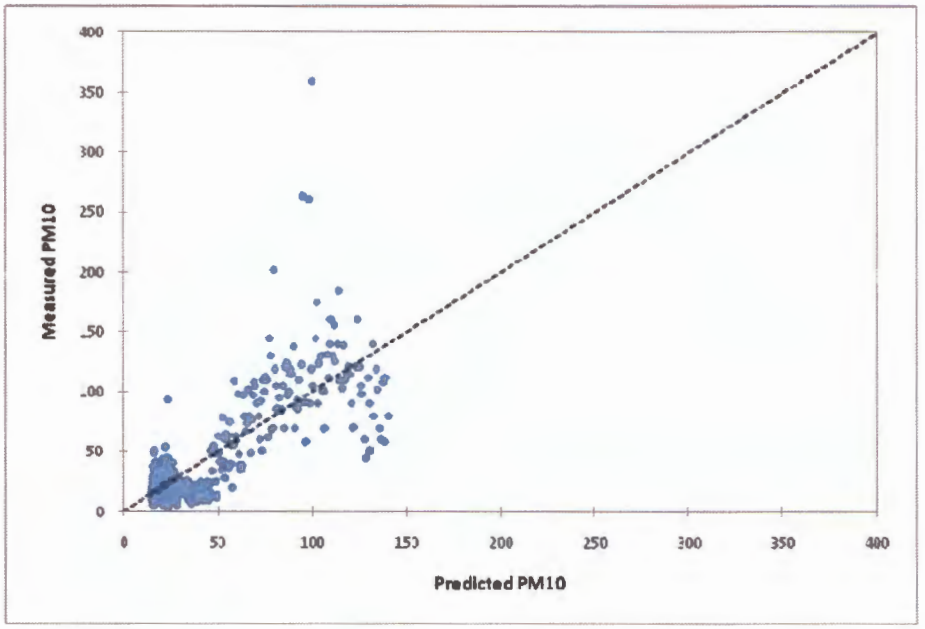

Figure 4.56: Correlation between Measured PM_{10} and Predicted PM_{10} for Jouberton, Klerksdorp

The R^2 value shows that there is a good agreement between measured and predicted concentrations of PM_{10} (0.75 for Rustenburg; 0.73 for Kelrksdorp) with a standard deviation of 15.69 for Rustenburg, and 24.38 for Klerksdorp. However, there is some degree of underestimation in both towns. Correlation plots for measured PM_{10} and modelled PM_{10} are presented in **Figures 4.55** and **4.56** respectively. Both plots show reasonable closeness, meaning the predicted PM_{10} concentrations are in agreement to the measured PM_{10} concentrations. Model parameters are presented in **Tables 4.5** and **4.6**. The A values are the points where the graph crosses the y axis. The B values are slopes of the graph at different times. The values assume a positive slope as the graph rises. They assume a negative slope as the graph drops.

Table 4.5: Model parameters for Rustenburg

Parameter	Value	Error
A	66.04278	8.91034
B1	-5.31278	1.40426
B2	0.25216	0.07185
B3	-0.00356	0.00167
B4	1.45379E-5	2.10603E-5
B5	7.55311E-8	1.55358E-7
B6	-9.46884E-10	6.91671E-10
B7	3.6644E-12	1.82765E-12
B8	-6.46509E-15	2.63747E-15
B9	4.41168E-18	1.60028E-18

Note: parameters are defined in section 4.5

Table 4.6: Model parameters for Klerksdorp

Parameter	Value	Error
A	79.59818	13.68274
B1	0.70379	2.10296
B2	0.0643	0.10554
B3	-0.00197	0.00245
B4	2.10646E-5	3.08389E-5
B5	-1.1651E-7	2.28097E-7
B6	3.73773E-10	1.01771E-9
B7	-7.17013E-13	2.69223E-12
B8	7.88618E-16	3.88542E-15
B9	-3.96917E-19	2.35547E-18

Note: parameters are defined in section 4.5

CHAPTER 5

CONCLUSION AND RECOMMENDATIONS

5.1 CONCLUSION

The objective of this study was to address the lack of data for the extent of atmospheric aerosol loading in the North-West Province, South Africa. Three approaches were used to arrive at this objective. The first approach was to determine quantitatively, atmospheric aerosol loading in the North-West Province of South Africa, with emphasis on Rustenburg and Klerksdorp mining towns. This approach was imperative so that the data acquired could be used to compare with the South African Air Quality Standards for the attention of the stakeholders, and also to compare with international standards such as the WHO standards. The second approach was to determine qualitatively, atmospheric aerosols loading in this Province. The third approach was to determine the chemical composition of the atmospheric aerosols and model it.

The concentrations of atmospheric aerosols were determined by utilising the Grimm equipment. Values of the concentrations given as μgm^{-3} were then used to compare with the SAAQS. It was observed that the atmospheric aerosols represented by PM_{10}, were in some seasons, above the acceptable limits. The second objective was achieved by treating AOD information retrieved from MISR satellite. From the AOD values, the atmospheric aerosols prevalent in the study area were those of the anthropogenic activities. These are the major source of health concerns as they are believed to cause diseases like cancer, respiratory, and cardiovascular problems, as outlined in Chapter two.

From the results obtained from this study, the following conclusion can be drawn. The results obtained were compared to the National Ambient Air Quality Standards for South African (2004) and the World Health Organization, WHO (2005). It was observed that the PM_{10} values for 24 hourly periods exceeded the 75 μgrn^{-3} maximum permissible limit for the South African Guidelines, and those of the World Health Organization permissible limits of $50\mu gm^{-3}$.

The North West Province, with major contribution from Rustenburg and Klerksdorp mining areas, gets over 50 percent of its GDP through mining activities. It is therefore tempting to conclude that the PM_{10} values measured are mostly from the mining activities. This however, would be over simplifying the complex situation. Industrial activities emit particulates such as CO, SO_2, NO_x, incineration processes emissions, sand blasting generated particulate matter, and etc. The transport sector emits entrained road dust, including tailpipe aerosols. The agriculture activities on the other hand contribute dust particles into the atmosphere as well as fuel burning from agricultural equipment. The domestic activities generate fuel combustion related aerosols. Cross-regional air pollution cannot be ignored. Pollutants generated in one area can be transported over distances to other areas. As such, it is not the intention of this study to pinpoint exact sources of emissions of the measured atmospheric aerosols. Chapter 1 highlighted the problem statement. Through this study, atmospheric aerosol loading in the North West Province with emphasis on Rustenburg and Klerksdorp has been documented. The highlighted objectives have been met as outlined in the Experimentation Chapter. Thus it has been shown that measured PM_{10} values have at several times gone beyond the acceptable limit that is stipulated in the SAAQS. The same can be said when compared to the WHO standards. South Africa has four seasons, namely Autumn, Winter, Spring, and Summer. From the data presented, there is more aerosol loading during the Winter season than any other season. On relating meteorological conditions, it is noted that humidity mostly affects the aerial residence time of the aerosols. In Winter, there is less humidity and so less wet deposition of aerosols. In Summer humidity, is highest and so there is greater wet deposition leading to lowest aerosols in the atmosphere.

The third objective was the determination of heavy metal composition of aerosols. This was achieved by analysing the collected samples with an the ICP-MS equipment. The heavy metals were found to be toxic and are a cause for concern. In the case of arsenic, for example, the United States Food and Drug Agency (USEPA) concluded that sufficient evidence existed to conclude that arsenic is a human carcinogen, based upon increased lung cancer mortality in humans, increased internal organ cancers in humans (liver, kidney, lung, and bladder), and an increased incidence of skin cancer in humans (USEPA, 1998c). Mercury causes hand tremours, increase in memory disturbance and slight subjective and objective evidence of autoimmune dysfunction in adults (Fawer et al.,

1983). South Africa gives a guideline for lead only. The SAAQS (2009), set lead levels at 0.5 μgm^{-3} per year. Lead has the effect of changing the levels of certain blood enzymes among other things (USEPA, 1988). The following extract is from "Air Quality in Europe" (European Envronment Agency, 2011): The heavy metals arsenic (As), cadmium (Cd), lead (Pb), mercury (Hg) and nickel (Ni) are common air pollutants, mainly emitted as a result of various industrial activities and combustion of coal. Although the atmospheric levels are low, they contribute to the deposition and build-up of heavy metal contents in soils, sediments and organisms. Heavy metals are persistent in the environment and some bioaccumulate in food chains. Arsenic exposure is associated with increased risk of skin and lung cancer. Cadmium is associated with kidney and bone damage and has also been identified as a potential human carcinogen, causing lung cancer. Lead exposures have developmental and neuro-behavioural effects on foetuses, infants and children, and elevated blood pressure in adults. Mercury is toxic in the elemental and inorganic forms but the main concern is associated with the organic compounds, especially methylmercury. It accumulates in the food chain, for example in predatory fish in lakes and seas and reaches humans. Nickel is a known carcinogen and also has other non-cancerous effects, e.g. on the endocrine system. Air pollution is only one source of exposure to these metals but their persistence and potential for long-range atmospheric transport means that atmospheric emissions of heavy metals affect even the most remote regions. The European Envronment Agency, as a result of these metal toxicity, set the following guidelines: Arsenic – 0.006 μgm^{-3}; cadmium – 0.005 μgm^{-3}; nickel – 0.02 μgm^{-3}; lead – 0.5 μgm^{-3}.

5.2 RECOMMENDATIONS

Two recommendations are made because of the findings in the chemical composition analysis. The first recommendation is that a detailed quantitative analysis should be done in both mining areas. The second recommendation is that a follow up research work that could correlate atmospheric aerosol composition and health should be done.

Atmospheric aerosol concentrations in the two towns of Rustenburg and Klerksdorp were modelled. The rebuilding of the atmospheric aerosol concentrations from the daily PM_{10} data and the subsequent comparison with the measured atmospheric aerosol

concentrations has resulted in a very close agreement. The value of r^2 obtained as indicated in the results, the modelling or the forecast can be said to be good. It must be borne in mind that results modelled are just estimates. It can be said therefore that from the results obtained from this model, it can be considered as a complementary tool that can be employed by anyone for the prediction of atmospheric aerosol concentrations.

REFERENCES

Abdul-Razzak, H. & Ghan, S.J., (2000). A parameterization of aerosol activation. Part 2: Multiple aerosol types. *Journal of Geophysics Research* 105: 6837–6844.

Ackerman, T.P., & Coauthors, (2004). Integrating and interpreting aerosol observations and within the PARAGON framework. *Bulletin of American Meteorological Society* 85: 1523–1533.

Adams, P.J. & Seinfeld, J.H., (2002). Predicting global aerosol size distributions in general circulation . *Journal of Geophysics Research* 107: 4370, doi:10.1029/2001JD001010.

Agency for Toxic Substances and Disease Registry (ATSDR), (2007). Toxicological Profile for Arsenic *(Update)*. Atlanta, GA: U.S. Department of Health and Human Services, Public Health Service.

Agranovski, I., (2010). *Aerosols – Science & Technology*. KgaA, Weinheim Wiley-VGH Verlag GmbH and Co. 455pp.

Amundson, N.R., Caboussat, A., He, J.W., Martynenko, A.V., Savarin, V.B., Seinfeld, J.H. & Yoo, K.Y., (2005). A computationally efficient inorganic atmospheric aerosol phase equilibrium model (UHAERO). *Atmospheric Chemistry and Physics Discussions* 5: 9291-9324.

Anderson, B.E., Grant, W.B., Gregory, G.L., Browell, E.V., Collins, J.E., Sachse, G.W., Bagwell, D.R., Hudgins, C.H., Blake, D.R. & Blake, N.J., (1996). Aerosols from biomass burning over the tropical South Atlantic region: Distribution and impacts. *Journal of Geophysics Research* 101: 24117- 24137.

Andreae, M.O., Andreae, T.W., Annegarn, H., Beer, J., Cachier, H., le Canut, P., Elbert, W., Maenhaut, W., Salma, I., Wienhold, F.G. & Zenker, T., (1998). Airborne Studies of Aerosol Emissions from Savanna Fires in Southern Africa: 2. Aerosol Chemical Composition. *Journal of Geophysical Research* 103 (32): 119 – 128.

Artaxo, P., Reinaldo, C.C., Fernandes, E.T., Martins, J.V., Xiao, Z., Lindqvist, O.F. J.J., Maria, T., & Maenhaut, W. (2000). Large scale mercury and trace element measurements in the Amazon basin. *Atmospheric Environment* 34: 4085 – 4096.

Atkinson, W.R., Ross, H.A., Sunyer, J., Ayres, J., Baccini, M., Vonk, J.M., Boumghar, A., Forastiere, F., Forsberg, B., Touloumi, G., Schwartz, J., & Katsouyanni, K., (2001). Acute Effects of Particulate Air Pollution on Respiratory Admissions. *American Journal of Respiratory and Critical Care Medicine* 164: 1860 – 1866.

Ballester, F., (2002). The EMECAM project: A multicentre study on air pollution and mortality in Spain: combined results for particulates and for sulphur dioxide. *Occupational and Environmental Medicine* 59: 300 – 308.

Barrie, L.A., (1986). Arctic air pollution: an overview of current knowledge. *Atmospheric Environment* 20 (4): 643–663.

Barth, M., Rasch, P.J., Kiehl, J.T., Benkovitz, C.M. & Schwartz, S.E., (2000). Sulfur chemistry in the NCAR CCM: Description, evaluation, features and sensitivity to aqueous chemistry. *Journal of Geophysics Research* 105: 1387–1415.

Bates, T.S., Huebert, B.J., Gras, J.L., Griffiths, F.B. & Durkee, P.A., (1998). International Global Atmospheric Chemistry (IGAC) Project's First Aerosol Characterization Experiment (ACE 1): Overview. *Journal of Geophysics Research* 103: 16 297–16 318.

Bates, T.S., & Coauthors, (2006). Aerosol direct radiative effects over the northwest Atlantic, northwest Pacific, and North Indian Oceans: Estimates based on in-situ chemical and optical measurements and chemical transport modeling. *Atmospheric Chemistry and Physics* 6: 1657–1732.

Begum, B.A., Kim, E., Biswas, S.K., & Hopke, P.K., (2004). Investigation of sources of atmospheric aerosol at urban and semi-urban areas in Bangladesh. *Atmospheric Environment* 38: 3025–3038.

Berglund, B., Brunekreef, B., Knoppel, H., Undvau, T., Maroni, M., Mblhave, L. & Skov, P., (1991). Effects of Indoor Air Pollution on Human Health. Indoor Air Quality and its Impact on Man: Environment and Quality of Life Report No. 10. Published by the COMMISSION OF THE EUROPEAN COMMUNITIES Directorate-General Information Market and Innovation Batiment Jean Monnet, LUXEMBOURG.

Bergstrom, R.W., Pilewskie, P., Russell, P. B., Redemann, J. Bond, T. C., Quinn, P. K. & Sierau, B., (2007). Spectral Absorption Properties of Atmospheric Aerosols. *Atmospheric Chemistry and Physics Discussions* 7: 10669–10686.

Bessagnet, B. & Rosset, R., (2001). Fractal modelling of carbonaceous aerosols—application to car exhaust plumes. *Atmospheric Environment* 35: 4751–4762.

Bessagnet, B., Hodzic, A., Vautard, R., Beekmann, M., Cheinet, S., Honore, C., Liousse, C. & Rouil, L., (2004). Aerosol modelling with CHIMERE – preliminary evaluation at the continental scale. *Atmospheric Environment* 38: 2803-2817.

Bhartia, P.K., Herman, J.R., McPeters, R.D. & Torres, O., (1993). Effect of Mount Pinatubo Aerosols on Total Ozone Measurements From Backscatter Ultraviolet (BUV) Experiments. *Journal of Geophysics Ressearch 98*: 18547-18554.

Bhatnagar, A. (2006). Environmental Cardiology Studying Mechanistic Links Between Pollution and Heart Disease. *Circulation Research* 99: 692-705.

Binkowski, F.S. & Shankar, U., (1995). The Regional Particulate Matter Model. 1. Model description and preliminary results. *Journal of Geophysical Research* 100 (D12): 26,191–26,209.

Bio, F.Y., Sadhra, S., Jackson, C. & Burge, P.S., (2007). Respiratory Symptoms and Lung Function Impairment in Underground Gold Miners in Ghana. *Ghana Medical Journal* 41: 38–47.

Blanchard, D.C. & Woodcock, A.H., (1957). Bubble formation and modification in the sea and its micrometeorological significance. *Tellus* 9: 145-158.

Boer, G.J., Flato, G. & Ramsden, D.A., (2000). Transient climate change simulation with greenhouse gas and aerosol forcing: Projected climate for the 21st century. *Climate Dynamics* 16: 427–450.

Bogo, H., Otero, M., Castro, P., Ozafran, M.J., Kreiner, A., Calvo, E.J. and Negri, R.M., (2003). Study of Atmospheric Particulate Matter in Buenos Aires City. *Atmospheric Environment* 37: 1135–1147.

Bradford, T. & Cook, N., (1997). *Inductively Coupled Plasma (ICP).* Available online at: http://www.cee.vt.edu/ewr/environmental/teach/smprimer/icp/icp.html. Last accessed 22th April 2011.

Brugge, D., Durant, J.L. & Rioux, C., (2007). Near-highway pollutants in motor vehicle exhaust: A review of epidemiologic evidence of cardiac and pulmonary health risks. *Environmental Health* 6:23 doi:10.1186/1476-069X-6-23.

Bullock, K.R., Duvall, R.M., Norris, G.A., McDow, S.R. & Hays M.D., (2008). Evaluation of the CMB and PMF using organic molecular markers in fine particulate matter collected during the Pittsburgh air quality study. *Atmospheric Environment* 42 (29): 6897–6904.

Callén, M.S., de la Cruz, M.T., López, J.M., Navarro, M.V. & Mastral, A.M., (2009). Comparison of receptor for source apportionment of the PM_{10} in Zaragoza (Spain). *Chemosphere* 76: 1120–1129.

Cardoso, A. A., Liu, H. & Dasgupta, P. K., (1997). Fluorometric fiber opticv drop sensor for atmospheric hydrogen sulphide. *Talanta* 44: 1099–1106.

Carlson, T. N. and Prospero, J.M., (1972). The Large-Scale Movement of Saharan Air Outbreaks over the Northern Equatorial Atlantic. *Journal of Applied Meteorology* 11: 283-297:

Cautreels, W., & Cauwenberghe, K.V., (1976). Determination of Organic Compounds in Airborne Particulate Matter by Gas Chromatography Mass Spectrometry. *Atmospheric Environment* 10: 447 – 457.

Charlson, R.J., Langner, J., Rodhe, H., Leovy, C.B. & Warren, S.G., (1991). Perturbation of the northern hemisphere radiative balance by backscattering from anthropogenic sulfate aerosols. *Tellus* 43AB: 152-163.

Chemclouds, (2001). Chemtrail Clouds and Volcanic Ash Clouds Compared. Aircraft Aerosol Operations. US.

Chin, M., Khan, R.A., Remer, L.A., Yu, H., Rind, D., Feingold, G., Quinn, P.K., Schwartz, S.E., Streets, D.G., DeCola, P. & Halthore, R., (2009). Atmospheric Aerosol Properties and Climate Impacts. Synthesis and Assessment Product 2.3 Report by the U.S. Climate Change Science Program and the Subcommittee on Global Change Research.

Chowdhury, Z., Zheng, M., Schauer, J.J., Sheesley, R.J., Salmon, L.G., Cass, G.R. & Russell, A.G., (2007). Speciation of fine organic carbon particles and source apportionment of $PM_{2.5}$ in Indian cities. *Journal of Geophysical Research* 112: 15303 – 15315.

Chung, S.H. & Seinfeld, J.H., (2002). Global distribution and climate forcing of carbonaceous aerosols. *Journal of Geophysics Research* 107: 4407, doi:10.1029/2001JD001397.

Coakley, J.A., Cess, R.D. & Yurevich, F.B., (1983). The effect of tropospheric aerosols on the earth's radiation budget: A parameterization for climate . *Journal of Atmospheric Science* 40: 116–138.

Collins, W.D., & Coauthors, (2006). The formulation and atmospheric simulation of the Community Atmosphere Model: CAM3. *Journal of Climate* 19: 2122–2143.

Colvile, R.N., Gómez-Perales, J.E. & Nieuwenhuijsen, M.J., (2003). Use of dispersion modelling to assess road-user exposure to $PM_{2.5}$ and its source apportionment. *Atmospheric Environment* 37 (20): 2773–2782.

Cooper, J.A. & Watson, J.G., (1980). Receptor oriented methods of air particulate source apportionment. *Journal of Air Pollution Control Association* 30 (10): 1116–1125.

Cousin, F., Tulet, P. & Rosset, R., (2004). Interaction Between Local and Regional Pollution During ESCOMPTE 2001: Impact on Surface Ozone Concentrations (IOP2a and 2b). *Atmospheric Research* 74: 117-137.

Cousin, F., Liousse, C., Cachier, H., Bessagnet, B., Guillaume, B. & Rosset, R., (2005). Aerosol modelling and validation during ESCOMPTE 2001. *Atmospheric Environment* 39 (8): 1539 – 1550.

Crassier, V., Suhre, K., Tulet, P. & Rosset, R., (2000). Development of a reduced chemical scheme for use in mesoscale meteorological . *Atmospheric Environment* 34: 2633–2644.

d'Almeida, G.A., (1987). On the variability of deser dust radiative characteristics. *Journal Geophysics Research* 92: 3017-3026.

d'Almeida, G.A., Koepke, P. & Shettle, E.C., (1991). Atmospheric Aerosols Global Climatology and Radiative Characteristics, 561pp, A. Deepak Publishing, Hampton, Va, USA.

Dave, J.V., (1978). Effect of Aersols on the Estimation of Total Ozone in an Atmospheric Column from the Measurements of Its Ultraviolet Radiance. *Journal of Atmospheric Science* 35: 899-911.

de Leeuw, G., Andreas, E. L., Anguelova, M. D., Fairall, C. W., Lewis, E. R., O'Dowd, C., Schulz, M. & Schwartz, S.E., (2011). Production flux of sea spray aerosol. *Revision Geophysics* 49: 1-39.

DeLuisi J.J., Furukawa, P.M., Gillette, D.A., Schuster, B.G., Charlson, R.J., Porch, W.M., Fegley, R.W., Herman, B.M., Rabinoff, R.A., Twitty J.T. & Weinman, J.A., (1976). Results of a comprehensive atmospheric aerosol-radiation experiment in the southwester United States. *Journal of Applied Meteorology* 15: 441-463.

Delworth, T.L. & Knutson, T.R., (2000). Simulation of early 20th century global warming. *Science* 287: 2246–2250.

Delworth, T.L., & Coauthors, (2006). GFDL's CM2 global coupled climate . Part I: Formulation and simulation characteristics. *Journal of Climate* 19: 643–674.

Department of Energy, (2001). Tropospheric Aerosol Program—Program plan. U.S. Department of Energy Report. DOE/SC-0034, 98 pp.

Diner, D. J., Beckert, J.C., Reilly, T.H., Bruegge, C. J., Conel, J. E., Kahn, R., Martonchik, J.V., Ackerman, T.P., Davies,R., Gerstl, S.A.W., Gordon, H.R., Muller, J.P., Myneni, R., Sellers, P.J., Pinty, B. & Verstraete, M.M., (1998). Multiangle imaging

spectroradiometer (MISR) instrument description and experiment overview. *IEEE Transactions on Geoscience and Remote Sensing* 36: 1072–1087.

Diner, D.J., & Coauthors, (2004). PARAGON: An integrated approach for characterizing aerosol climate impacts and environmental interactions. *Bulletin of American Meteorological Society* 85: 1491–1501.

Dockery, C.W., Pope, D.A., Xu, X., Spengler, J.D., Ware, J.H., Fay, M.A., Ferris, B.G. & Speizer, F.D. (1993). An association between air pollution and mortality in six US cities. *New England Journal of Medicine* 329: 1753–1759.

Dubovik, O., Holben, B. N., Kaufman, Y. J., Yamasoe, M., Smimov, A., Tan, D. & Slutsker, I., (1998). Single-scattering albedo of smoke retrieved from the sky radiance and solar transmittance measured from ground. *Journal of Geophysical Research* 103: (31): 903-31, 923.

Easter, R.C., & Coauthors, (2004). MIRAGE: Model description and evaluation of aerosols and trace gases. *Journal of Geophysics Research* 109: D20210, doi:10.1029/2004JD004571.

Eichel, C., M. Kramer, L., Schutz, & Wurzler, S., (1996). The watersoluble fraction of atmospheric aerosol particles and its influence on cloud microphysics. *Journal Geophysical Research and Atmosphere* 101: 29499-29510.

European Envronment Agency, (2011). Air quality in Europe — 2011 report. EEA Technical report No 12/2011.

Fawer, R.F., de Ribaupierre, Y., Guillemin, M.P., Berode, M. & Lob, M., (1983). Measurement of Hand Tremor Induced by Industrial Exposure to Metallic Mercury. *British Journal of Industrial Medicine* 40: 204-208.

Fountoukis, C. & Nenes, A., (2005). Continued development of a cloud droplet formation parameterization for global climate . *Journal of Geophysics Research* 110: D11212, doi:10.1029/2004JD005591.

Ghan, S.J., Leung, L.R., Easter, R.C. & Abdul-Razzak, H., (1997). Prediction of droplet number in a general circulatior model. *Journal of Geophysics Research* 102: 21 777–21 794.

Ghan, S.J., Easter, R.C., Hudson, J. & Breon, F.M., (2001a). Evaluation of aerosol indirect radiative forcing in MIRAGE. *Journal of Geophysics Research* 106: 5317–5334.

Ghan, S.J., Laulainen, N., Easter, R., Wagener, R., Nemesure, S., Chapman, E., Zhang, Y. & Leung, R., (2001b). Evaluation of aerosol direct radiative forcing in MIRAGE. *Journal of Geophysics Research* 106: 5295–5316.

Ghan, S.J. & Schwart, S.E., (2007). Aerosol Properties and Processes; A Path from Field and Laboratory Measurements to Global Climate . Climate Physics Group, Pacific Northwest National Laboratory, Richland, WA 99352.

Ginoux, P., Horowitz, L.H., Ramaswamy, V., Geogdzhayev, I.V., Holben, B.N., Stenchikov, G. & Tie, X., (2006). Evaluation of aerosol distribution and optical depth in the GFDL Coupled Model CM2.1 for present climate. *Journal of Geophysics Research* 111: D22210, doi:10.1029/2005JD006707.

Gomes, L. & Gillette, D.A., (1993). A comparison of characteristics of aerosol from dust storms in Central Asia with soil-derived dust from other regions. *Atmospheric Environment* 27A: 2539-2544.

Gong, S.L., Barrie, L.A., Blanchet, J.P., von Salzen, K., Lohmann, U., Lesins, G., Spacek, L., Zhang, L.M., Girard, E., Lin, H., Leaitch, R., Leighton, H., Chylek, P. & Huang, P., (2003). Canadian Aerosol Modulea size-segregated simulation of atmospheric aerosol processes for climate and air quality . 1. Module development. *Journal of Geophysical Research* 108 (D1): 4007 – 4025.

Gordon, G.E., (1980). Receptor . *Environmental Science and Technology* 14: 792–800.

Gordon, G.E., (1988). Receptor . *Environmental Science and Technology* 22: 1132–1142

Guo, H., Ding, A.J., So, K.L., Ayoko, G., Li, Y.S. & Hung, W.T., (2009). Receptor modelling of source apportionment of Hong Kong aerosols and the implication of urban and regional contribution. *Atmospheric Environment* 43: 1159–1169.

Gu, J., Pitz, M., Schenlle-Kreis, J., Diemer, J., Reller, A., Zimmermann, R., Soentgen, J., Stoelzel, M., Wichmann, H.E., Peters, A. & Cyrys, J., (2011). Source apportionment of ambient particles: comparison of positive matrix factorization analysis applied to particle size distribution and chemical composition data. *Atmospheric Environment* 45: 1849–1857.

Haber, S., Yitzhak, D. & Tsuda, A., (2003). Gravitational deposition in a rhythmically expanding and contracting alveolus. *Journal of Applied Physiology* 95: 657 – 671.

Halllett, J., Hudson, J.G., & Rogers, C.F., (1987). Characterization of combustion aerosols for haze and cloud formation, paper presented at the Third International Conference on

Carbonaceous Particles in the Atmosphere. *American Association Aerosol Research*, Berkeley, California, October 5-8.

Hansen, J., & Coauthors, (2005). Efficacy of climate forcings. *Journal of Geophysics Research* 110: D18104, doi:10.1029/2005JD005776.

Harrington, D.Y. & Kreidenweis, S.M., (1998). Simulations of sulfate aerosol dynamics-I. Model description. *Atmospheric Environment* 32: 1691–1700.

Harrison, R.M. & Kitto, A.M., (1992). Estimation of the rate constant for the reaction of acid sulfate aerosol with NH_3 gas from atmospheric measurements. *Journal of Atmospheric Chemistry* 15: 133–143.

Harrison, R.M., Smith, D.J.T. & Luhana, L., (1996). Source apportionment of atmospheric polycyclic aromatic hydrocarbons collected from an urban location in Birmingham, U.K. *Environmental Science and Technology* 30: 825–832.

Harrison, R.M., Deacon, A.R., Jones, M.R. & Appleby, R.S., (1997). Sources and processesaffecting concentrations of PM_{10} and $PM_{2.5}$ particulate matter in Birmingham (UK). *Atmospheric Environment* 31: 4103–4117.

Harrison, R.M., Smith, D.J.T., Pio, C.A. & Castro, L.M., (1997). Comparative receptor modelling study of airborne particulate pollutants in Birmingham (United Kingdom), Coimbra (Portugal) and Lahore (Pakistan). *Atmospheric Environment* 31: 3309–3321.

Harrison, R.M., Tilling, R., Callen Romero, M.S., Harrad, S. & Jarvis, K., (2003). A study of trace metals and polycyclic aromatic hydrocarbons in the roadside environment. *Atmospheric Environment* 37: 2391–2402.

Heald, C.L., Jacob, D.J., Park, R.J., Russell, L.M., Huebert, B.J., Seinfeld, J.H., Liao, H. & Weber, R.J., (2005). A large organic aerosol source in the free troposphere missing from current . *Geophysics Research Letters* 32: L18809, doi:10.1029/2005GL023831.

Henry, R.C., Lewis, C.W., Hopke, P.K. & Williamson, H.J., (1984). Review of receptor model fundamentals. *Atmospheric Environment* 18: 1507–1515.

Herman, J.R., Bhartia, P.K., Torres, O., Hsu, N.C., Seftor, C.J. & Celarier, E., (1997). Frequency of Ocurrence of absorbing aerosol. *Journal of Geophysics* Research 102 (D14): 16911-16922.

Hermanus, M., (2006). The Status of Occupational Health in the South African Mining Industry and Key Challenges for Practitioners. *Journal of the Mine Ventilation Society of South Africa* 59: 6 – 7.

Hinds, W.C., (1999). *Aerosols Technology: Properties, Behaviour and Measurement of Airborne Particles.* New York: John Wiley and Sons, Inc.

Hnizdo, E., Sluis-Cremer, G.K., Baskind, E. & Murray, J., (1994). Emphysema and Airway Obstruction in Non-smoking South African Gold Miners With Long Exposure to Silica Dust. *Occupational & Environmental Medicine* 51: 557 – 563.

Hnizdo, E., Murray, J. & Klempman, S., (1997). Lung cancer in relation to exposure to silica dust, silicosis and uranium production in South African gold miners. *Thorax* 52: 271 – 275.

Hnizdo, E. & Murray, J., (1998). Risk of Pulmonary Tuberculosis Relative to Silicosis and Exposure to Silica Dust in South African Gold Miners. *Occupational & Environmental Medicine* 55: 496 – 502.

Holben, B., Sundar, A., Christopher, X.L., Welch, R.M., Reid, J.S., Hobbs, P.V. & Eck, T.F., (1996). Estimation of Surface and Top-of-Atmosphere Shortwave Irradiance in Biomass-Burning Regions during SCAR-B. *Journal of Applied Meteorology* 39: 1742–1753.

Hopke, P.K., (1991). An introduction to receptor modelling. *Chemometrics and Intelligent Laboratory Systems* 10: 21–43.

Hoppel, W.A., Fitzgerald, J.W., Frick, G.M., Larson, R.E. & Mack, E.J., (1990). Aerosol size distributions and optical properties found in the marine boundary layer over the Atlantic Ocean. *Journal of Geophyscis Research* 95: 3659–3686.

Hoppel, W.A., Frick, G.M., Fitzgerald, J.W. & Wattle, B.J., (1994). A cloud chamber study of the effect which nonprecipitating water clouds have on the aerosol size distribution. *Aerosol Science Technology* 20: 1–30.

Horowitz, L.W., (2006). Past, present, and future concentrations of tropospheric ozone and aerosols: Methodology, ozone evaluation, and sensitivity to aerosol wet removal. *Journal of Geophysics Research* 111: D22211, doi:10.1029/2005JD006937.

Houghton, J. T., (1985). *The Global Climater.* New York. The Press Syndicate of the University of Cambridge.

Hsu, N.C., Herman, J.R., Bhartia, P.K., Seftor, C.J., Torres, O., Thompson, A.M., Gleason, J.F., Feck, T. & Holben, B.N., (1996). Detection of biomass burning smoke from TOMS measurements. *Geophysics Research Letters* 23: 745-748.

Hu, D., Qiao, L., Chen, J., Ye, X., Yang, X., Cheng, T. & Fang, W., (2010). Hygroscopicity of Inorganic Aerosols: Size and Relative Humidity Effects on the Growth Factor. *Aerosol and Air Quality Research* 10: 255 – 264.

Huebert, B.J., Bates, T., Russell, P.B., Shi, G., Kim, Y.J., Kawamura, K., Carmichael, G. & Nakajima, T., (2003). An overview of ACE-Asia: Strategies for quantifying the relationships between Asian aerosols and their climatic impacts. *Journal of Geophysics Research* 108: 8633, doi:10.1029/2003JD003550.

Husar, R.B. 1999. Atmospheric Aerosol Science Before (1900). *History of Aerosol Science Conference*, August, 31 to September, 2 1999, Austria.

Hussein K., (2011). GEOG 4110/5100 Advanced Remote Sensing Background Material Review of Material from GEOG/GEOL 4093/5093. http://cires.colorado.edu/esoc/classes/geog5100/Lecture_2.pdf

Jacob, D., (2000). Heterogeneous chemistry and tropospheric ozone. *Atmospheric Environment* 34: 2131–2159.

Jacob, D.J., and Coauthors, (2003). Transport and Chemical Evolution over the Pacific (TRACEP) aircraft mission: Design, execution, and first results. *Journal of Geophysics Research* 108: 9000, doi:10.1029/2002JD003276.

Jacobson, M.Z., (1997). Development and application of a new air pollution modelling system. Part II. Aerosol module structure and design. *Atmospheric Environment* 31: 131–144.

Jaecker-Voirol, A., & Mirabel, P., (1989). Heteromolecular nucleation in the sulfuric acid-water system. *Atmospheric Environment* 23: 2053–2057.

Jimenez, J.L. & Coauthors, (2003). New particle formation from photooxidation of diiodomethane (CH_2I_2). *Journal of Geophysics Research* 108: 4318, doi:10.1029/2002JD002452.

Johnson, R.L., (2004). Relative Effects of Air Pollution on Lungs and Heart. *Circulation* 109: 5 – 7.

Jonathan, M., Samet, M.D., Dominici, F., Curriero, F.C., Coursac, I. & Zeger, S.L., (2000). Fine Particulate Air Pollution and Mortality in 20 U.S. Cities 1987–1994. *The New England Journal of Medicine* 343: 1742 – 1749.

Kahn, R.A., Garay, M.J., Nelson, D.L., Levy, R.C., Bull, M.A., Diner, D.J., Martonchik, J.V., Hansen, E.G., Remer, L.A. & Tanre, D., (2011). Toward unified satellite climatology of

aerosol properties. 3. MODIS versus MISR versus AERONET. *Journal of Quantitative Spectroscopy & Radiative Transfer* 112 (5): 901-909.

Kaneyasu, N., Ohta, S. & Murao, N., (1995). Seasonal variation inthe chemical composition of atmospheric aerosols andgaseous species in Sapporo, Japan. *Atmospheric Environment* 29: 1559–1568.

Kaufman, Y. J., & Coauthors, 1998: Smoke, Clouds, and Radiation-Brazil (SCAR-B) experiment. *Journal of Geophysics Research* 103: 31 783–31 808.

Kim, J.J., Smorodinsky, S., Lipsett, M., Brett, C.S., Alfred, T.H. & Bart, O., (2004). Traffic-related Air Pollution near Busy Roads. *American Journal of Respiratory and Critical Care Medicine* 170: 520 – 526.

Kinne, S., & Coauthors, (2003). Monthly averages of aerosol properties: A global comparison among , satellite data, and AERONET ground data. *Journal of Geophysics Research* 108: 4634, doi:10.1029/2001JD001253.

Koch, D., Schmidt, G.A. & Field, C., (2006). Sulfur, sea salt and radionuclide aerosols in GISS ModelE. *Journal of Geophysics Research* 111: D06206, doi:10.1029/2004JD005550.

Koepke, P. & Hess, M., (1988). Scattering functions of tropospheric aerosols: the effects of nonspherical particles. *Applied Optics* 27: 2422-2430.

Kometani, T.Y., Bove, J.L., Nathanson, B., Siebenberg, S. & Magyar, M., (1972). Dry Ashing of Airborne Particulate Matter on Paper and Glass Fiber Filters For Trace Metal Analysis by Atomic Absorption Spectrometry. *Environmental Science & Technology* 6: 617.

Kong, S., Han, B., Bai, Z., Chen, L., Shi, J. & Xu, Z., (2010). Receptor modelling of $PM_{2.5}$, PM_{10} and TSP in different seasons and long-range transport analysis at a coastal site of Tianjin, China. *Science of the Total Environment* 408: 4681–4694.

Krotkov, N.A., Krueger, A.J. & Bhartia, P.K. (1997). Ultraviolet optical model of volcanic clouds for remote sensing of ash and sulfur dioxide. *Journal of Geophysical Research D: Atmospheres*, 102 (18): 21891-21904.

Kulmala, M., Laaksonen, A. & Pirjola, L., (1998). Parameterizations of sulphuric acid/water nucleation rates. *Journal of Geophysical Research* 103: 8301–8307.

Kumar, A.V., Patil, R.S. & Nambi, K.S.V., (2001). Source apportionment of suspended particulate matter at two traffic junctions in Mumbai, India. *Atmospheric Environment* 35: 4245–4251.

Laakso, L., Vakkari, V. , Laakso, H., Virkkula, A., Backman, J., Kulmala, M., Beukes, J. P., van Zyl, P. G., Tiitta, P., Josipovic, M., Pienaar, J.J., Chiloane, K., Gilardoni, S., Vignati, E., Wiedensohler, A., Tuch, T., Birmili, W., Piketh, S., Collett, K., Fourie, G.D., Komppula, M., Lihavainen, H., de Leeuw, G. & Kerminen, V.M., (2010). South African EUCAARI measurements: seasonal variation of trace gases and aerosol optical properties. *Atmospheric Chemistry and Physics* 12: 1847–1864.

Lai, C.H., Chen, K.S., Ho, Y.T., Peng, Y.P. & Chou Y., (2005). Receptor modeling of source contributions to atmospheric hydrocarbons in urban Kaohsiung, Taiwan. *Atmospheric Environment* 39: 4543–4559.

Langford, I.H. & Bentham, G., (1993). *The Potential Effects of Climate Change on Winter Mortality in England and Wales*. East Anglia: Centre for Social and Economic Research on the Global Environment, University of East Anglia.

Larsen, R.K. & Baker, J.E., (2003). Source apportionment of polycyclic aromatic hydrocarbons in the urban atmosphere: a comparison of three methods. *Environmental Science and Technology* 37: 1873–1881.

Larson, S.M., Gass, G.R., Hussey, K.J. & Luce, F., (1988). Verification of image processing-based visibility . *Environmental Science and Technology* 22: 629–637.

Laupsa, H., Denby, B., Larssen, S. & Schaug J., (2009). Source apportionment of particulate matter ($PM_{2.5}$) in an urban area using dispersion, receptor and inverse modelling. *Atmospheric Environment* 43 (31): 4733–4744.

Lee, S.H., Reeves, J.M., Wilson, J.C., Hunton, D.E., Viggiano, A.A., Miller, T.M., Ballenthin, J.O. & Lait, L.R., (2003). New particle formation by ion-induced nucleation in the upper troposphere and lower stratosphere. *Science* 301: 1886–1889.

Lee, W. Liu, Wang, Y., Russell, A.G. & Edgerton, E.S., (2008). Source apportionment of $PM_{2.5}$: comparing PMF and CMB results for four ambient monitoring sites in the southeastern United States. *Atmospheric Environment* 42: 4126–4137.

Levin, Z. & Lindberg, J.D., (1979). Size distribution, chemical composition, and optical properties of urban and desert aerosols in Israel. *Journal of Geophysics Ressearch* 84: 6941-6950.

Levin Z., Joseph, J.H. & Mekler, Y., (1980). Properties of Sharav (Khamsin) dust-comparison of optical and direct sampling data. *Journal of Atmospheric Science* 37: 882-891.

LifeExtension, (2012). Heavy Metal Toxicity. Life Extension Foundation, USA.

Lindberg, J.D. & Laude, L.S., (1974). Measurement of the absorption coefficient of atmospheric dust, *Applied Optics* 13: 1923-1927.

Lindberg, J.D., Gillespie, J.B., & Hinds, B.D., (1976). Measurements of imaginary refractive indices of atmospheric particulate matter from a variety of geographic locations in *Proceedings of the International Symposium of radiation in the Atmosphere, Garmisch-Parterkirchen* , edited by H.J. Bolle, Science Press, New York.

Lippmann, M., (1998). The 1997 US EPA standards for particulate matter and ozone. *Environmental Science and Technology* 10: 75–99.

Liu, X., Penner, J.E. & Herzog, M., (2005). Global modeling of aerosol dynamics: Model description, evaluation, and interactions between sulfate and nonsulfate aerosols. *Journal of Geophysics Research* 110: D18206, doi:10.1029/2004JD005674.

Longtin, D.R., Shettle, E.P., Hummel, J.R. & Pryce, J.D., (1988). A wind dependent Desert Aerosol Model: Radiative Properties, *AFGL-TR-88-0112*, Air Force Geophysics Laboratory.

Lovejoy, E.R., Curtius, J. & Froyd, K.D., (2004). Atmospheric ion-induced nucleation of sulfuric acid and water. *Journal of Geophysics Research* 109: D08204, doi:10.1029/2003JD004460.

Lundgren, D.A. & Burton, R.M., (1995). Effect of particle size distribution on the cut point between fine and coarse ambient mass fraction. *Inhalation Toxicology* 7: 131–148.

Ma, Q., Liu, Y. & He, H., (2010). The Utilization of Physisorption Analyzer for Studying the Hygroscopic Properties of Atmospheric Relevant Particles. *Journal of Physical Chemistry* 114: 4232–4237.

Mahoney, J. R., and Coauthors, 2003: Strategic plan for the U.S. Climate Change Science Program. Climate Change Science Program and the Subcommittee on Global Change Research Rep., 211 pp. www.climatescience.gov/Library/stratplan2003/final/ccspstratplan2003-all.pdf.

Malm, W.C., Schichtel, B.A., Pitchford, M.L., Ashbaugh, L.L. & Eldred, R.A., (2004). Spatial and monthly trends in speciated fine particle concentration in the United States. *Journal of Geophysics Research* 109: D03306, doi:10.1029/2003JD003739.

Marchand, R.T., Ackerman, T.P. & Moroney, C., (2007). An assessment of Multiangle Imaging Spectroradiometer (MISR) stereo-derived cloud top heights and cloud top winds using ground-based radar, lidar, and microwave radiometers. *Journal of Geophysical Research* 112: D06204, doi:10.1029/2006JD007091.

Martins, J.V., Hobbs, P.V., Weiss, R.E. & Artaxo, P., (1996). Shapes of smoke particles from biomass burning in Brazil, SCAR-B Proceedings, edited by V.W.J.H. Kirchhoff, Transtec Editorial, 1996 , Upwelling UV spectral irradiances and surface albedo measurements at Lauder, New Zealand. *Geophysics Research Letters* 23: 1757-1760.

Maurer, J., (2001). Overview of NASA's Terra satellite. University of Hawaii, HI 96822, USA.

McGraw, R., (1997). Description of aerosol dynamics by the quadrature method of moments. *Aerosol Science Technology* 27: 255–265.

McGraw, R. & Wu, D., (2003). Kinetic extensions of the nucleation theorem. *Journal of Chemistry and Physics* 118: 9337–9347.

McGraw, R., (2005). Nucleation and vapor composition: Statistical analysis and interpretation of rate measurements using PCA. *Proc. of the Hyytiala Conf. on Formation and Growth of Secondary Atmospheric Aerosols,* Hyytiälä, Finland, International Global Atmospheric Chemistry Project, 69–74.

McMahon, C.K., (1983). Characteristics of forest fuel, fires and emissions. Paper No. 83-45.1. Presented at 76th Annual Meeting of the Air Pollution Control Association, Atlanta, GA, 19-24 June.

McMurry, P.H., (2000). A Review of Atmospheric Aerosol Measurements. *Atmospheric Environment* 34: 1959 – 1999.

McMurry, P.H. & Coauthors, (2005). A criterion for new particle formation in the sulfur-rich Atlanta atmosphere. *Journal of Geophysics Research* 110: D22S02, doi:10.1029/2005JD005901.

Medina, S., Plasencia, A., Ballester, F., Miicke, H.G. & Schwartz, O.N., (2004). Apheis: Public Health Impact of PM_{10} in 19 European Cities. *Journal of Epidemiology and Community Health* 58: 831 – 836.

Meehl, G.A., Washington, W.M., Wigley, T.M.L., Arblaster, J.M. & Dai, A., (2003). Solar and greenhouse gas forcing and climate response in the twentieth century. *Journal of Climate* 16: 426–444.

Meehl, G.A., & Coauthors, (2006). Climate change projections for the 21st century and climate change commitment in the CCSM3. *Journal of Climate* 19: 2597–2616.

Melillo, J.M., Callaghan, T.V., Woodward, F.I., Salati, E. & Sinha, S.K., (1990). Effects on Ecosystems. *Climate Change IPCC full report*, 283-309

Meng, Z., Dabdub, D. & Seinfeld, J.H., (1998). Size-resolved and chemically resolved model of atmospheric aerosol dynamics. *Journal of Geographical Research* 103: 3419-3435.

Mitchell, J.F.B., Johns, T.C., Gregory, J.M. & Tett, S.F.B., (1995). Climate response to increasing greenhouse gases and sulphate aerosols. *Nature* 376: 501–504.

Mishchenko, M.I., Lacis, A.A., Carlson, B.E. & Travis, L.D., (1995). Nonsphericity of dust-like tropospheric aerosols: implications for aerosol remote sensing and climate modeling. *Geophysics Research Letters* 22: 1077-1080.

Moon, K.A. & Chae, H.K., (2007). What is the Meaning of Heavy Metals ?: A Case Study in Korean Textbooks. Proceeding of the 2nd NICE Symposium July 30-31, Taipei, TAIWAN.

Motulsky, H. & Christopoulos, A., (2012). Fitting to biological data using linear and nonlinear regression. A Practical Guide to Curve Fitting. GraphPad Software. 2236 Avenida de la Playa La Jolla, CA 92037 USA.

Moucheron, M.C. & Milford, J., (1996). Development and testing of a process model for secondary organic aerosols. *Air and Waste Management Association, Nashville.*

Municipal Dermacation Board, (2008). North West Province Environment Outlook Draft Environment Outlook Report. North West Department of Agriculture, Conservation and Environment.

Nafziger, Sabine, (1996). Heavy Metals. *CAOBISCO*, Secretary General Rue Defacqz 1/7. Brussels.

Nakajima, T., King, M.D., Spinhrine, J.D. & Radke, L.F., (1991). Determination of the optical thickness and effective particle radius of clouds from reflected solar radiation measurements. Part II: Marine stratocumulus observations. *Journal of Atmospheric Science* 48: 728–750.

Napari, I., Noppel, M., Vehkamäki, H. & Kulmala, M., (2002a). An improved model for ternary nucleation of sulfuric acid-ammonia-water. *Journal of Chemistry and Physics* 116: 4221–4227.

Napari, I., Noppel, M., Vehkamäki, H. & Kulmala, M., (2002b). Parametrization of ternary nucleation rates for H2SO4-NH3-H2O. *Journal of Geophysics Research* 107: 4381, doi:10.1029/2002JD002132.

National Ambient Air Quality Standards for South Africa (2004).

http://www.google.co.za/url?sa=t&rct=j&q=national+ambient+air+quality+standards+south+africa&source=web&cd=84&ved=0CE4QFjADOFA&url=http%3A%2F%2Fwww.greengazette.co.za%2Fdocuments%2Fnational-gazette-32816-of-24-dec-2009-vol-534_20091224-GGN-32816.pdf&ei=HZgbUKSmCNKzhAe4g4DQAw&usg=AFQjCNGp9WCcONBasu6REAVJ0wLLaJvnwg Accessed: November 10, 2011.

National Institute for Occupational Safety and Health (NIOSH), (2002). Health Effects of Occupational Exposure to Respirable Crystalline Silica. Department of Health and Human Services Centers for Disease Control and Prevention National Institute for Occupational Safety and Health, Publication No. 129.

National Research Council, C.o.A.C., (1993). Board on Atmospheric Sciences and Climate, Commission on Geosciences, Environment and Resources, Understanding and predicting atmospheric chemical change: An imperative for the U.S. Global Change Research Program, National Academy Press, Washington, D.C.

InfoHub. http://events.infohub.co.za/venue-details.htm?id=648__north-west-province-events. Accessed May 02, 2012.

Ohta, S. & Okita, T., (1990). A chemical characterization of atmospheric aerosol in Sapporo. *Atmospheric Environment* 24A: 815–822.

Ohta, S., Murao, N. & Moriya, T., (1990). Evaluation of absorption properties of atmospheric aerosols at solar wavelengths based on chemical characterization. *Atmospheric Environment* 24A: 1409–1416.

OpenLearn, (2012). Global warming. The Open University, Milton Keynes, United Kingdom.

Oregon Museum of Science and Industry, (2006). A Guide for Educators in Grades 3-8. Traveling Exhibits 1945 SE Water Avenue Portland, OR 97214.

Ovtchinnikov, M., & Ghan, S.J., (2005). Parallel simulations of aerosol influence on clouds using a cloud-resolving model and a single column model. *Journal of Geophysics Research* 110: doi:10.1029/2004JD005088.

Palheta, D. and Taylor, A., (1995). Mercury in environmental and biological samples from a gold mining area in the Amazon region of Brazil.

Pallavi Pant &Roy M. Harrison., (2012). Critical review of receptor modelling for particulate matter: A case study of India. *Atmospheric Environment* 49: 1-12.

Pandis, S.N., Wexler, A.S. & Seinfeld, J.H., (1995). Dynamics of Tropospheric Aerosols. *Journal of Physical Chemistry* 99: 9646-9659

Panchenko, M. V., Kozlov, V. S. & Terpugova, S. A., (2001). Estimation of the Single Scattering Albedo from the Data on the Content of Submicron Aerosol, Absorbing Substance, and the Parameter of Condensation Activity In a Local Volume. Eleventh ARM Science Team Meeting Proceedings, Atlanta, Georgia, March 19-23, 2001.

Pankow, J.F., (1994). An absorption model of gas/particle partitioning of organic compounds in the atmosphere. *Atmospheric Environment* 28: 185–188.

Parungo, F., Bodhaine, B. & Bortniak, J., (1981). Seasonal variation in Antarctic Aerosol. *Journal of Aerosol Science* 17: 491-504.

Patterson, E.M., Gillette, D.A. & Stockton, B., (1977). Complex Index of Refraction between 300 and 700 nm for Saharan Aerosols. *Journal of Geophysics Research* 82: 3153-3160.

Patterson E.M. & McMahon, C.K., (1984). Absorption characteristics of forest fire particulate matter. *Atmospheric Environment* 18: 2541-2551.

Penner, J.E., Dickinson, R.E. & O'Neill, C.E., (1992). Effects of Aerosol from Biomass Burning on the Global Radiation Budget. *Science* 256: 1432-1434.

Penner, J. E., Charlson, R.J., Schwartz, S.E., Hales, J.M., Laulainen, N.S., Travis, L., Leifer, R., Novakov, T., Ogren, J. & Radke, L.F., (1994). Quantifying and minimizing uncertainty of climate forcing by anthropogenic aerosols. *Bulletin of American Meteorological Society* **75:** 375–400.

Penner, J.E., & Coauthors, (2001). Aerosols, their direct and indirect effects. *Climate Change 2001: The Scientific Basis,* J. T. Houghton et al., Eds., Cambridge *University Press, 289–348.*

Penner, J.E., & Coauthors, (2002). A comparison of modeland satellite-derived aerosol optical depth and reflectivity. *Journal of Atmospheric Science* 49: 441–460.

Peters, A., Dockery, D.W., Muller, J.E., Murray, A. & Mittleman, M.D., (2001). Increased Air Pollution and the Triggering of Myocardial Infarction. *Circulation* 103: 2810 – 2815.

Pey, J., Alastuey, A., Querol, X., Pérez, N. & Cusack, M., (2010). A simplified approach to the indirect evaluation of the chemical composition of atmospheric aerosols from PM mass concentrations. *Atmospheric Environment* 44: 5112-5121.

Petzold, A., Schonlinner, M., (2004). Multi-angle absorption photometry: A new method for the measurement of aerosol light absorption and atmospheric black carbon. *Journal of Aerosol Science* 35: 421–441.

Pilat, M.J., Ensor, D.S. & Bosch, J.C., (1970). Source Test Cascade Impactor. *Atmospheric Environment* 4: 671-679.

Pilinis, C., (1989). Numerical simulation of visibility degradation due to particulate matter: Model development and evaluation. *Journal of Geophysical Research* 94: 9937–9946.

Politis, M., Pilnis, C. & Lekkas, T.D., (2008). Ultrafine Particles (UFP) and Health Effects, Dangerous, Llike no Other PM? Review and Analysis. *Global NEST Journal* 10: 439-452.

Pope, C.A. & Burnett, R.T., (2002). Lung Cancer, Cardiopulmonary Mortality, and Long-term Exposure to Fine Particulate Air Pollution. *Journal of the American Medical Association* 287: 1132 – 1141.

Pope III, C.A., Schwartz, J. & Ransom, M., (1992). Daily mortality and PM10 pollution in Utah Valley. *Archives Environmental Health* 42: 211–217.

Pöschl, U., (2005). Atmospheric Aerosols Composition, Transformation, Climate and Health Effects. *Chemical International Edition* 44: 7520 – 7540.

Radke, L.F., Hegg, D.A., Hobbs, P.V., Nance, J.D., Lyons, J.H., Laursen, K.K., Weiss, R.E., Riggan, P.J. & Ward, D.E., (1991). Particulate and trace gas emissions from large biomass fires in North America, in *Global Biomass Burning: Atmospheric, Climatic, and Biospheric Implications*, edited by J.S. Levine, chap. 28, pp. 209-224, MIT Press, Cambridge, Mass.

Ramadan, Z., Eickhout, B., Xin-Hua Song, Buydens, L.M.C. & Hopke, P.K., (2003). Comparison of positive matrix factorization and multilinear engine for the source apportionment of particulate pollutants. *Chemometrics and Intelligent Laboratory Systems* 66: 15–28.

Ramanathan, V., Crutzen, P. J., Lelieveld, J., Mitra, A.P., Althausen, D., Anderson, J., Andreae, M.O., Cantrell, W., Cass, G. R., Chung, C. E., Clarke, A. D., Coakley, J. A., Collins, W.D., Conant, W.C., Dulac, F., Heintzenberg, J., Heymsfield, A. J., Holben, B., Howell, S., Hudson, J., Jayaraman, A., Kiehl, J.T., Krishnamurti, T.N., Lubin, D., McFarquhar, G., Novakov, T., Ogren, J.A., Podgorny, I.A., Prather, K., Priestley, K., Prospero, J.M., Quinn, P.K., Rajeev, K., Rasch, P., Rupert, S., Sadourny, R., Satheesh, S.K., Shaw, G.E., Sheridan, P. & Valero, F.P.J., (2001). Indian Ocean

experiment: An integrated analysis of the climate forcing and effects of the great Indo-Asian haze. *Journal of Geophysics Research*: 106 (D22): 28 371–28 398.

Rau, J.A. & Khalil, M.A.K., (1993). Anthropogenic contributions to the carbonaceous content of aerosols over the Pacific Ocean. *Atmospheric Environment* 27A (8): 1297–1307.

Raes, F., Bates, T., McGovern, F. & Van Liederkerke, M., (2000). The 2nd aerosol characterization experiment (ACE-2): General overview and main results. *Tellus* 52B: 111–125.

Reyes, M., (1997). Aerosols in the Atmosphere. http://icp.giss.nasa.gov/research/ppa/1997/reyes/. Accessed: May 02, 2012.

Rhoades, D., (2006). *Particle Size with a Graseby-Anderson Mark III Cascade Impactor.* Wood Street Palatine: Clean-Air Engineering, Inc.

Rios, A., (2004). *MODIS Observations of Desert Dust, Forest Fire Smoke and Anthropogenic Aerosols*: *Significant Opportunities in Atmospheric Research and Science*. Sacramento: California State University.

Roberts, J.R., (1999). Metal Toxicity in Children. Training Manual on Pediatric Environmental Health: Putting It Into Practice. Emeryville, CA: Children's Environmental Health Network.

Robinson, A.L., Subramanian, R., Donahue, N.M., Bernardo-Bricker, A. & Rogge, W.F., (2006). Source apportionment of molecular markers and organic aerosol. 2. Biomass smoke. *Environmental Science and Technology* 40: 7811–7819.

Rosen, H., Hansen, A.D.A., Gundel, L. & Novakov, T., (1978). Identification of the graphitic component of source and ambient particulates by Raman sprectroscopy and an optical attenuation technique. *Applied Optics* 17: 3859-3861.

Roulet, M., Lucotte, M., Farella, N., Serique, G., Coetho, H., Sousa, P., Scarone, A.P., Mergler, D., Guimaràes, J.R.D., & Amorim, M., (1999). Effects of Recent Human Colonisation on the Presence of Mercury in Amazon Ecosystems. *Journal of Water, Air, and Soil Pollution* 112: 3 – 4.

Russell, P.B., Hobbs, P.V. & Stowe, L.L., (1999). Aerosol properties and radiative effects in the United States East Coast haze plume: An overview of the Tropospheric Aerosol Radiative Forcing Observa1082 | JULY 2007 tional Experiment (TARFOX). *Journal of Geophysics Research* 104: 2213–2222.

Rustenburg. (2010). In *South African History Online*. Available at www.sahistory.org.za (retrieved: May 02, 2012).

Salma, I., Balásházy, I., Winkler-Heil, R., Hofmann, W. & Záray, G., (2002). Effect of particle mass size distribution on the deposition of aerosols in the human respiratory system. *Journal of Aerosol Science* 33: 119 – 132.

Salma, I., Balásházy, I., Winkler-Heil, R., Hofmann, W. & Záray, G., (2002). Effect of physical exertion on the deposition of urban aerosols in the human respiratory system. *Journal of Aerosol Science* 33: 983 – 997.

Schauer, J.J., Rogge, W.F., Hildemann, L.M., Mazurek, M.A. & Cass, G.R., (1996). Source apportionment of airborne particulate matter using organic compounds as tracers. *Atmospheric Environment* 30: 3837–3855.

Schmidt, G.A., & Coauthors, (2006). Present day atmospheric simulations using GISS ModelE: Comparison to in-situ, satellite and reanalysis data. *Journal of Climate* 19: 153–192.

Schroeder, W.H., Dobson, M., Kane, D.M. & Johnson, N.D., (1987). Toxic Trace Elements Associated With Airborne Particulate Matter: A review. *Journal of Air Pollution Control Association* 37: 1267 – 1285.

Schroeder, W.H. & Munthes, J., (1998). Atmospheric Mercury-an Overview. *Atmospheric Environment* 32: 809 – 822.

Schütz, L., (1980). Long-range transport of desert dust with special emphasis on the Sahara. *Annals of the New York Academy of Sciences* 338: 515-532.

Schwartz, J., Dockery, D.W. & Neas, L.M., (1996). Is daily mortality associated specifically with fine particles? *Journal of Waste Management Association* 46: 927–939.

Seftor, C.J., Hsu, N.C., Herman, J.R., Bhartia, P.K., Torres, O., Rose, W.I., Schneider, D.J., & Krotkov, N., (1997). Detection of Volcanic Ash Clouds from Nimbus 7/total Ozone Mapping Spectrometer. *Journal of Geophysical Research D: Atmospheres* 102 (14): 16749-16759.

Seinfeld, J.H., & Coauthors, (1996). Aerosol Radiative Forcing and Climate Change. *National Research Council*, National Academy Press, 161 pp.

Seinfeld, J.H., (2004). Air Pollution: A Half Century of Progress. *American Institute of Chemical Engineers Journal* 50: 1096–1108.

Seinfeld, J.H. & Pandis, S.N., (2006). *Atmospheric Chemistry and Physics: From Air Pollution to Climate Change*. New York: John Wiley and Sons, Inc.

Şen, Z., (2008). *Solar Energy Fundeamentals and Modelling Techniques: Atmosphere, Environment, Climate Change and Renewable energy*. London: Springer-Verlag Limited.

Sharmaa, A., Sivakumara, V., Bolliga, C., van der Westhuizena, C. & D. Moemaa., (2009). The System description of the mobile LIDAR. *South African Journal of Science* 105.

Shaw, G.E., (1979). Considerations on the origin ans properties of the Antarctic aerosol. Reviews of Geophysics and Space Physics 8: 1983-1998.

Shi, G.L., Zeng, F., Li, X., Feng, Y.C., Wang, Y.Q., Liu, G.X. & Zhu, T., (2011). Estimated contributions and uncertainties of pca/mlr-cmb results: source apportionment for synthetic and ambient datasets. *Atmospheric Environment* 45: 2811–2819.

Shrivastava, M.K., Subramanian, R., Rogge, W.F. & Robinson, A.L., (2007). Sources of organic aerosol: positive matrix factorization of molecular marker data and comparison of results from different source apportionment . *Atmospheric Environment* 41: 9353–9369.

Ska, D.D., Wojtylak, M., (2010). Air Pollution Forecasting Model Control. *Journal of Medical Informatics and Technologies* 14: ISSN 1642-6037.

Skull, R.B., (1988). *An introduction to boundary layer meteorology*. Dordrecht: Kluwer Academic Publishers, 666pp.

Slanina, S., (Lead Author); Davis, W., (Topic Editor), 2008. "Air pollution emissions." In: Encyclopedia of Earth (Cleveland C J, ed.). Environmental Information Coalition, National Council for Science and the Environment. http://www.eoearth.org/article/Air pollution emissions, Washington DC.

Sloane, C.S., (1984). Optical properties of aerosols of mixed composition. Atmospheric Environment 18: 871–878.

Sluis-Cremer, G.K., Walters, L.G. & Sichel, H.S., (1967). Chronic Bronchitis in Miners and Non-Miners: An Epidemiological Survey of a Community in the Gold Mining Area in the Transvaal. *British Journal of Industrial Medicine* 24: 1–12.

Song, Y., Zhang, Y., Xie, S., Zeng, L., Zheng, M., Salmon, L.G., Shao, M. & Slanina, S., (2006). Source apportionment of $PM_{2.5}$ in Beijing by positive matrix factorization. *Atmospheric Environment* 40: 1526–1537.

Sokolik, I., Andronova, A. & Johnson, T.C., (1993). Complex Refractive Index of Atmospheric Dust Aerosols. *Atmospheric Environment* 27A: 2495-2502.

Sportisse, B., (2010). *Fundamentals in Air Pollution: From Processes to Modelling.* London: Springer Dordrecht Heidelberg.

Stedman, J.R., (1997). A UK wide episode of elevated particle (PM_{10}) concentration in March 1996. *Atmospheric Environment* 31: 2381–2383.

Stockwell, W.R., Kirchner, F., Kuhn, M. & Seefeld, S., (1997). A new mechanism for regional atmospheric chemistry modeling. *Journal of Geophysical Research* 22: 25,847–25,879.

Stone, E., Schauer, J., Quraishi, T.A. & Mahmood, A., (2010). Chemical characterization and source apportionment of fine and coarse particulate matter in Lahore, Pakistan. *Atmospheric Environment* 44: 1062–1070.

Stott, P.A., Tett, S.F.B., Jones, G.S., Allen, M.R., Mitchell, J.F.B. & Jenkins, G.J., (2000). External control of twentieth century temperature by natural and anthropogenic forcings. *Science* 290: 2133–2137.

Swap, J.R., Annegarn, J. H., Suttles, J.T., King, D.M., Platnick, S., Privette, L.J. & Scholes, J.R., (2003). Africa Burning: A Thematic Analysis of the Southern Africa Regional Science Initiative 2000. *Journal of Geophysical Research* 108: 8465.

Tasić, M., Rajšić, S., Novaković, V. & Mijić, Z., (2006). Atmospheric Aerosols and their Influence on Air Quality in Urban Areas. *Physics, Chemistry and Technology* 4: 83 – 91.

Tauler, R., Viana, M., Querol, X., Alastuey, A., Flight, R.M., Wentzell, P.D. & Hopke, P.K., (2009). Comparison of the results obtained by four receptor modelling methods in aerosol source apportionment studies. *Atmospheric Environment* 43: 3989–3997.

Tegen, I., Lacis, A.A. & Fung, I., (1996). The influence on climate forcing of mineral aerosols from disturbed soils. *Nature* 380: 419-422.

Temime, B., (2012). Atmospheric Aerosols : physical properties, chemical composition, health & environmental effects. Department of Chemistry, UCC.

Tesche, T.W., McNally, D.E., Loomis, C., Stella, G.M. & Wilkinson, J.G., (2002). *Scientific Peer –Review of the HgCAMx Atmospheric Mercury Model and its Application Report.* Madison: WDNR Mercury Modeling Team, Wisconsin Department of Natural Resources.

Tett, S.F.B., & Coauthors,(2002). Estimation of natural and anthropogenic contributions to twentieth century temperature change. *Journal of Geophysics Research* 107: 4306, doi:10.1029/2000JD000028.

The Shared Research Instrumentation Facility, (1998). Computerized Instrumentation, The Shared Research Instrumentation Facility Room 221 Discovery Hall, MSN 4D7 10900 University, BLVD Manassas VA, 20110.

Thurston, G.D. & Spengler, J.D., (1985). A quantitative assessment of source contributions to inhalable particulate matter pollution in metropolitan Boston. *Atmospheric Environment* 19: 9–25.

Thurston, G.D. & Lioy, P.J., (1987). Receptor modelling and aerosol transport. *Atmospheric Environment* 21: 687–698.

Tie, X., & Coauthors, (2005). Assessment of the global impact of aerosols on tropospheric oxidants. *Journal Geophysics Research* 110: D03204, doi:10.1029/2004JD005359.

Tsai, Y.I. & Chen, C., (2006). Atmospheric aerosol composition and source apportionments to aerosol in southern Taiwan. *Atmospheric Environment* 40: 4751–4763.

Torres, O. & Bhartia, P.K., (1995). Effect of stratospheric aerosol on ozone profile from BUV Measurements. *Geophysics Research Letters* 22: 235-238.

Torres, O., Ahmad, Z. & Herman, J.R., (1992). Optical effects of polar stratospheric clouds on the retrieval of TOMS total ozone. *Journal of Geophysics Research 97*: 13015-13024.

Torres, O., Bhartia, P.K., Herman, J.R., Ahmad, Z. & Gleason, J., (1998). Derivation of aerosol properties from satellite measurements of backscattered ultraviolet radiation: Theoretical basis. *Journal of Geophysical Research D: Atmospheres* 103 (D14): 17099-17110.

Turco, R., (1992). Acid rain also occurs from air pollution. American Geophysical Union Special Report: Volcanism and Climate Change.

U.S. Climate Change Science Program (CCSP) Strategic Plan, (2009).Atmospheric Aerosol Properties and Climate Impacts. Synthesis and Assessment Product 2.3 Report by the U.S. Climate Change Science Program and the Subcommittee on Global Change Research.

U.S. Environmental Protection Agency, (1988). Recommendations for and Documentation of Biological Values for use in Risk Assessment. EPA 600/6-87/008, NTIS PB88-1798774/AS.

U.S. Environmental Protection Agency, (1997). Chemical Mass Balance Receptor Model Version 8(CMB8), User Manual. Research Triangle Park, NC Desert Research Institute, Reno, NV.

U.S. Environmental Protection Agency, (1998c). *Iris File: Arsenic, Inorganic.*

U.S. Environmental Protection Agency, (2000). *Toxicological Review of Trivalent Chromium and Toxicological Review of Hexavalent Chromium.* Washington DC: National Center for Environmental Assessment.

U.S. Environmental Protection Agency, (2007). *Research Programs: Particulate Matter (PM) Health Effects, Health and Environmental Effects Research.* Washington DC: National Center for Environmental Assessment.

U.S. Geological Survey, (2010). Volcanic Gases and their Effects. non –US Department of the Interior. 12201 Sunrise Valley Drive, MS 904, Reston VA 20192.

Vehkamäki, H., Kulmala, M., Napari, I., Lehtinen, K.E.J., Timmreck, C., Noppel, M. & Laaksonen, A., (2002). An improved parameterization for sulfuric acid–water nucleation rates for tropospheric and stratospheric conditions. *Journal of Geophysics Research* 107: 4622, doi:10.1029/2002JD002184.

Viana, M., Kuhlbusch, T.A.J., Querol, X., Alastuey, A., Harrison, R.M., Hopke, P.K., Winiwarter, W. & Vallius, M., (2008). Source apportionment of particulate matter in Europe: a review of methods and results. *Journal of Aerosol Science* 39: 827–849.

Viana, M., Pandolfi, M., Minguillón, M.C., Querol, X., Alastuey, A., Monfort, E. & Celades, I., (2008b). Inter-comparison of receptor for PM source apportionment: case study in an industrial area. *Atmospheric Environment* 42: 3820–3832.

Virtanen, A., Joutsensaari, J., Koop, T., Kannosto, J., Yli-Pirilä, P., Leskinen, J., Mäkelä, J.M., Holopainen, J. K., Pöschl, U., Kulmala, M., Worsnop, D. R. & Laaksonen, A., (2010). An amorphous solid state of biogenic secondary organic aerosol particles. *Nature* 467: 824–827.

Volkamer, R. & Coauthors, (2006). Secondary organic aerosol formation from anthropogenic air pollution: Rapid and higher than expected. *Geophysics Research Lettters* 33: L17811, doi:10.1029/2006GL026899.

von Salzen, K., (2005). Piecewise log-normal approximation of size distributions for aerosol modeling. *Atmospheric Chemistry and Physics Discussions* 5: 3959–3998.

Wahlin, P., (2003). COPREM: a multivariate receptor model with a physical approach. *Atmospheric Environment* 37: 4861–4867.

Wall, S.M., John, W. & Ondo, J.L., (1988). Measurement of aerosol size distributions for nitrate and major ionic species. *Atmospheric Environment* 22: 1649–1656.

Wang, G., Huang, L., Gao, S. & Wang, L., (2002). Measurement of PM_{10} and $PM_{2.5}$ in Urban Area of Nanjing, China and The Assessment of Pulmonary Deposition of Particle Mass. *Chemosphere* 48: 689 – 695.

Warrick, R. & Oerlemans, A.J., (1990). Sea Level Rise. Climate Change IPCC full report, 257-281.

Washington Department of Health, (2003). Fact Sheet Arsenic in the Environment. http://www.doh.wa.gov/ehp/oehas/pubs/arsenic.pdf. Accessed: May 02, 2012.

Weber, R.J., McMurry, P.H., Mauldin, L., Tanner, D., Eisele, F., Clarke, A.D. & Kapustin, V.N., (1999). New particle formation in the remote troposphere: A comparison of observations at various sites. *Geophysics Research Letters* 26: 307–310.

Weiss, R.E., Kapustin, V.N. & Hobbs, P.V., (1992). Chain-aggregate aerosols in smoke from the Kuwait oil fires. *Journal of Geophysical Research* 97: 14527-14531.

Weizmann Institute of Science, (2007). Tiny airborne particles are a major cause of climate change. http://www.newmaterials.com/Customisation/News/Research_&_Development/University/Tiny_airborne_particles_are_a_major_cause_of_climate_change.asp. Accessed: May 02, 2012.

Westphal, D.L. & Toon, O.B., (1991). Simulations of Microphysical, Radiative, and Dynamical Processes in a Continental-Scale Forest Fire Smoke Plume. *Journal of Geophysics Research* 96: 22379-22400.

Whitby, K.T., (1978). The physical characteristics of sulfur aerosols. *Atmospheric Environment* 12: 135–159.

Whitby, E.R., & McMurry, F.H., (1997). Modal aerosol dynamics modeling. *Aerosol Science and Technology* 27: 673–688.

Wikipedia, the free encyclopedia. http://en.wikipedia.org/wiki/Stratospheric_sulfur_aerosols. Accessed: May 02, 2012.

Windows To The Universe, (2011). Aerosols, Cloud Nucleation and Global Dimming http://www.windows2universe.org/earth/Atmosphere/aerosol_cloud_nucleation_dimming.html. Accessed: May 02, 2011.

Wiscombe, W.J. & Mugnai, A., (1988). Scattering from nonspherical Chebyshev particles. 2: Means of angular scattering patterns. *Applied Optics* 27: 2405-2421.

World Health Organization, (2000). *Transport, Environment and Health*. Copenhagen: Regional Publications, European Series.

World Health Organisation, (2003). Health Aspects of Air Pollution with Particulate Matter, Ozone and Nitrogen Dioxide: Report on a WHO Working Group. Bonn: WHO.

World Health Organization, (2004). Public Health Monitoring of the Metro Manila Air Quality Improvement Sector Development Program. Manila: Asian Development Bank (ADB) and Department of Health (DOH), Philippines.

World Health Organization Air quality guidelines for particulate matter, ozone, nitrogen dioxide and sulfur dioxide. Global update 2005. http://whqlibdoc.who.int/hq/2006/WHO_SDE_PHE_OEH_06.02_eng.pdf Accessed: November 10, 2011.

World Health Organization, (2011). Air Quality and Health. Fact sheet N°313. http://www.who.int/mediacentre/factsheets/fs313/en/index.html. Accessed: May 02, 2012.

Wright, D.L., Kasibhatla, P.S., McGraw, R. & Schwartz, S.E., (2001). Description and evaluation of a sixmoment aerosol microphysical module for use in atmospheric chemical transport . *Journal of Geophysics Research* 106: 20 275–20 291.

Wynn, T.A., (2007). Common and unique mechanisms regulate fibrosis in various fibroproliferative diseases. *The Journal of Clinical Investigation* 117: 524 – 529.

Wynn, T.A., (2011). Integrating mechanisms of pulmonary fibrosis. Journal of Experimental Medicine 208(7): 1339–1350.

Yatkin, S. & Bayram, A., (2008). Source apportionment of PM_{10} and $PM_{2.5}$ using positive matrix factorization and chemical mass balance in Izmir, Turkey. *Science of the Total Environment* 390: 109–123.

Yigiletu, M.T., Yigiletu, V., Botai, J.O. & Mengistu, G., (2011). Aerosol climatology over South Africa based on 10 years of Multi-angle Imaging SpectroRadiometer (MISR) Data. *Journal of Geophysical Research*, doi:10.1029/2011JD016023, in press. [Abstract] [PDF] (accepted 12 August 2011).

Yoon, C., & McGraw, R., (2004a). Representation of generally mixed multivariate aerosols by the quadrature method of moments: I. Statistical foundation. *Journal of Aerosol Science* 35: 561–576.

Yoon, C., & McGraw, R., (2004b). Representation of generally mixed multivariate aerosols by the quadrature method of moments: II. Aerosol dynamics. *Journal of Aerosol Science* 35: 577–598.

Zemp, E., Elsasser, S., Schindler, C., Kunzli, N., Perruchoud, A.P., Domenighetti G., Medici, T., Ackermann-Liebrichi, U., Leuenberger, P., Monn, C., Bolognini, G., Bongard, J., Brändli, O., Karrer, W., Keller, R., Schöni, M.H., Tschopp, J., Villiger, B. & Zellwege,r J., (1999). Long-Term Ambient Air Pollution and Respiratory Symptoms in Adults (SAPALDIA Study). *American Journal of Respiratory and Critical Care Medicine* 159: 1257 – 1266.

Zeng, F., Shi, G., Li, X., Fang, Y., Bi, X., Wu, J. & Xue, Y., (2010). Application of a combined model to study the source apportionment of PM_{10} in Taiyun, China. *Aerosol and Air Quality Research* 10: 177–184.

Zhang, Y., Easter, R.C., Ghan, S.J. & Abdul-Razzak, H., (2002). Impact of aerosol size representation on modelling aerosol-cloud interactions. *Journal of Geophysics Research* 107: 4558, doi:10.1029/2001JD001549.

Zhang, R., Suh, I., Zhao, J., Zhang, D., Fortner, E.C., Tie, X., Molina, L.T. & Molina, M.J., (2004). Atmospheric new particle formation enhanced by organic acids. *Science* 304: 1487–1490.